Aus dem Institut für klinische Neuroimmunologie der

Ludwig-Maximilians-Universität München

Direktoren: Prof. Dr. Reinhard Hohlfeld und Prof. Dr. Martin Kerschensteiner

Analysis of oligoclonal band antibodies from patients with neurological diseases

Dissertation

zum Erwerb des Doktorgrades der Naturwissenschaften

an der Medizinischen Fakultät

der Ludwig-Maximilians-Universität München

vorgelegt von

Simone Maren Brändle

aus Reutlingen

Juni 2016

Betreuer: PD Dr. rer. nat. Klaus Dornmair

Zweitgutachter: Prof. Dr. Axel Imhof

Dekan: Prof. Dr. med. dent. Reinhard Hickel

Tag der mündlichen Prüfung: 14.12.2016

Zusammenfassung

Bei den meisten Patienten mit akut- und chronisch-entzündlichen Erkrankungen des zentralen Nervensystems (CNS) können expandierte Antikörperspezies, sogenannte oligoklonale Banden (OCB), in Liquor cerebrospinalis (CSF) nachgewiesen werden. OCBs werden intrathekal produziert und stellen ein wichtiges diagnostisches Kriterium dar. Bei Infektionen des CNS, wie beispielsweise Neuroborreliose, ist bekannt, dass OCB Antikörper gegen den Erreger gerichtet sind. Bei Enzephalitiden mit unklarer Ursache, und insbesondere bei Multiple Sklerose (MS), der häufigsten entzündlichen CNS-Erkrankung, sind die Zielantigene der OCB Antikörper unbekannt.

Ziel dieser Studie war die Identifizierung von Antigenen von OCB Antikörper aus CSF von Patienten mit neurologischen Erkrankungen. Die OCB Antikörper wurden bereits in früheren Arbeiten aus CSF isoliert und charakterisiert. Sie stammten aus vier MS Patienten und einem Patienten mit γ-Aminobuttersäure-A Rezeptor ($GABA_AR$-) Enzephalitis.

In früheren Arbeiten wurden unfraktionierte CSF-Proben oder Antikörper aus Einzelzellen verwendet, um Antigene zu identifizieren. Diese Studien ermöglichten aber keine Zuordnung der Antigene zu einer definierten OCB. Kürzlich wurde in der AG Dornmair eine Methode etabliert, die die Zuordnung schwerer und leichter Ketten bei definierten OCB Antikörpern aus CSF erlaubt. Dies ermöglicht es nun Antigene definierter OCBs zu bestimmen. Hier wurden sechs OCB-basierte Antikörper als IgG1-Moleküle rekombinant hergestellt und mittels Proteinmicroarrays auf Reaktivität gegen Proteine untersucht. Drei der identifizierten Kandidatenantigene wurden durch Immunpräzipitation und „enzyme-linked immunosorbent assays“ unabhängig validiert. Diese drei Antigene sind intrazelluläre Proteine deren Expression nicht auf das CNS beschränkt ist. Reaktivität der OCBs gegen ubiquitäre, intrazelluläre Strukturen, könnte auf eine nicht-pathogene Rolle der OCBs in der MS hindeuten. OCBs könnten als Reaktion auf die vermehrte Bildung von Zelltrümmern in der Frühphase der Erkrankung gebildet werden und deren Beseitigung durch Opsonisierung beschleunigen.

Die $GABA_AR$-Enzephalitis ist eine besonders schwere, akute Enzephalitis mit unklarer Etiologie. Ein monoklonal expandierter Antikörper aus CSF eines $GABA_AR$-Enzephalitis Patienten wurde als IgG1-Molekül exprimiert und seine Spezifität für die extrazelluläre Domäne des $GABA_AR$ nachgewiesen. Unter der Annahme, dass die $GABA_AR$-Enzephalitis als paraneoplastisches neurologisches Syndrom im Zusammenhang mit einer Tumorerkrankung zu sehen ist, wurde dieser Antikörper mittels Proteinmicroarrays auf Reaktivität gegen weitere Proteine untersucht. Es wurden mehrere Zink-bindende Proteine, die Mehrzahl mit „LIM-Domäne“, identifiziert. Es ist bekannt, dass diese Proteine tumor-reaktive Immunantworten auslösen können. Die Erkennung des LIM-Proteins „cystein-rich protein 2“ (CSRP2) wurde durch Immunpräzipitation unabhängig validiert. Da sowohl $GABA_AR$, als auch CSRP2 über Zink-Bindestellen verfügen, könnten diese die Grundlage für eine Kreuzreaktivität auf molekularer Ebene bilden.

Summary

Expanded antibody species can be detected in cerebrospinal fluid (CSF) samples in most patients with acute or chronic inflammatory conditions of the central nervous system (CNS). These so-called oligoclonal bands (OCB) are produced intrathecally and provide an important diagnostic tool. In infectious conditions, such as neuroborreliosis, OCBs recognize the causing agent. In idiopathic encephalitides, and in particular multiple sclerosis (MS), the most common inflammatory disease of the CNS, target antigens are not known.

The aim of this study was to identify target structures of distinct OCB antibodies derived from CSF of patients with neurologic disorders. The OCB antibodies had been identified and characterized in previous studies. They were derived from four MS patients and one patient with γ-aminobutyric acid-A receptor ($GABA_AR$)-encephalitis.

In previous studies, target antigens were identified using unfractionated CSF samples or single cell derived antibodies. In these studies, target antigens could not be assigned to a distinct OCB. Recently, a new method was established, which identifies matching heavy and light chains of expanded antibody species in CSF. This now allows for the search for target antigens of distinct OCBs. Here, six OCB-derived antibodies were expressed as IgG1-molecules and screened for reactivity to protein antigens on microarrays. Three target antigens were validated independently using immunoprecipitation and enzyme-linked immunosorbent assays. All three antigens are intracellular proteins expressed in most tissues of the human body, indicating that OCB antibodies may recognize ubiquitous, intracellular proteins. Although more OCB-antigens need to be analyzed, these results suggest that OCB-antibodies may be raised in response to cell debris caused by primary immune reactions and may take part in debris removal by opsonizing cellular debris.

$GABA_AR$-encephalitis is a rare and severe form of acute encephalitis of unknown etiology. A monoclonally expanded antibody species from CSF of a $GABA_AR$-encephalitis patient was recombinantly expressed and found to recognize the extracellular domain of the $GABA_AR$ α1-subunit. $GABA_AR$-encephalitis may have a paraneoplastic background, i.e. it may be associated with malignancies. To identify a potential link to a paraneoplastic syndrome, the $GABA_AR$ α1-subunit specific antibody was tested for reactivity to potential tumor antigens on microarrays. A number of zinc-binding proteins, most of them LIM-domain proteins, were identified as targets. Reactivity with “cysteine-rich protein 2” (CSRP2) was validated by immunoprecipitation. LIM-proteins are involved in transcriptional regulation and other members of this family of proteins are strongly associated with malignancies. Since $GABA_AR$ and CSRP2 contain zinc-binding motifs, this structure may provide a potential molecular basis for the cross-reactivity of the antibody to both proteins.

Danksagung

Ich möchte mich herzlich bei allen bedanken, die mich in der Zeit meiner Promotion begleitet und unterstützt haben.

Ein großer Dank gilt meinem Betreuer PD Dr. Klaus Dornmair für die interessante Fragestellung und die Unterstützung während meiner Doktorarbeit. Er hatte jederzeit ein offenes Ohr und hilfreiche Denkanstöße für mich, die das Projekt voranbrachten.

Außerdem möchte ich mich bei der Leitung des Instituts für klinische Neuroimmunologie des Klinikums der Universität München, Professoren Hohlfeld und Kerschensteiner, für die Unterstützung meiner Arbeit und die Infrastruktur der Abteilung bedanken.

Mit größter Geduld hat Dr. Eduardo Beltrán mich während der gesamten Arbeit unterstützt und meinen Alltag erheitert. Dr. Kathrin Held hat stets ihr Know-how mit mir geteilt und stand mir mit Ratschlägen und Diskussionsbereitschaft zur Seite. Vielen Dank hierfür!

Weiterhin gilt meinen Kollegen in der Arbeitsgruppe mein Dank für die gute und inspirierende Zusammenarbeit. Besonders möchte ich mich bei Reini, Joachim und Ingrid dafür bedanken, dass sie mich an ihrem reichen Erfahrungsschatz teilhaben ließen. Großer Dank gilt auch den früheren Labormitgliedern Dr. Jessica Bruder und Dr. Birgit Obermeier für die Schaffung der Grundlagen meines Projekts.

Professor Dr. Hyrettin Tumani und Dr. Makbule Senel von der Klinik für Neurologie der Universität Ulm haben durch die Bereitstellung klinischer Proben einen großen Beitrag zu dieser Arbeit geleistet. Außerdem haben Makbules Erkenntnisse aus der Neuroborreliose eine wichtige Grundlage für meine Arbeit gebildet.

Vielen Dank auch an Dr. Kerstin Berer, unsere Diskussionen haben mir immer wieder neue Blickwinkel auf die Dinge eröffnet!

Nicht zuletzt möchte ich meinen Eltern und Timo für die jahrelange Unterstützung danken.

Content

1 Introduction

Since the first description of immunoglobulins (Ig) in the late 19th century [1], enormous progress was made in understanding their role in the human immune system. Generally, antibodies recognize foreign structures, induce immunologic processes, and thereby prevent harmful actions by a foreign invader. The complex mechanism producing a highly diverse repertoire, which allows the recognition of virtually every invader, was revealed and greatly advanced research in the field of immunology. In contrast to the protective function of antibodies, autoimmunity occurs as an adverse effect of effective host defense. In an aberrant immune response, antibodies may target self-structures and cause a variety of diseases. Despite the broad knowledge that has accumulated on antibodies over time, their role and function in distinct diseases remain puzzling.

1.1 Immunoglobulins

Antibodies may display a highly diverse and versatile repertoire of specificities, which is needed for efficient recognition and clearance of foreign invaders. The antibody repertoire is created by random recombination of gene segments, somatic hypermutation (SHM) and class switch recombination during B-cell development. These processes enable the immune system to increase the specificity of the antibody to the foreign invader and clear the infection more efficiently. Fully differentiated B-cells (plasma cells) produce large amounts of antigen-specific antibodies and build up memory to effectively clear a second infection (memory B-cell).

1.1.1 B-cell Maturation and BCR Rearrangement

B-cell precursors arise from hematopoetic progenitors in the bone marrow, where the formation of the B-cell receptor (BCR) is initiated. Pro-B-cells start to rearrange the heavy (H-) chain gene locus, as schematically depicted in Figure 1-1.

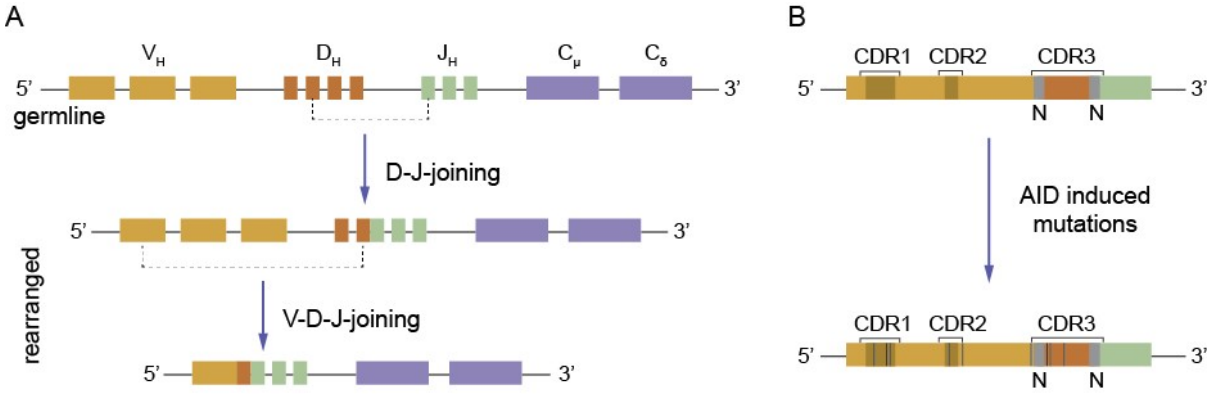

Figure 1-1: Schematic illustration of V(D)J-recombination and somatic hypermutation.

V(D)J-recombination is exemplarily depicted for the H-chain locus. At first, a single randomly selected D- segment is joined to one J- segment (middle row) in an AID dependent mechanism, followed by selection and joining of an upstream V-segment (bottom row). The gene segments are joined imprecisely (A). Upon completion of the V(D)J-recombination of the H-chain locus, one V- and one J-segment on either of the two L-chain loci is selected and joined (not depicted). In germinal centers, Ig-coding DNA-sequences undergo somatic hypermutation that introduces single amino acid exchanges (horizontal black bars) in the V-region of H- and L-chains (B). The illustration is adapted from [2].

The H-chain gene locus codes for three gene segments: variable (V), diversity (D) and junction (J). Each segment is made up of numerous copies of V-, D, and J-genes. In a first step, a randomly selected D-gene is connected to any J-gene of the H-chain locus, which is subsequently combined with a V-gene. Cells in the pre-B state rearrange the light (L-) chain locus in the same manner. Random addition or deletion of nucleotides at the combination sites further diversifies the receptor repertoire. Upon successful rearrangement of H- and L-chain locus, the immature B-cell expresses membrane-bound BCR that is capable of binding an antigen.

Such immature B-cells leave the bone marrow and encounter their antigen in the periphery. Upon antigen encounter, mature B-cells migrate to secondary lymphatic tissues, such as lymph nodes or the spleen, where they form germinal centers (GC) and undergo affinity maturation [3]. Within these structures, B-cells up-regulate the protein “activation-induced cytidine deaminase” (AID) that introduces point mutations in the Ig-coding DNA-sequences. These somatic hypermutations (SHM) result in increased affinity for the antigen and further diversification of the receptor repertoire [4]. The affinity maturation process is active until the antigen is cleared from the system. The random selection process in cooperation with imprecise joining and somatic hypermutation creates a highly diverse receptor repertoire that may form more than 10^{18} different specificities. A schematic overview of the development of B-cells is given in Figure 1-2.

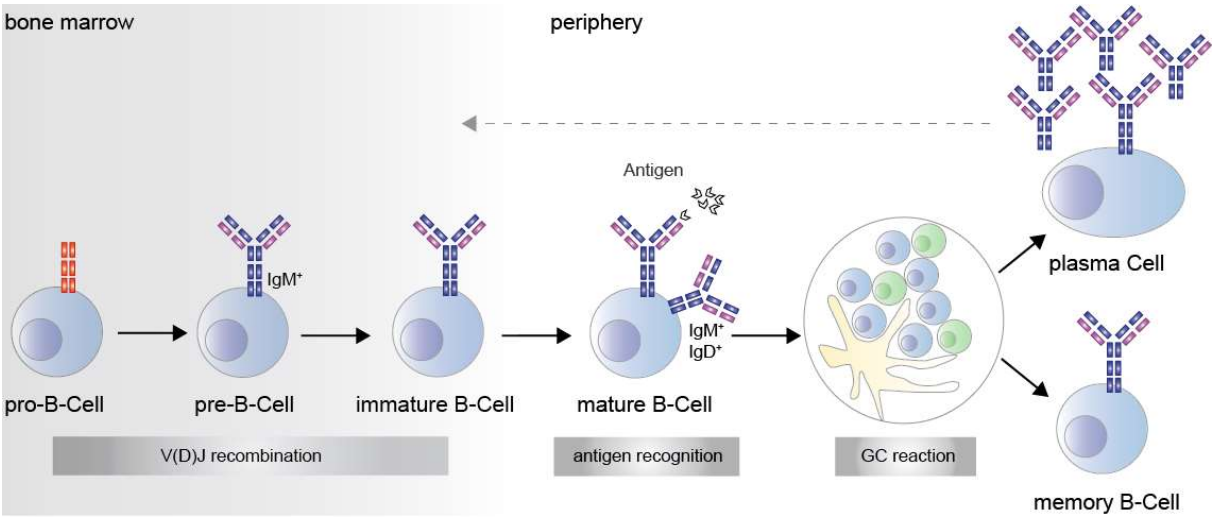

Figure 1-2: Schematic illustration of B-cell maturation.

B-cell precursors start their maturation process in the bone marrow. Upon successful V(D)J-rearrangement of the H- and L-chain, immature B-cells leave the bone marrow and eventually recognize an antigen in the periphery. Antigen-experienced B-cells (mature B-cells) migrate to germinal centers (GC) where they are in close contact with T-cells (green) and antigen-presenting cells (APC, yellow). Up-regulation of AID, that introduces point mutations in the variable region of the BCR, fine-tunes the receptor specificity. B-cells that display increased antigen specificities are positively selected, leave the GC, and proliferate. The progeny differentiate into plasma cells that produce large amounts of antibodies and memory B-cells that ensure immunologic memory. The illustration is modified from [5].

B-cells expressing high-affinity receptors are positively selected in the GC, proliferate, and differentiate into plasmablasts and finally plasma cells that produce large amounts of soluble Ig. Some cells give rise to antigen-specific memory B-cells that circulate the system after infection clearance to promptly elicit a specific immune response in case of re-infection.

Fully differentiated plasma cells usually undergo AID-mediated class switch recombination that allows production of five different Ig-subclasses, each of them adapted to a distinct task. Antibodies can be secreted in forms of IgM, IgD, IgG, IgA and IgE, with IgG being the subclass with highest prevalence in human serum [6] and CSF [7].

1.1.2 Antibody Structure and Function

IgG makes up the majority of circulating antibodies. The basic structure of all Ig-molecules is a Y-shaped heterodimer consisting of two identical H- and two identical L-chains (Figure 1-3). Structurally, antibodies consist of Ig-domains, a common protein fold that consists of antiparallel β-sheets forming one β-barrel per domain. H-chains possess four Ig-domains and L-chains possess two Ig-domains. The heterodimeric molecule is stabilized by disulfide bridges in the constant regions between H- and L- chain and in the hinge region between the two H-chains. Once the chains are split by treatment with a reducing agent, the molecular weight (MW) of H-chains is approximately 50 kDa and the one of L-chains is about 25 kDa, generating a fully assembled IgG-molecule with a MW of 150 kDa.

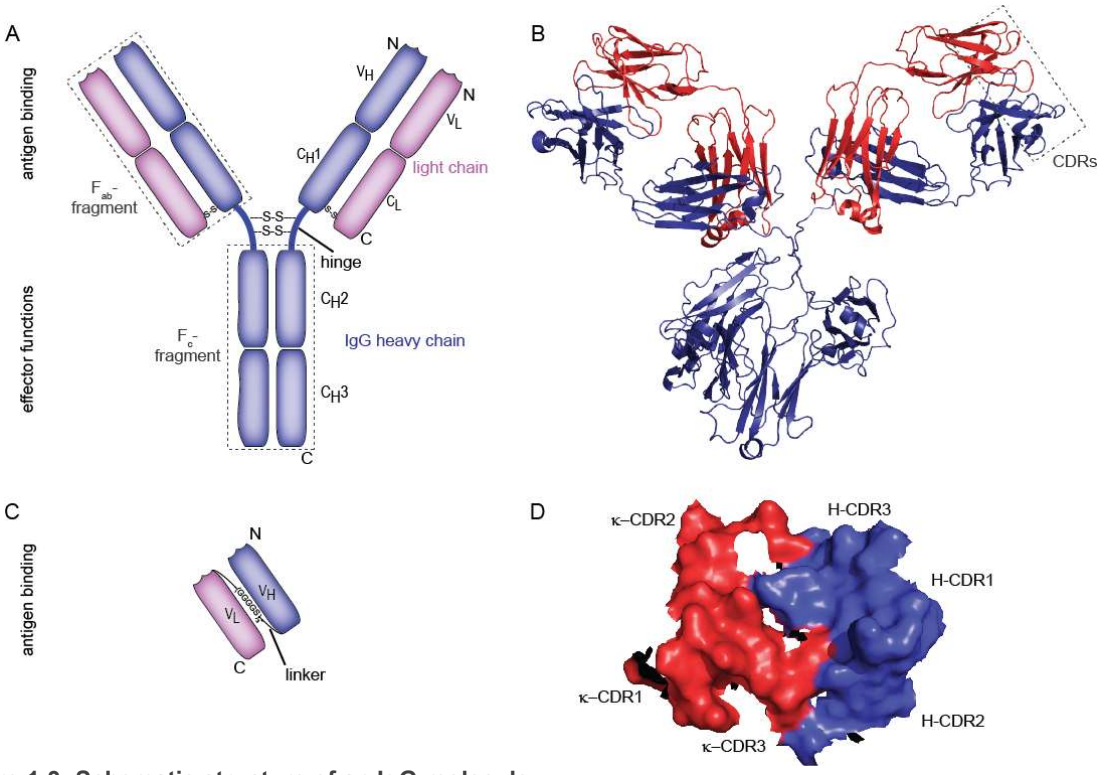

Figure 1-3: Schematic structure of an IgG-molecule.

The molecule consists of two identical H- (blue) and two identical L-chains (magenta) that are interconnected by disulfide bridges in the constant (C_H1 and C_L) and hinge regions. Antigens are bound via the antigen binding site, made up of the N-terminus of one H- and one L-chain. C_H2 and C_H3-domains of the H-chains form the Fc-fragment that controls the antibody effector function. The complete L-chain and the two N-terminal Ig-domains of the H-chains form the F_{ab}-fragment (A). The ribbon diagram of an antibody illustrates the folding of antiparallel β-sheets into β-barrels in each of the Ig-domains. The loops of the variable region contain the CDRs that interact with the antigen. The illustration of PDB 1IGY is modified from [8] (B). Single-chain Fv-fragments consist of the variable regions of H- and L-chain that are linked via a polypeptide linker (C). The ribbon diagram of x-ray diffraction analysis of a scF_V-molecule illustrates the retained structural characteristics of the Ig-domains in the artificial antibody-fragment. The illustration of PDB 4H0G is modified from [9] (D).

An antibody-molecule combines two fundamental functions that are reflected by its structure: First, specific antigen recognition via the variable region and second, mediation of effector functions by the constant region. Both chains carry a highly variable region that confers specificity to the Ig-molecule and is subject to affinity-maturation as described above. The N-terminal Ig-domain constitutes the variable region and consists of three complementary determining regions (CDR). CDRs 1 and 2 are encoded by the V-gene segment, the CDR3 in contrast is the site of joining of V(D)J-segments (Figure 1-1). The CDR-loops interconnect the β-sheets of the framework regions. These loops engage prominent positions in the molecule and interact directly with the target antigen. The complete antigen binding site is constituted by the variable regions of one H- and one L-chain; however, the fraction which is actually involved in antigen recognition varies. The surface area available for antigen recognition is approximately 1000 square Ångström [10] (Figure 1-3D).

Both H- and L-chains have constant regions that consist of three Ig-domains (C_H1-3) in case of the H-chain and a single one in L-chains (C_L). In H-chains, the Ig-domains of the constant region are interconnected by a hinge region that confers flexibility to the molecule. This way a single IgG-antibody may complex two antigens in varying distances and angles. The constant regions, especially those of H-chains, mediate the effector functions of antibodies. The different antibody subclasses are specifically recognized by receptors on effector cells or activate specific, non-cellular downstream mechanisms like the complement cascade. Proteolytic cleavage of IgG-molecules by papain was found to separate these functions creating two distinct fragments: one carrying the antigen binding site, named F_{ab}-fragment and one consisting of the H-chain constant domains C_H2 and C_H3, named F_c.

Naturally produced antibodies always have both F_{ab} and F_c-fragment and at least two identical binding sites. In some instances, the constant regions are abandoned due to specific experimental requirements or to reduce the molecule's size. Commonly used truncated antibody formats are F_{ab}-fragments and single chain variable fragments (scF_v). A schematic illustration of an IgG-molecule and an exemplary ribbon diagram depicting the folded structure as well as the F_{ab}- and scF_v-counterparts are shown in Figure 1-3. Both synthetic molecules possess the full variable region, that confers antigen-specificity, but the F_{ab}-fragment lacks the F_c-fragment whereas the scF_v lacks the constant regions entirely. Classically, F_{ab}-fragments are heterodimers of the full length L-chain and a truncated H-chain stabilized by one disulfide bridge, with each of the chains being approximately 25 kDa in size. In contrast, scF_v-molecules consist of a single chain that carries the variable regions of the H- and L-chains connected by a flexible linker of 5-15 small amino acids (AA), like glycine or serine, generating a 28 kDa protein. Both antibody-fragments carry a single antigen binding site and are capable of antigen recognition. However, higher avidity stabilizes antigen-antibody-interactions and therefore full antibodies are generally better suited to study interactions with low to medium affinities.

The discrimination of antibody subclasses is based on their different constant regions. They are specialized to the requirements of different inflammatory conditions and thus elicit distinct effector functions. The pentameric structure of IgM is well suited to recognize repetitive patterns because the high avidity compensates for lower affinity before SHM. IgG-antibodies have usually undergone somatic hypermutation, thus have higher affinities and are better suited to quickly reach the inflammatory site due to the smaller size. The major effector functions elicited by IgG-molecules are neutralization, antibody-dependent cell-mediated cytotoxicity (ADCC) and complement activation (Figure 1-4). Antibodies that encounter their antigen prevent interaction of the foreign molecule with host cells by charging its surface epitopes. Following this neutralization step, the immune system aims at clearing the foreign molecule. Clearance may be achieved by the complement system that is activated by antibody-antigen-complexes via the classical pathway. The membrane attack complex forms the final stage of the amplification cascade and initiates the lysis of the target microbe. Antibodies cross-linking membrane-bound molecules on pathogen-infected host cells recruit effector cells like natural killer cells and macrophages that then lyse the antibody-coated cell. The process of antibodies coating a molecule to initiate clearance is called opsonization.

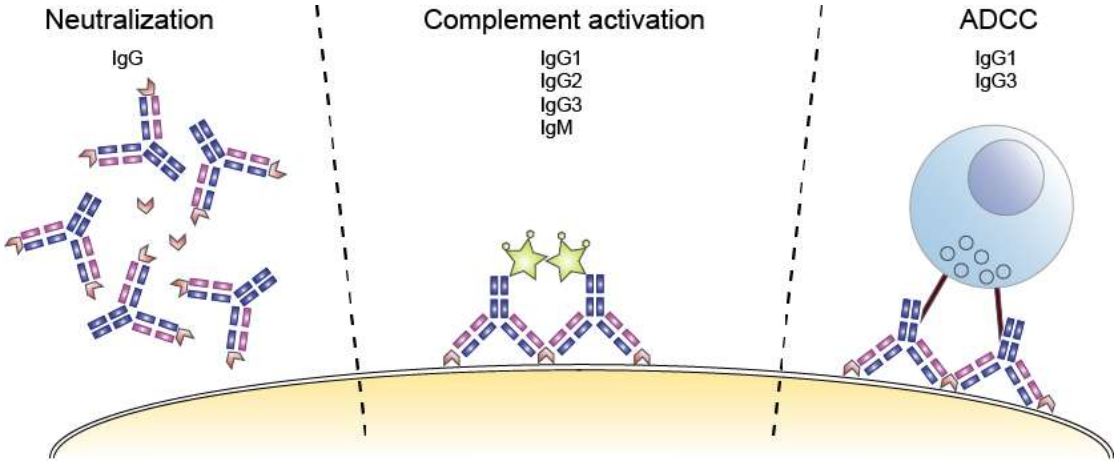

Figure 1-4: Effector functions of antibodies.

Antibodies neutralize soluble antigens and prevent toxic effects or their entry into host cells. Cross-linking of an antigen by multiple IgG-molecules activates the complement cascade leading to the formation of the membrane attack complex that eliminates the foreign invader. Antibodies that recognize an antigen on the surface of a pathogen-infected cell can recruit effector cells that bind the F_c-fragment of the antibodies and induce apoptosis in the infected cell (antibody-dependent cell-mediated cytotoxicity, ADCC). The illustration is modified from [11].

1.1.3 Specificity of Antibodies

Although the B-cell maturation process aims at creating antigen-specific antibodies, cross-reactivity is frequently encountered. Classically, polyreactivity of antibodies is defined as reactivity of a monoclonal antibody to DNA, lipopolysaccharide and insulin [12]. This reactivity profile is commonly associated with germline or near-germline configuration of Ig-chains [13]. Clearly, reactivity to multiple antigens (multireactivity) is not restricted to the above mentioned antigen classes and recognition of two or more related or unrelated protein antigens by a single antibody is a common finding [14]. Such multispecificity is an accepted phenomenon in the naïve antibody

repertoire. These multi- and autoreactive receptors are kept in check during the maturation process of B-cells, limiting harmful autoreactivity [12]. It is conceivable that multireactivity of antibodies in the healthy system helps the rapid neutralization of infectious agents at the site of entry besides a variety of other potential functions [14].

In addition to the well-accepted multireactivity in (near-) germline antibodies, affinity-matured, supposedly antigen-specific, antibodies were found to be multireactive as well. To this end, broadly neutralizing antibodies to an HIV-1 envelope protein in HIV-infected individuals were found to simultaneously recognize cardiolipin with comparable affinity [15]. Furthermore, autoantibodies derived from autoimmune hepatitis [16], rheumatoid arthritis [17] and systemic lupus erythematousus (SLE) patients [18] show signs of multireactivity as well.

Closely related molecules and similar secondary structures can cause cross-reactivity of an antibody. However, the examples mentioned above identified an unrelated molecule as “cross-reactive antigen”. In Figure 1-5, different mechanisms to explain the specific recognition of unrelated antigens by a monoclonal antibody are depicted. Those are rigid adaptation, induced fit and differential ligand positioning. A prominent example illustrating the fact that only a fraction of the binding pocket is actually involved in antigen binding is the murine 8-18C5 antibody specific for myelin oligodendrocyte glycoprotein (MOG). Introducing an alternative L-chain to this antibody leaves the MOG-reactivity unchanged, demonstrating that the interaction mostly relies on the variable region of the H-chain [19]. The relatively large area of the antigen binding site enables specific recognition of multiple distinct antigens, related and unrelated epitopes, by a single antibody (see Figure 1-3).

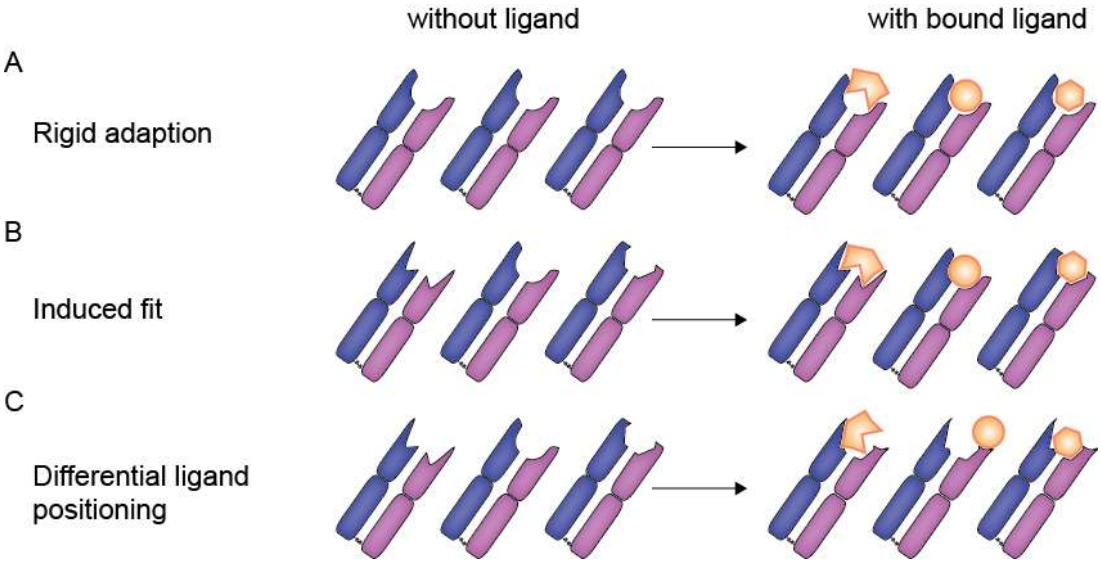

Figure 1-5: Schematic illustration of three potential mechanisms of polyreactivity.

Structurally different antigens (orange) are bound by the same, rigid binding site (depicted in form of F_{ab}-fragments). The rigid adaptation theory predicts different residues or areas within the binding pocket to combine with distinct antigen surfaces without major conformational changes (A). The induced fit-mechanism is based on the conformationally flexible binding pocket that adapts to structurally distinct antigens upon encounter (B). The third option predicts differential positioning of antigens. The antigen binding site carries multiple specific and spatially distinct regions that can interact with unrelated antigens (C). The illustration is adapted from [20].

The rigid adaptation theory views the binding site as a whole that accommodates structurally distinct antigens using different subsites within the binding pocket without major conformational changes [21]. On the contrary, the induced fit theory is based on the conformational flexibility of antibodies [22]. The hinge region has long been appreciated to arrange for simultaneous binding of two epitopes with varying distances from each other, but more recently, it becomes apparent that the variable regions may also undergo more or less subtle conformational changes during antigen recognition [23].

This flexibility may enhance antigen specificity by an induced-fit mechanism, but also could further increase the receptor repertoire diversity as it may allow specific binding to multiple structures [24, 25]. Differential positioning theory assumes pre-defined subsites within an antigen binding pocket that allows specific recognition of distinct, structurally unrelated antigens [26].

At least for naturally occurring multireactive antibodies from the naïve repertoire, it was shown that these antibodies can bind to late apoptotic cells, activate complement and thereby enhance phagocytosis by macrophages [27]. Thus, multireactive antibodies may assist efficient clearing of cell debris produced by mechanical stress, infectious insults or other processes [28].

1.2 Autoimmunity and Autoantibodies

B-cell maturation involves mechanisms that are prone to create self-reactive receptors and antibodies. The random process that creates the highly diverse receptor repertoire concomitantly causes the formation of auto-reactive receptors. The immune system has evolved various strategies to restrain these cells: First, early B-cells with self-reactive receptors [12] may rearrange the L-chain sequence (receptor editing) [29], second, cells may be entirely deleted from the repertoire, i.e., undergo apoptosis [30], or third, may lose the capacity to respond to their antigens (anergy) [31]. The presence of autoreactive antibodies in the healthy human system is well known and may even have a beneficial role as part of first line defense mechanisms or through immunoregulatory functions [14, 32].

However, autoreactivity may also occur during affinity-maturation in an appropriate immune response to a disease-related agent [33] or a malignancy [34]. In susceptible individuals, appropriate regulation of these self-reactive clones may fail, initiating an immune response against the host with production of vast amounts of auto-antibodies. A number of autoimmune diseases manifest themselves by prominent autoantibody production such as anti-nuclear antibodies found in SLE and Sjörgen’s syndrome, anti-thyroid antibodies in Hashimoto thyroiditis, rheumatoid factor in rheumatoid arthritis and antibodies targeting Aquaporin-4 in neuromyelitis optica (NMO, [35]). In contrast, anti-tumor immunity may raise antibodies directly targeted at autoantigens. Anti-tumor responses that elicit neurological deficits are termed paraneoplastic neurologic syndromes. In this case, tumors are thought to ectopically express neuronal antigens [36, 37] that become the target of the immune response that may also attack CNS-tissue [38].

In many cases, the etiology of autoimmune diseases is not very well understood. Often, an interplay between genetic and environmental factors is assumed to trigger the onset of the disease that is then perpetuated by autoreactivity in a dysregulated immune system [39]. Autoimmune diseases can manifest themselves in a variety of ways. In total, around 80 different autoimmune conditions are known so far that affect approximately 4.5 % of the world's population [40] and for some conditions increasing prevalence rates have been reported [41]. The most common autoimmune disease of the central nervous system (CNS) is MS with 2-2.5 million people affected worldwide.

1.2.1 Pathogenesis of Multiple Sclerosis

MS is a presumably autoimmune-mediated disorder of the CNS. Focal inflammation in different CNS-regions is a hallmark of the disease. Within such lesions, the myelin sheath surrounding neurons is destructed. Symptoms and disease course of the disorder vary widely between affected individuals. MS patients often experience relapsing-remitting forms of the disease in early stages. These are characterized by the occurrence of new symptoms that ameliorate over time. In later stages, the disease course may become secondary-progressive, in which persisting impairment accumulates [42].

The precise mechanisms that cause this heterogeneous chronic inflammatory disorder of the CNS remain elusive. MS-pathology is currently viewed as myelin destruction due to autoimmune processes in susceptible individuals. For a long time, MS was considered a $CD4^+$ T-cell mediated disease. This is supported by a strong genetic association of MS with the HLA class II variant DRB1*1501 [43]. Also, the rodent model for MS "experimental autoimmune encephalomyelitis" (EAE) is driven by myelin-specific T-cells [44].

The fact that the concordance between monozygotic twins is relatively low has drawn attention to environmental factors [45]. External influences, like smoking [46], may cause sustained activation of the immune system and possibly trigger autoimmunity. The concentration of vitamin D has also been associated with modified disease risk [47]. Another factor may be microbial infections. Similar to smoking, infection with Epstein-Barr virus represents a persistent immune activator and is tightly associated with MS incidence [48].

Another matter of debate is whether the triggers originate in the CNS-compartment or the periphery. First, an immune response targeted at a CNS-specific antigen may occur in the periphery and migrate into the CNS. Second, the initiating event may take place inside the CNS and could recruit other immune cells in a secondary event. Whether the triggers are cryptic self-molecules, foreign molecules that cause autoreactivity by molecular mimicry, or the general highly inflammatory setting, which may dysregulate the immune system, remains unclear as well [49]. Molecular mimicry as basis of a misdirected immune response has been shown to be involved in the pathogenesis of Gullaine-Barré-Syndrom that is commonly associated with a preceding *Campylobacter jejuni* infection [50].

In recent years, multiple findings have drawn the attention to B-cells and antibodies in the disorder and argue for a more complex pathogenesis than previously thought [51]. For instance, transgenic mice with MOG-specific T-cells were found to recruit MOG-specific B-cells and trigger anti-MOG antibody production. These antibodies were pathogenic and the mice spontaneously developed a relapsing-remitting disease course resembling the most common form of MS [52]. Anti-CD20 antibodies rapidly deplete B-cells from the system and were found to be of considerable therapeutic value, although they spare CD20-negative pro-B-cells and antibody-producing plasmablasts/plasma cells. B-cell depletion has proven effective in reduction of relapses, illustrating the wide effects on the disease performed by B-cells. Besides secreting antibodies, they modulate the immune response by secreting cytokines [53] and serving as antigen-presenting cell (APC, [54]). Precisely because the role of antibodies in the disease course remains enigmatic, it is important to characterize them in depth.

Importantly, human serum contains large amounts of antibodies of various specificities. These polyclonal antibodies are also, although in low concentrations, present in human CSF. Yet, MS patients often have additional expanded antibody species of distinct biochemical properties, named oligoclonal bands (OCB). Understanding the role of OCB-antibodies may be one step towards unraveling the processes triggering disease onset and progression.

1.2.2 Expanded Antibodies in CSF of MS Patients

Clonally expanded antibody species in CSF are a hallmark and diagnostic marker of MS. CSF is a clear fluid that surrounds the brain and spinal cord and is an ultrafiltrate of blood. The fluid environment protects the brain from concussions and is an important route to transport molecules [55]. Although CSF is directly derived from blood, the protein content is very low and smaller proteins are over-represented due to the ultrafiltration process that is sensitive to the proteins' MW [56]. Only 0.2 % of the IgG-concentration of blood are present in healthy human CSF and immune responses are generally absent from the CNS, thus intrathecal antibody production suggests a pathogenic process [57]. The specific expansion allows differentiation of distinct antibody species from the polyclonal background of antibodies by isoelectric focusing (IEF), so that OCBs can be demonstrated as distinct bands (Figure 1-6). OCBs were first visualized by IEF in the 1940s [58-60]. The detection of OCBs in CSF is not specific for any single condition, but rather a hint to an inflammatory condition in the CNS. Although there is a strong association with pathogenic conditions, OCBs may appear in healthy individuals as well. Expanded antibody species forming OCBs in CSF are observed in infectious disorders such as neuroborreliosis, neurosyphilis or HIV encephalitis and are also found in autoimmune conditions like SLE, Sjörgen's syndrome, besides MS [61]. In contrast to antibodies, which react to foreign invaders in inflammatory settings, OCBs in autoimmune diseases, especially in MS, remain enigmatic because their antigens are still unknown.

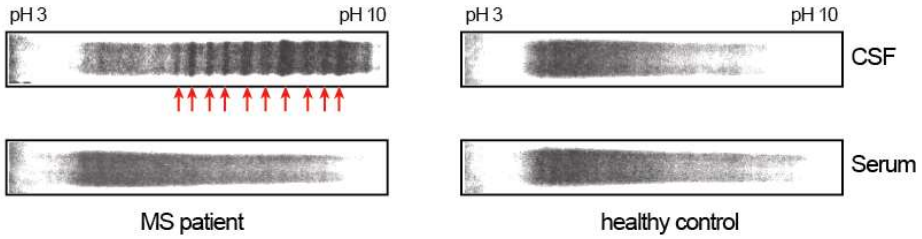

Figure 1-6: Clinical IEF and anti-IgG immunofixation of CSF and serum.

The left panel shows the IEF-analysis of CSF (upper) and serum (lower) of an MS patient. Multiple strong bands superimpose the polyclonal background of antibodies in the CSF sample of the MS patient (red arrows). In contrast, the serum of the same patient does not exhibit oligoclonal banding, but only a polyclonal background. On the right side, the same analysis with CSF and serum of a healthy donor shows polyclonal antibody background in both samples. IEF analysis was done by the Institute of Clinical Chemistry, Klinikum Großhadern, LMU München.

Infectious conditions, and other immunologic challenges, induce the secretion of vast amounts of antibodies once antigen-specific cells have undergone affinity maturation. Hence, a small number of individual, positively selected clones will mass-produce a highly restricted antibody repertoire that targets the infectious agent and can be detected as OCB. It is very well conceivable, and has been demonstrated for a number of disease conditions, that these OCB antibodies recognize the infectious agent [62-65]. Upon clearance of the infectious cause, antigen-specific antibodies are no longer needed in vast amounts thus their production is downregulated and OCBs disappear eventually. In contrast to neuroinflammatory conditions that elicit OCB production, the expanded antibodies in MS do not vanish, but persist basically unchanged for years even under most treatments [66].

MS is the most prominent autoimmune disorder associated with OCBs. The vast majority, around 95 %, of all patients display OCBs [67] and at least a fraction of these antibodies is produced intrathecally, in the CNS [68]. Furthermore, B-cells present in CSF of MS patients are closely related arguing for an ongoing B-cell maturation and proliferation inside the CNS [69]. These findings point to the persistence of a recurring antigenic stimulus that perpetuates the immune response and antibody production. As mentioned above, a supposedly persistent stimulus could arise from microbial infections, environmental factors or recurring production of cell debris, but has not been identified so far.

Classically, OCBs are formed by affinity-matured, class-switched IgG-molecules, further supporting an underlying antigen-driven process. On a functional level, IgG-molecules are capable of complement activation. IgG and complement deposits were detected in acute demyelinating lesions of autopsy brain material of MS patients [70], implicating a role of OCB-antibodies in disease. The effectiveness of plasma exchange in a subset of MS patients also points to an impact of antibodies on disease progression [71]. So far, it is not well understood what the role of OCB-antibodies in MS is, likewise their specificity remains to be elucidated. It is unclear whether antibodies are being produced in an irrelevant bystander activation mechanism due to the highly inflammatory status of the CNS [72] or play an active role in the disease. Thus,

identification of the target structures of OCB antibodies may hold clues on the pathogenesis of the disease.

1.2.3 Target Antigens of OCB-antibodies

Based on EAE-models, antibodies to myelin components like myelin oligodendrocyte glycoprotein (MOG), myelin basic protein (MBP) or proteolipid protein (PLP) are considered prime candidates due to their prominent localization in the myelin sheath. Besides myelin antigens, other oligodendroglial molecules were described, such as oligodendrocyte-specific protein [73], transketolase [74] or transaldolase [75]. Direct targeting of oligodendrocytes may explain the vanishing reconstruction of the myelin sheath with disease duration [76]. Similarly, neuronal and axonal structures seem to be targets of autoantibodies in MS. Neurofascin, located at the node of Ranvier, where the myelin sheath is intermittent, might be a target that enables direct axonal damage [77]. Neurofilament is released from axons upon an insult and is targeted by autoantibodies [78], but this is also observed in other CNS-diseases [79, 80]. A major advance in MS research was the identification of Aquaporin-4 on astrocytes as targets of antibodies [35] in a subset of patients that are now diagnosed with NMO [81].

Furthermore, ubiquitous proteins, expressed in virtually all cells, were found to be targeted by antibodies in CSF and/or serum of MS patients. These include heat shock proteins [82], heterogeneous nuclear ribonucleoprotein [83] or components of the proteasome [84]. Furthermore, non-protein ubiquitous target structures were identified as targets of antibodies from CSF of MS patients including DNA [85] and lipids [86, 87].

In line with a proposed infectious trigger of the disease, a variety of viral components have been described to be recognized by antibodies from MS samples [88]. The most prominent association is the “MRZ-reaction”, describing the reactivity of around 89 % of CSF-samples from MS patients with measles (M), rubella (R), and varicella zoster (Z) virus particles [89]. Furthermore, virtually all MS patients show seroreactivity to human herpes viruses, particularly Epstein-Barr-Virus [90].

1.2.3.1 Antigen Identification Strategies

Though incomplete, the above examples of target antigens compile a highly diverse set of molecules with heterogeneous structural and functional features. A detailed analysis revealed more than 30 antigens [91]. The individual entities of the large conglomerate of different target structures are widely accepted, but a common pattern was not identified so far. Thus, the antigens could not shed light on disease etiology [91]. Generally, the relevance of the autoantigens described above remains unclear due to the missing link between the individual antigens. On the one hand this finding may suggest antibodies have only marginal impact on MS pathology [92, 93], on the other hand this may, at least in part, reflect the heterogeneity of the disease itself [70].

The different methods used to identify target antigens further complicate the interpretation. Two fundamental approaches are in use. First, unfractionated CSF samples are directly applied in antigen searches [94, 95]. Second, antibodies are reconstructed from single plasma cells and recombinant antibodies used for antigen identification [96, 97]. In both cases, it remains unclear if detected signals derive from an expanded antibody species or the polyclonal background. Further, an antigen-specificity may not be attributed to a distinct oligoclonal band. CSF contains serum derived antibodies [57]. These are not produced in the CNS-compartment and form the polyclonal background of antibodies. Due to the low overall IgG-concentration of CSF [57], weak signals are expected. Thus, using the first approach, signals from OCB-antibodies may be superimposed by signals from irrelevant polyclonal antibodies. The second approach requires selection of single CSF B-cells from which matching IgG H- and L-chains are cloned allowing for production of recombinant antibodies. Besides the expanded B-cell clones that produce OCB-antibodies, irrelevant B-cells are found in CSF that may produce non-expanded antibodies. Thus, it is not clear whether the selected antibody represents an OCB or not. Such antibodies may also contribute to the polyclonal background and thus will not advance the search of antigens to OCB-antibodies [98]. This uncertainty applies to all antigens mentioned above.

An exception to these considerations constitutes the CSF-sample of patient MS2. This patient sample is characterized by a persisting single expanded antibody species as shown by clinical isoelectric focusing depicted in Figure 1-7 [99]. In such a sample, the serum derived polyclonal background of antibodies is present but the clonal expansion is very limited. Accordingly, next generation sequencing and Ig-proteome analysis of this sample confirmed a monoclonal expansion.

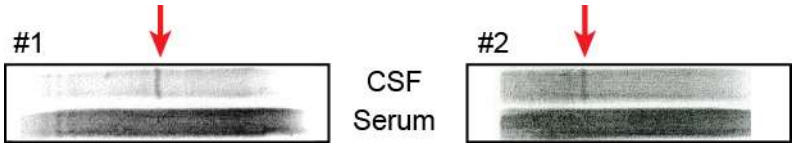

Figure 1-7: Clinical IEF and immunoblotting of CSF and serum samples from patient MS2.

CSF and serum samples at two different time points are shown. A single band was detected in the CSF samples at both time points but in neither of the serum samples. Samples and IEF analysis were provided by W. Kristoferitsch, Vienna. The illustration is modified from [99].

As persisting OCBs are found in most patients, it is assumed that they may hold clues to unravel disease etiology. Thus, it is important to study distinct OCB-antibodies in the absence of other OCB-antibodies and polyclonal background. Limited diversity facilitates the characterization of relevant antibodies and their target antigens. In addition, samples taken at early time points during disease onset could prove particularly helpful for the identification of initiating factors or processes in pathogenesis.

1.2.3.2 Identifying expanded Antibody Species forming distinct OCBs in CSF

To overcome the shortcomings of previous antigen identification strategies, a new method to identify, characterize and clone distinct OCB-antibodies from CSF was established by B. Obermeier [100]. The overall workflow is illustrated in Figure 1-8. This method allows the correlation of expanded H- and L-chains that form a distinct OCB in a patient sample and thereby enables in depth analysis of its antigen specificity.

CSF from MS patients is separated into its cellular and soluble components and both fractions are analyzed individually. In a first step, IgG-molecules are collected by protein G affinity-chromatography and deglycosylated to reduce sample complexity. The antibodies are then separated based on their isoelectric point by IEF followed by classical polyacrylamide gel electrophoresis (PAGE) separation. All experimental procedures are run under strictly non-reducing conditions to preserve disulphide bridges between the individual chains and thereby ensure the parallel purification of matching H- and L-chains. Staining with Coomassie brilliant blue reveals a number of distinct spots that each represent IgG H_2L_2 complexes. Such spots are selected for subsequent mass spectrometric analysis.

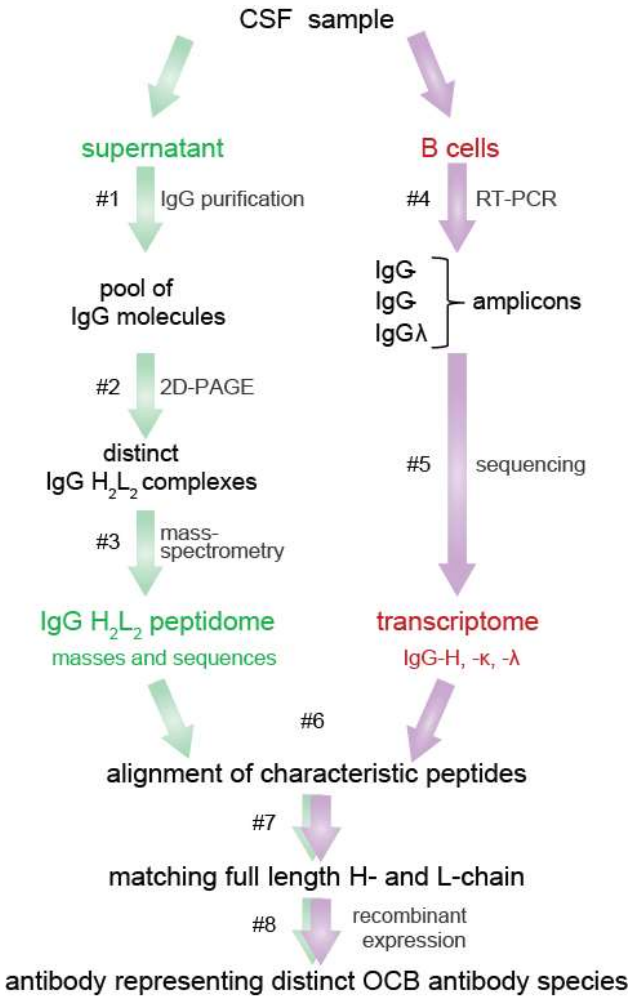

Figure 1-8: Workflow to identify matching H- and L-chains of OCB-antibodies from CSF.

The method is based on parallel analysis of the IgG-transcriptome of CNS-resident B-cells and the IgG-proteome of the CSF sample. IgG-molecules are isolated by protein G affinity chromatography and deglycosylated (#1). The antibody population is separated according to the isoelectric point of the molecules by IEF that yields bands with concentrated biochemically highly similar antibody species. In a second dimension, the antibodies are separated based on their MW by SDS-PAGE (#2). This separates free H- and L-chains and incomplete heterodimers from the full length IgG molecules of interest. These are isolated from the gel, analyzed by mass spectrometry (#3). The IgG-repertoire is analyzed in parallel. mRNA is obtained and transcribed into cDNA followed by nested PCR on IgG H- and L-chains (#4). The IgG-transcriptome is determined by either Sanger sequencing or next generation sequencing (#5) and peptide fragments are aligned to the full length sequences of H- and L-chains from the transcriptome (#6). This will yield full length sequences of matching H- and L-chains from an OCB-forming antibody (#7). The antibody is then recombinantly produced (#8) and applied in antigen search experiments. The illustration is adapted from [101].

Mass spectrometry allows the identification of a number of peptides from the expanded H- and L-chains. As in almost all mass-spectrometric experiments, the sequence coverage is not complete, i.e. full length sequences are not revealed. Therefore, the IgG-transcriptome of B-cells present in the CSF sample is analyzed in parallel. Following two rounds of nested PCR on IgG H- and L-chains, products are either sequenced by Sanger sequencing or by next generation sequencing. Both methods reveal full length sequences of the entire IgG H- and L-chain repertoire in CSF of a patient. The peptides detected by mass spectrometry are then aligned to the full length sequences from transcriptome analysis and this allows the definite identification of an expanded antibody species. The alignments are highly patient-specific due to somatic hypermutations and CDRs. The matching H- and L-chain are then recombinantly expressed in human embryonic kidney (HEK293E) cells. The substantial amounts of antibody obtained by recombinant expression enable the search for antigen structures of distinct OCB-derived antibodies.

In contrast to earlier efforts to identify target antigens of OCB-antibodies, this method ensures that the studied antibodies represent a truly expanded antibody species from a patient. Using this method, B. Obermeier identified five distinct OCB-derived antibodies applicable for antigen searches. OCB-derived antibodies were expressed as F_{ab}-fragments at first and used in initial antigen search experiments [100, 102], which however did not yield consistent results. Additionally, an MS-OCB-derived antibody was studied here with regard to its antigen specificity that represented a monoclonal antibody expansion in an MS patient [99].

1.3 Pathogenesis of $GABA_AR$-encephalitis

In contrast to the chronic inflammation of the CNS observed in MS, acute forms of encephalitis exist. Viral and bacterial encephalitides are most commonly encountered, but autoimmune conditions can also cause acute inflammation of the CNS [103].

Such autoimmune encephalitides have come into focus in recent years. A number of neurologic syndromes are associated with antibodies, mainly of the IgG-isotype. They target neuronal cell surface and synaptic proteins, and the list of encephalitogenic antibodies continually expands [104]. Those antibodies in serum and CSF may target the N-methyl-D-aspartate receptor (NMDAR, [36]), α-amino-3-hydroxy-5-methyl-4-isoxazolepropionic acid receptor (AMPAR, [105]), γ-aminobutyric acid-B receptor ($GABA_BR$, [106]) and receptor associated proteins such as the leucine-rich glioma inactivated protein 1 (LGI1) and contactin-associated protein-like 2 (CASPR2) [107]. In all cases, the condition is probably caused by an autoimmune reaction and some of these syndromes may be associated with malignancies [108]. In such paraneoplastic syndromes, symptoms arise from the host's immune response to a malignancy anywhere in the body [109].

A prominent example of a paraneoplastic syndrome is NMDAR-encephalitis, which seems to be triggered by ovarian teratoma expressing neuronal antigens including NMDAR [36]. The precise molecular mechanisms of paraneoplastic syndromes however remain unclear [110].

Most recently, $GABA_AR$-encephalitis was identified as a new form of autoimmune encephalitis. This severe form of encephalitis causes seizures and refractory *status epilepticus*. Antibodies from CSF and serum of $GABA_AR$-encephalitis patients recognize synaptic $GABA_AR$ and were found to substantially downregulate the number of receptors on the cell surface [111]. Similarly, a loss of $GABA_AR$ surface expression was observed in *status epilepticus* of other causes [112]. $GABA_AR$ is a ligand-gated ion channel that exerts inhibitory effects on neurotransmission. In most cases, binding of the neurotransmitter γ-aminobutyric acid (GABA) triggers a net influx of chloride into neurons by opening the chloride selective channel via a conformational switch mechanism [113]. The hyperpolarization raises the threshold for excitatory signals and thereby inhibits action potentials.

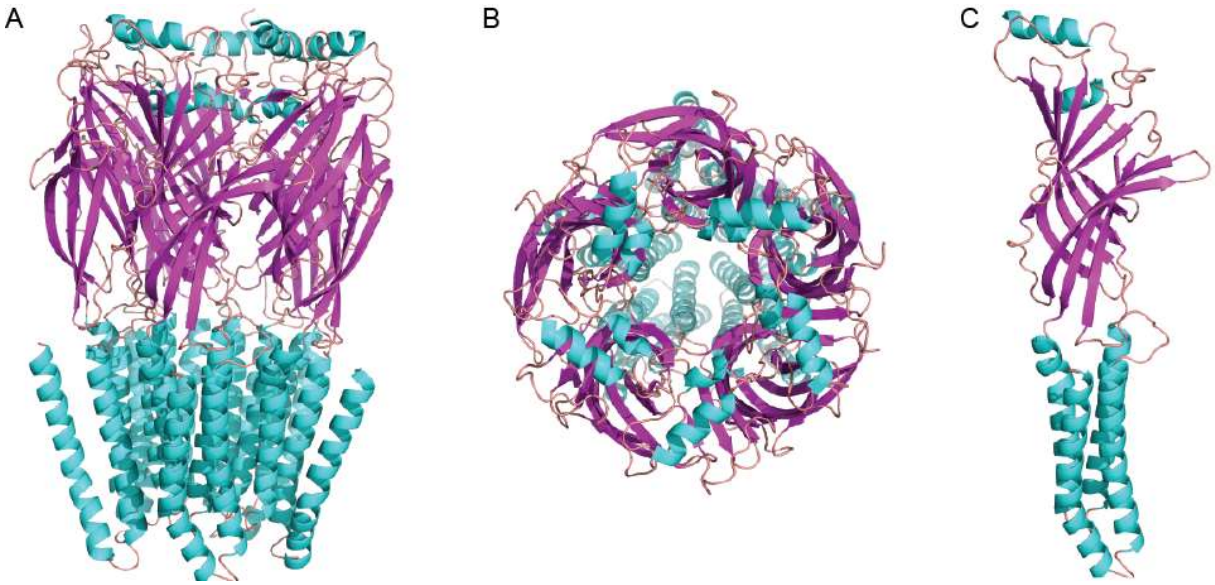

Figure 1-9: Ribbon-diagram of a $GABA_AR$ β3 homopentamer.

The fully assembled $GABA_AR$ β3 consist of five identical subunits anchored to the plasma membrane. Correctly arranged subunits form a channel that selectively allows chloride-ions to pass once the receptor is activated. (A and B). Each subunit is anchored to the plasmamembrane with 4 transmembrane helices (cyan), consisting of the 200-250 N-terminal AA. The extracellular domain mainly consists of β-sheets (magenta) (C). This illustration of PDB 4COF is modified from [114].

The receptor may form a pentameric structure using a variety of subunits from the pool of six α-, three β-, γ- and ρ-, and single δ-, ε-, θ-, and π-subunits [115]. Mostly, heteropentamers are formed that contain two α- and two β-subunits along with one other subunit [116]. $GABA_AR$ is mainly found in the neuropil and cerebral cortex in the central neurvous system and the subunit composition crucially influences function [117]. Figure 1-9 depicts the $GABA_AR$ β3-homopentamer crystal structure as a model for heteropentameric equivalents. The extracellular domain of the receptor consists of the 200-250 N-terminal AA of each of the subunits. The subunits are anchored into the membrane via four α-helical transmembrane domains with an

intracellular loop between the third and fourth helix [118]. Besides its natural ligand GABA, $GABA_AR$ may be regulated by a number of other substances including general anaestetics and drugs to treat epilepsy, insomnia and anxiety [119]. Among other endogenous modulators, $GABA_AR$ was also found to be regulated by zinc ions [120].

The number of patients with $GABA_AR$-encephalitis is small and so far a mainly non-paraneoplastic autoimmune cause is assumed [111]; however a fraction of these patients was found to present with thymoma [121, 122].

1.3.1 Identification of systemic Antigens of a $GABA_AR$-encephalitis related Antibody

$GABA_AR$-encephalitis was described as a novel form of autoimmune non-paraneoplastic encephalitis in a series of essentially six patients [111]. By definition, paraneoplastic syndromes are associated with any kind of malignancy, however it was found that in the majority of cases neurologic symptoms occur prior to cancer diagnosis [123, 124]. In some cases the underlying malignancies are small or possibly undetectable [34], thus the apparent absence of a malignancy does not exclude a possible paraneoplastic syndrome. This led to investigate potential cross-reactivity of an antibody targeting the $GABA_AR$ α1-subunit with other proteins, which might possibly be related to malignancy. The antibody used for these experiments was identified from the IgG repertoire of B-cells found in CSF of one of the index patients (Ip2) described by Petit-Pedrol et al. [111]. Using next generation sequencing, a single expanded antibody species was detected in this sample (E. Beltrán, unpublished data). This expanded antibody provided the basis for the search of a potential systemic antigen in $GABA_AR$-encephalitis that might possibly have initiated an immune response to $GABA_AR$ in a cross-reactive or paraneoplastic manner.

1.4 Objective

The aim of this study was to elucidate target antigens of expanded antibody species found in CSF of patients with CNS-disorders. The knowledge of target structures should help to understand the role of these antibodies in the pathogenesis of MS and $GABA_A$-receptor encephalitis.

So far, the involvement and role of OCB-antibodies in MS remains enigmatic. The major aim of this study was the identification of antigens of distinct OCBs, because knowledge of the targets of OCBs is likely to offer insights into their function in this disease. The recently established MS-OCB-derived recombinant antibodies are a particularly valuable tool to identify antigenic structures of expanded antibody species as they are the first antibodies which are unambiguously derived from distinct OCBs in CSF of MS patients. Identification of antigens of different distinct OCBs might disclose similarities and a common pattern may provide hints to a potential role of OCB antibodies in MS. Besides understanding the role of antibodies in MS, identification of antigens targeted at disease-onset may help to elucidate early processes leading to manifestation of the disease. In particular, the monoclonally expanded antibody found in CSF of patient MS2 at the time of first clinical signs of disease could identify target structures that play a role early in disease.

Previous antigen searches were carried out with OCB-derived F_{ab}-fragments but did not yield consistent results. Thus, OCB-derived full length antibodies were produced that form more stable antigen-antibody-complexes due to higher avidity and therefore may facilitate antigen identification. Protein microarrays were screened to identify candidate antigens, which subsequently were validated using independent methods such as immunoprecipitation, enzyme-linked immunosorbent assays and fluorescence microscopy.

In $GABA_A$-receptor encephalitis, the target structure in the CNS was known. Based on the assumption that $GABA_A$-receptor encephalitis might relate to paraneoplastic mechanisms, the aim was to identify a target antigen that possibly raised an anti-tumor immune response in the periphery. The monoclonally expanded antibody found in patient CSF that strongly reacted to the α1-subunit of the $GABA_A$-receptor, is used here to investigate this possibility. The reactivity of the recombinantly expressed antibody rAb-Ip2 to the $GABA_AR$ α–subunit was confirmed by enzyme-linked immunosorbent assay.

Using similar methods as mentioned above, rAb-Ip2 was tested for reactivity to proteins to identify potential cross-reactive antigens that may form the basis for a paraneoplastic neurologic syndrome in the patient.

2 Materials and Methods

2.1 Materials

All chemicals were purchased from Merck (Darmstadt), Sigma-Aldrich (Taufkirchen) or Qiagen (Hilden). Consumables were obtained from Biozym (Oldendorf), Eppendorf (Hamburg), Corning Incorporated (New York, USA), Millipore (Schwalbach) and Nunc (Langenselbold). Manufacturers other than those stated above are mentioned in the respective sections.

2.1.1 Patient Material

Patient material MS1 used in this study was provided by the Institute of Clinical Neuroimmunology, LMU Munich (T. Kümpfel). The sample was taken at first diagnosis. All other samples from different neurological conditions were provided by the Clinic of Neurology, University of Ulm (M. Senel). Informed consent was obtained from all patients. The study was approved by the Institutional Review Boards of the Ludwig-Maximilians-University Munich and the University of Ulm. Table 2-1 summarizes the demographic data and basic CSF findings of patient material used in this study.

Table 2-1: Demographic Data on Samples used for antigen-reactivity Screening in larger Patient Cohorts.

The cohort included patients with multiple sclerosis (MS), other inflammatory disorders (OID), neuroborreliosis (NB), cranial nerve palsies (CNP) and non-inflammatory neurologic disorders (NIND). The first column shows the number of cases per disease entity and distribution of sexes. The following columns show the mean age at sampling, mean cell count and IgG-content of the CSF samples, mean IgG-content of the serum samples and the range of each parameter within one group. The last column gives the percentage of OCB-positive patients.

	N (Male/ Female)	Age (Years)	CSF cell # (/µl)	CSF IgG (mg/l)	Serum IgG (g/l)	OCB (%)
MS	20 (8/12)	44 (30-48)	2 (1-3)	39.3 (35.5-49)	10.9 (9.75-11.7)	16 of 20 (80.0)
OID	7 (4/3)	53 (39-72)	1360 (107-3000)	317 (210-1370)	6.7 (5-14.5)	1 of 7 (14.3)
NB	13 (9/4)	41 (25-64)	103 (57-190)	167 (132-313)	10 (9.1-11.3)	12 of 13 (92.3)
CNP	8 (5/8)	54 (45-67)	2 (1-2)	30.8 (25.3-49.7)	10.9 (9.4-12.2)	0 of 8 (0)
NIND	17 (11/6)	55 (49-67)	1 (0-1)	21.9 (15.9-25.3)	10.5 (8.27-11.5)	0 of 17 (0)

2.1.2 General Equipment

Table 2-2: List of General Equipment in use

Purpose	Device	Source
Autoclave	Varioklav Classic 500	H+P Labortechnik, Oberschleißheim, Germany
Bunsen burner	Fireboy eco	Integra Bioscience, Fernwald, Germany
CD-spectrometer	J-715	Jasco, Gross-Umstadt, Germany
Cell count	Neubauer improved counting chamber	Carl Roth, Karlsruhe, Germany
Centrifugation	Benchtop centrifuge 5417 R	Eppendorf, Hamburg, Germany
	Sorvall RC-5C Plus	Thermo Fisher Scientific, Waltham, MA, USA

Purpose	Device	Source
Centrifugation (cont.)	Megafuge1.0 R	Heraeus, Hanau, Germany
	Ultracentrifuge Optima L90K	Beckman Coulter, Brea, CA, USA
Gelelectrophoresis	Electro blotting chamber	In-house workshop
	XCell SureLock™ Mini-Cell	Invitrogen, Darmstadt, Germany
	Agarose gels	In-house workshop
ELISA reader	Victor 2 1420 multilabel counter	Perkin Elmer, Waltham, MA, USA
Flow cytometry	FACSverse	Becton Dickinson, Heidelberg, Germany
FPLC-System	LCC 501 Plus	Amersham Farmacia (GE Healthcare), Solingen, Germany
	UV-detector Uvicord SD	
Incubation	HT Multitron Standard	Infors HT, Basel, Switzerland
	Thermotron	Thermo Fisher Scientific
	Heratherm	
Gel documentation	Molecular imager Gel doc™ XR	Bio-Rad, München, Germany
	QuantityOne Basic Software	
	Perfection 4990 Photo	Epson, Meerbusch, Germany
Heating	Thermomixer comfort 5436	Eppendorf
	Waterbath MA6	Lauda, Lauda-Königshofen, Germany
Ice machine	Scotsman AF30	Scotsman, Suffolk, UK
Mass spectrometry	Proteomics Analyzer 4700 or 4800 MALDI-TOF/TOF	AB Sciex, Darmstadt, Germany
Microarray Scanning	GenePix 4000B	Axon Instruments, Union City, CA, USA
Microscopy	AxioVert 200M	Carl Zeiss, Jena, Germany
	Wilovert®	Will, Wetzlar, Germany
Microwave	-	Privileg, Stuttgart, Germany
Mixing	Vortex Genie 2	Scientific Industries, New York, NJ, USA
Concentration determination	NanoDrop® ND-1000 Spectrophotometer	PeqLab, Erlangen, Germany
PCR	GeneAMP® PCR system 9600	Perkin Elmer
	T personal Thermocycler	Biometra, Göttingen, Germany
pH-meter	pH521	Bruno Kummer, Freiburg, Germany
	Pipetboy acu	Integra Bioscience
	Gilson Pipetman® P	Gilson, Middleton, WI, USA
Power supply	EPS 400/500	Amersham Farmacia
	EPS 2A200	
Rotors	JA-10	Beckman Coulter
	JA25.50	
	70Ti	Beckman Coulter
Shaker	Duomax 1030	Heidolph Instruments, Schwabach, Germany
	Unimax 2010	
Sonification	Sonifier 450	Branson, Geneva, Switzerland
Sterile workbench	Lamin Air®	Heraeus
Stirring	Ikamag RCT magnetic stirrer	IKA, Staufen, Germany
UV-transillumination	UV-Transilluminator 312 nm	Bachofer Laborgeräte, Reutlingen, Germany
Water purification	Milli-Q Advantage	Millipore, Schwalbach , Germany
Weighing	Analytical balance 2001 MP2	Sartorius, Göttingen, Germany
	Precision balance L2200P	
Western blot detection	OPTIMAX®	Protec, Oberstenfeld, Germany
	GE Imager 4000	GE Healthcare,
	Odyssey Fc	LI-COR, Bad Homburg, Germany

2.1.3 General Buffers and Reagents

Table 2-3: List of generally used Buffers

Name	Composition	Use
PBS pH 7.4	150 mM NaCl 8.4 mM Na_2HPO_4 1.9 mM NaH_2PO_4 x H_2O	Protein biochemistry
PBS-T	1x PBS 0.05 % (w/v), Tween-20	Washing buffer
SDS Running buffer Tris-Glycine	0.1 % (w/v) SDS, 0.02 M tris, 0.2 M glycine	run Tris-Glycin SDS-PAGE
SDS Running buffer Bis-Tris	50 mM MOPS, 50 mM tris base, 0.1 % SDS, 1 mM EDTA	run Bis-Tris SDS-PAGE
reducing SDS sample buffer (3x)	0.15 M tris-HCl pH6.8, 7.5 % (w/v) SDS, 45 % (w/v) glycerol, 0.01 % (w/v) bromphenol blue, 6 % (v/v) β-mercaptoethanol	reducing SDS-PAGE
non-reducing SDS sample buffer (5x)	0.2 M tris-HCl pH6.8, 7.5 % (w/v) SDS, 20 % (w/v) glycerol, 0.02 % (w/v) bromphenol blue	non-reducing SDS-PAGE
anode buffer	50 mM boric acid 20 % methanol in H_2O, pH9	Western blotting
cathode buffer	50 mM boric acid 5 % methanol in H_2O, pH9	Western blotting
ECL A	0.25 % (w/v) luminol in 1 M tris pH8.6	membrane development
ECL B	0.11 % (w/v) para-hydroxycoumaric acid in DMSO	membrane development
trypan blue (0.1 %)	0.4 % trypan blue solution 1:4 in 1x PBS	cell counting
LB-medium	1 % (w/v) NaCl 0,5 % (w/v) Bacto™ Yeast Extract 1 % (w/v) Bacto™ Tryptone, pH 7	bacterial cultures
DNA sample buffer (6x)	50 % (v/v) glycerol, 0,02 % (w/v) bromphenol blue, 0,02 % (w/v) xylene cyanole, 10 mM tris-HCl, pH7.5	agarose gels
TBE-buffer (10x)	0.89 M tris, 0.89 M boric acid, 0.02 M EDTA, pH 8	agarose gels

Table 2-4: List of generally used Reagents

Name	Use	Source
Nucleic acids 10 mM dNTPs	PCR reaction	Invitrogen
10x PCR buffer		Roche Diagnostics, Mannheim, Germany
Taq polymerase		
TMB substrate (1x)	ELISA detection	eBioscience

2.1.4 Restriction Enzymes

Table 2-5: List of Restriction Enzymes in use

Name	Manufacturer
*Bam*HI, *Bss*HII, *Kas*I, *Nco*I, *Nde*I, *Sac*II, *Sal*I, *Msc*I, *Bsu*36I	New England Biolabs

2.1.5 Primer

Primers were synthesized by Metabion (Martinsried) and delivered in 100 µM stock solutions. M13 sequencing primers were obtained from Invitrogen. AA exchanges introduced by the primer are printed in bold, restriction sites are underlined (Table 2-6 to Table 2-9).

Table 2-6: List of Primers for cloning FAM84Awt and FAM84A-mutants

Primer	Sequence
FAM84Awt *Bss*HII for	5′-CACAGGCGCGCGATGTGACATCCAGATGGGCAACCAACTGGACC-3′
FAM84Awt*Bam*HI V5/His_6 rev	5′-AGGGATCCTTAGTGGTGGTGGTGGTGGTGTTGTGAATCTAGTCCTAGTAG TGGATTTGGTATTGGTTTTCCCTCCTTATCGTCCACGAGG-3′
FAM84A *Nde*I for	5′-CACCCATATGGGCAACCAACTG-3′
FAM188VA *Msc*I rev	5′-ggAGGTGGCCACAGGCATTCTGCACCACCAGTTCGGC**CGC**CAGG-3′
FAM190EA *Msc*I rev	5′-taAGGTGGCCACAGGCATTCTGCACCACCAG**TGC**GGC-3′
FAM191LA *Msc*I rev	5′-AGGTGGCCACAGGCATTCTGCACCAC**CGC**TTCGG-3′
FAM84 *Msc*I for	5′-AATGCCTGTGGCCACCTGG-3′
FAM *Bsu*36I-for	5′-aACGCCTC**A**GGCAGACTGAG-3′
FAM323EA *Bsu*36I rev	5′-TCTGCCTGAGGCGTCGATCCGCCGCTTCTCGCGGATCAGATC**TGC**CAGGC -3′
FAM324DA *Bsu*36I rev	5′-TCTGCCTGAGGCGTCGATCCGCCGCTTCTCGCGGATCAG**AGC**TTCCAGGC -3′
FAM327RA *Bsu*36I rev	5′-TCTGCCTGAGGCGTCGATCCGCCGCTTCTC**GGC**GATC-3′
FAM328EA *Bsu*36I rev	5′-TCTGCCTGAGGCGTCGATCCGCCGCTT**CGC**GCGG-3′
FAM331RA *Bsu*36I rev	5′-TCTGCCTGAGGCGTCGAT**CGC**CCGC-3′

Table 2-7: Primers for cloning AKAP17A

Primer	Sequence
AKAP17A *Sac*II for	5′-GGCTCCGCGGTGGGTCCTGTCCATGGCAGCGGCTACCATC-3′
AKAP17A *Bam*HI/His_6 rev	5′-CAAGGATCCTTAATGGTGATGGTGATGGTGTCGGGAACGACAGACGAGC-3′
AKAP17A *Bam*HI/V5/His_6 rev	5′-CTAGGATCCTTAATGGTGATGGTGATGGTGGGTGCTGTCCAGGCCCAGCA GAGGATTAGGGATGGGCTTGCCTCGGGAACGACAGACGAGCGCTACAC-3′

Table 2-8: Primers for cloning GABAα1ex

Primer	Sequence
GABAα1ex *Nco*I for	5′-GAGCCATGGGGCAGCCGTCATTACAAGATGAAC-3′
GABAα1ex *Bam*HI/V5/His_6/*Bgl*II rev	5′-AAGAGATCTTTAATGGTGATGGTGATGGTGGGTGCTGTCCAGGCCCAGCA GAGGATTAGGGATGGGCTTGCCTCCTCCGGATCCGCCAATCTTTCTCTTC

	AAGTG-3′

Table 2-9: List of sequencing primers in use

Primer	Sequence
pTT5 forward	5´-CTTTCTCTCCACAGGTGTC-3´
pTT5 reverse	5´-CCTTCCGAGTGAGAGACAC-3´
M13 forward	5´-GTAAAACGACGGCGTC-3´
M13 reverse	5´-GAGGAAACAGCTATGAC-3´
T7 promotor	5´-TAATACGACTCACTATAGGG-3´
T7 terminator	5´-GCTAGTTATTGCTCAGCGG-3´

2.1.6 Vectors

Table 2-10: List of Vectors

Name	Resistance gene	Size	Description	Source
pET19b	amp^R,	5.7 kb	expression vector	Novagene
pET33b(+)	kan^R	5.4 kb	expression vector	Novagene
pCR®2.1-TOPO®	amp^R, kan^R	3.9 kb	TOPO-TA cloning	Invitrogen
pQE30	amp^R	3.4 kb	expression vector	Qiagen
pTT5	amp^R	4.4 kb	expression vector	Yves Durocher, NRC Biotechnology Research Institute

2.1.7 Bacterial Strains

Table 2-11: List of Bacterial Strains

Name	Genotype	Source
E. coli TOP10	F- *mcr*A Δ(*mrr-hsd*RMS-*mcr*BC) φ80*lac*ZΔM15 Δ*lac*X74 *deo*R *rec*A1 *end*A1*ara*Δ139 Δ(*ara, leu*) 7697 *gal*U *gal*K λ- *rps*L(StrR) *nup*G	One Shot® TOP 10 Chemically Competent Cells (Invitrogen)
E. coli BL21-Star™-DE3	F- *omp*T *hsd*SB (rB-mB-) *gal dcm rne*131(DE3)	Invitrogen

2.1.8 Cell Line

Table 2-12: Cell Line in Use

Name	Description	Source
HEK293E Large Scale Transient Expression System	human embryonic kidney cell line, G418-resistence	D. Jenne (Yves Durocher NRC Biotechnology Research Institute)

2.1.9 Antibodies

Table 2-13: List of Primary Antibodies

Name	reactivity	use	dilution used	conjugate	host	source
α-V5-HRP	V5-tag	WB, ELISA	1:5 000-1:10 000	HRP	mouse	LifeTechnologies
α-V5	V5-tag	ELISA		---	rabbit	Millipore
α-His_6-HRP	His_6-tag	WB, ELISA	1:1 000 1:2 000	HRP	mouse	SigmaAldrich

mono α-DDK	DDK-tag	WB	1:2 000	---	mouse	Origene
poly α-AKAP17A	human AKAP17A	IP, WB	1:2 000	---	rabbit	MyBioSource
mono α-AKAP17A	human AKAP17A	IP, WB	1:1 000	---	mouse	Biorad
poly α-FAM84A	human FAM84A	IP, WB, ELISA	1:2 000	---	rabbit	ThermoScientific
mono α-FAM84A	human FAM84A	IP, WB, ELISA	1:1 000	---	mouse	abcam
poly α-MKNK1	human MKNK1	ELISA	1:1 000	---	rabbit	ThermoScientific
mono α-MKNK1	human MKNK1	ELISA	1:1 000	---	mouse	abcam
poly α-$GABA_AR$	human $GABA_AR$ α1-subunit	ELISA	1:175		rabbit	abcam

Table 2-14: List of Secondary Antibodies

Name	Reactivity	Use	Dilution used	Conjugate	Host	Scource
α-mouse HRP	Mouse IgG heavy + light chain	WB	1:5 000	HRP	Rabbit	LifeTechnologies
α-rabbit HRP	rabbit IgG heavy + light chain	WB	1:10 000	HRP	Donkey	abcam
α-rabbit IgG Fc HRP	Rabbit IgG Fc	ELISA	1:50 000	HRP	goat	AbD Serotec
α-human IgG-HRP	human IgG Fc region	WB, ELISA	1:1 000	HRP	Mouse	Invitrogen
α-human IgG HRP	human IgG heavy + light chain	WB, ELISA	1: 10 000	HRP	goat	Invitrogen

2.1.10 Proteins

Table 2-15: List of commercially obtained Proteins

Short name	Full name	UniProt #	~ MW [kDa]	Scource	Manufacturer
MKNK1	MAP kinase-interacting kinase 1	Q9BUB5-1	51	HEK	Origene
FAM20B	Family with sequence similarity 20 B	O75063	44	CHO	R&D Systems
CHD2	Chromodomain helicase DNA binding protein 2	O14647	81	Wheat germ	Abnova
MAPK7	Mitogen-activated protein kinase 7	Q13164	88	HEK	Origene
CRIP2	Cystein-rich protein 2	P52943	22	HEK	Origene
CSRP2	Cysteine- and glycine-rich protein 2	P16527	21	HEK	Origene

2.2 Molecular Cloning and Microbiological Methods

Molecular cloning techniques in cooperation with microbiological methods allow rapid production and amplification of desired DNA-constructs. The following sections describe the individual steps that are necessary to construct expression vectors that allow the production of large amounts of recombinant target proteins.

2.2.1 Polymerase Chain Reaction (PCR)

Amplification of certain DNA-sequence and their modification are basic applications of the PCR-technique. When preparing expression vectors, this method is used to introduce restriction sites to the gene of interest, to introduce mutations at a specific site or to determine if the desired sequence is present. The basic parameters and reaction mix setup is listed in detail in Table 2-16. Elongation times were adjusted to the target sequence, 1 min elongation time is allowed per 1 000 bp fragment length.

Table 2-16: Basic PCR Reaction Mix and Parameters

basic reaction mix
1X PCR buffer (Roche)
200 µM dNTP-Mix
0.5 µM forward primer
0.5 µM reverse primer
5 U *Taq* DNA-polymerase
100 ng DNA matrix
ad 50 µl dH_2O

basic PCR parameters			
Function	**Temperature**	**Time**	
initial denaturation	94 °C	3 min	
denaturation	94 °C	1 min	25-40 cycles
hybridization	55 °C	1 min	
elongation	72 °C	1.5 min	
final elongation	72 °C	10 min	
	4 °C	∞	

2.2.1.1 Bacterial Colony Screening

Material from single colonies of freshly transformed bacteria was directly used to screen for the gene of interest. The PCR-mix was set up in 20 µl reaction volume and colony material transferred to the reaction tube. The reaction was carried out over 25 cycles with 55 °C annealing temperature using 1 U of *Taq* polymerase.

2.2.1.2 *In vitro* PCR-Mutagenesis

To analyze binding characteristics of antibody-antigen-complexes, *in vitro* PCR mutagenesis was applied to introduce single AA exchanges at specific sites in the candidate antigen nucleotide sequence. Primers were complementary to the target sequence with few desired nucleotide exchanges that induce AA mutations. Additionally, these primers contain restriction sites that allow easy integration of the PCR-product into the target vector. Constructs obtained by PCR mutagenesis are described in detail in section 2.2.11.

2.2.2 Isolation of Plasmid-DNA

Plasmid DNA was recovered from bacterial cultures using either the QIAprep Spin Miniprep Kit or the QIAGEN Plasmid Maxi kit, depending on the culture volume. Purification was done according to the manufacturer's instructions, with elution volumes of 35 µl or 200 µl elution buffer respectively.

DNA-fragments were purified from PCR mixes and agarose gels using the QIAquick Kit or QIAgen MinElute and were eluted in 12 µl or 30 µl of elution buffer respectively.

2.2.3 Agarose Gelelectrophoresis

DNA-fragments were separated based on their size using agarose gel electrophoresis. Agarose gels were casted at concentrations of 1-2 % agarose in TBE buffer, to allow optimal separation of the specific fragments. Samples in sample buffer and DNA standard are loaded to the gel and the electric field is applied at 90 V. Addition of 0.5 µg/ml final concentration of ethidium bromide to the TBE-buffer enables detection of DNA-bands with UV-light at 312 nm wavelength. In case of preparative agarose gels, the DNA-bands of interest were cut out of the gel and purified using the QIAquick Kit as described in section 2.2.2.

2.2.4 DNA Digestion using Endonucleases

Restriction enzymes recognize specific nucleotide sequences and cut these by a particular pattern. This yields DNA-fragments with compatible ends which are exploited when ligating insert and vector. The restriction enzymes used in this study are listed in Table 2-5. All restriction digests were carried out in the buffer recommended by the manufacturer, using the appropriate amount of enzyme units. Mostly, double digests were possible, however, in case of contiguous recognition sites or incompatible digestion buffers sequential digests were carried out. If so, the first restriction enzyme was heat inactivated or the buffer exchanged using the MinElute PCR Purification Kit prior to the second digestion step. Digestions were carried out overnight at the optimal temperature of the restriction enzyme in use.

2.2.5 DNA Ligation

Prior to ligation of insert and vector, the vector was dephosphorylated to prevent its self-ligation. Up to 1 µg of vector DNA was dephosphorylated using rAPid alkaline phosphatase (Roche) in a reaction volume of 20 µl for 15 min at 37 °C. The phosphatase was inactivated by incubation for 2 min at 75 °C before proceeding to ligation.

T4 DNA-ligase (Invitrogen) was used to ligate vector- and insert-DNA. 100 ng of open, dephosphorylated vector and 4-times molar excess of insert were incubated in 20 µl reaction volume overnight at 16 °C. Ligated vector-insert-constructs were transformed to chemically competent *E. coli* bacteria as described in section 2.2.12.

2.2.6 TOPO-TA Cloning

The TOPO-TA cloning kit allows direct integration of a PCR product into the pCR®2.1-TOPO® vector (LifeTechnologies). Amplification of DNA using *Taq* polymerase yields PCR products containing 3' adenine overhangs which allow hybridization of the fragment to the thymidine overhang of the linearized vector of the cloning kit. DNA-fragments were cloned into the vector as described by the manufacturer and subsequently transformed into chemically competent OneShot® TOP10 *E. coli* (section 2.2.12).

2.2.7 DNA Quantification

DNA-concentration was determined using either absorbance of UV light at 260 nm wavelength or by comparison with standard amounts of ethidium bromide stained bands in agarose gels. UV-absorbance was measured using the ND1000 spectrophotometer according to the manufacturer's instructions. DNA bands in agarose gels were stained during the separation process by including ethidium bromide in the running buffer as described in section 2.2.3.

2.2.8 DNA Sequencing

To confirm the identity of a sequence, samples were sent for Sanger-sequencing at the "LMU Genetics Sequencing Service". Primers used for sequencing reactions are listed in Table 2-7. Results were analyzed and edited using "Chromas Lite Version 2.01".

2.2.9 Cloning of full length recombinant Antibodies

To recombinantly express proteins in a eukaryotic system, the pTT5 vector was chosen as it is well suited for production of secreted proteins by the HEK293E system [125]. Plasmids are propagated in the cells via their EBV latency origin of replication (oriP) thereby increasing the total number of plasmids throughout the expression period. Furthermore, the human cytomegalovirus promotor (pCMV) encoded on the plasmid, in cooperation with the trans-activating adenoviral protein E1a that is constitutively expressed in the HEK293E cells, ensures high expression rates of recombinant proteins [126].

Table 2-17 lists the patient-derived recombinantly produced antibodies used in the present study, deviant original naming and their source.

Table 2-17: List of recombinantly produced Antibodies from Patient CSF.

The first column gives the name of the antibody used throughout this work, followed by the according nomenclature in the original publication and the source.

antibody	original nomenclature	source
rOCB-MS3-s1	Fab-1039-s1	Obermeier [100]
rOCB-MS1-s8	Fab-HM-63-s8	
rOCB-MS1-s9	Fab-HM-63-s9	
rOCB-MS4	Fab-NS-52	
rOCB-MS1-s2	Fab-HM-63-s2	
r8-18C5	8-18C5	Obermeier [100], Linington [127]
rOCB-MS2-s5	Fab7/AB7	Brändle [99]
rAb-Ip2	---	E. Beltrán (unpublished data)

Cloning of a full length IgG1-molecule from OCB-derived antibody H- and L-chains was described in detail in the preceding master's thesis [99]. The construct obtained from this prior study was subsequently used to transform all previously cloned F_{ab}-fragments of OCB-derived antibodies [100] into full length antibody constructs with IgG1 backbone. Additionally, the humanized F_{ab}-fragment [100] of the mouse myelin oligodendrocyte glycoprotein (MOG)–specific antibody 8-18C5 [127] was cloned into a full length construct. The Ab-Ip2 was cloned into the full length pTT5-construct accordingly.

The heavy chain variable regions of the five previously existing OCB-derived F_{ab}-fragments were cut out of the existing F_{ab}-encoding pTT5 H-chain vectors by *Sal*I and *Sac*II. The original full length rOCB-MS2-s5 H-chain vector was linearized using the same restriction enzymes and variable regions were ligated into the open vector. The light chain constructs remained unchanged (Figure 2-1).

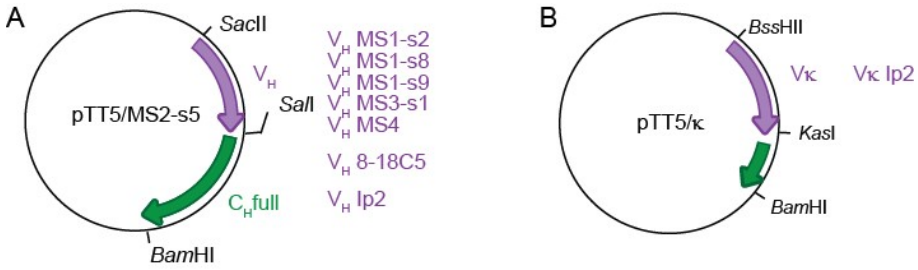

Figure 2-1: Schematic of the cloning strategy used to obtain full length antibody constructs.

The pTT5/MS2-s5-construct encodes the full length H-chain of rOCB-MS2-s5. The vector was opened using *Sac*II and *Sal*I restriction sites. H-chain variable regions (VH) of MS-derived antibodies rAb-MS1-s2, -MS1-s8, -MS1-s9, -MS3-s1, -MS4 and the MOG-specific r8-18C5 were cut from F_{ab}-coding vectors using the same sites. VH of rAb-Ip2 was obtained by PCR (A). The pTT5-constructs coding for L-chains remained unchanged in case of MS-derived antibodies and r8-18C5. The L-chain variable region (Vκ) of rAb-Ip2 was obtained by PCR and inserted into the pTT5/κ-vector via *Bss*HII and *Bam*HI restriction sites.

The sequences of the variable regions of the H- and L-chains of an expanded antibody from CSF of a $GABA_AR$-encephalitis patient were extended by *Sac*II and *Sal*I restriction sites (H-chain, Figure 2-1A) and *Bss*HII and *Kas*I (L-chain, Figure 2-1B) respectively. PCR-products were then introduced in the full length pTT5 H- or L-chain-vector using these restriction sites (in cooperation with E. Beltrán). All antibodies were cloned in two variants, with and without C-terminal V5-tag. The V5-tag was a useful tool to detect reactivity in protein microarray experiments, whereas some validation assays required the absence of this tag. The amino acid sequences of all recombinant antibodies are included in the appendix.

2.2.10 Cloning of single chain variable Fragment (scF_v)

For rOCB-MS2-s5, recombinant expression in HEK293E cells was not possible as previously described in the master's thesis. Alternatively, this OCB-derived antibody was produced in *E. coli* using the pET19-vector system. The vector carries the T7 promotor and terminator sequence, which allows for recombinant production in bacterial strains expressing T7 RNA polymerase. The

intrinsic His_6-tag, enteropeptidase coding sequence and Proteinkinase A recognition site of the vector were not employed here. C-terminal V5- and His_6-tags were introduced by PCR.

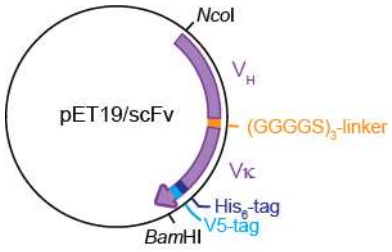

Figure 2-2: Schematic illustration of the scFv- MS2-s5-construct.

The N-terminal V_H region was linked to the V_K region by a triple glycine linker. The His_6- and V5-tags form the C-terminus of the construct. The gene-construct was purchased from GeneArt and inserted into the pET19-vector via the *Nco*I and *Bam*HI restriction sites.

rOCB-MS2-s5 was cloned as single chain variable fragment (scF_v). Recombinant expression of proteins often creates protein aggregates that need to be refolded in order to be active. However, refolding large multi-domain proteins is complicated, thus a minimized format of the antibody was constructed. This construct contains the variable regions of H- (N-terminal) and L- (C-terminal) chain, connected by a flexible triple glycine linker (GGGGS). These small molecules are easily refolded and thereby better suited for prokaryotic expression [128]. The scF_v-construct was C-terminally tagged with V5 and His_6. The construct was obtained from GeneArt® (LifeTechnologies) and inserted in the pET19 expression vector via *Nco*I and *Bam*HI restriction sites. The amino acid sequence of scFv-MS2-s5 is included in the appendix.

2.2.11 Cloning of Candidate Antigens

Candidate antigens were cloned for recombinant expression to obtain large amounts of protein to independently validate antibody-antigen recognition. Apart from AKAP17A, candidate antigens were expressed in *E. coli*. All constructs were C-terminally His_6-and V5-tagged. In addition, an AKAP17A-construct without V5-tag was used.

2.2.11.1 FAM84A

The FAM84A-gene (UniProt: Q96KN4-1) was codon-optimized and synthesized with *Bss*HI and *Bam*HI restriction sites by GeneArt® (LifeTechnologies). The construct was cloned into the pTT5 vector and used for eukaryotic expression. Additionally, the *Nde*I restriction site was introduced at the 3'-end by PCR that allows for directed insertion of the FAM84A-gene into the pET33b(+)-vector via *Nde*I and *Bam*HI. Both constructs were C-terminally tagged with V5 and His_6-tags.

Additionally, single alanine exchanges were introduced into the FAM84A-gene by PCR mutagenesis. Alanine is the second smallest AA and does not feature distinguished characteristics and therefore does in most cases not influence the overall properties of the protein, particularly its folding behavior. Mutations to be inserted were located at two distinct sites of the gene and therefore demanded for two individual cloning strategies. To mutate AA188, AA190 and AA191 to alanine, the existing *Nde*I and *Msc*I restriction sites were used. To exchange AA263, AA264, AA267, AA268 and AA271 with alanine, the *Msc*I restriction site was used and a *Bsu*36I motif, which was newly introduced. Reverse primers contained nucleotide

mismatches that encoded the individual AA-exchange and the *Msc*I or *Bsu*36I site respectively. All primers used to obtain the wild type and mutant sequences are listed in Table 2-6.

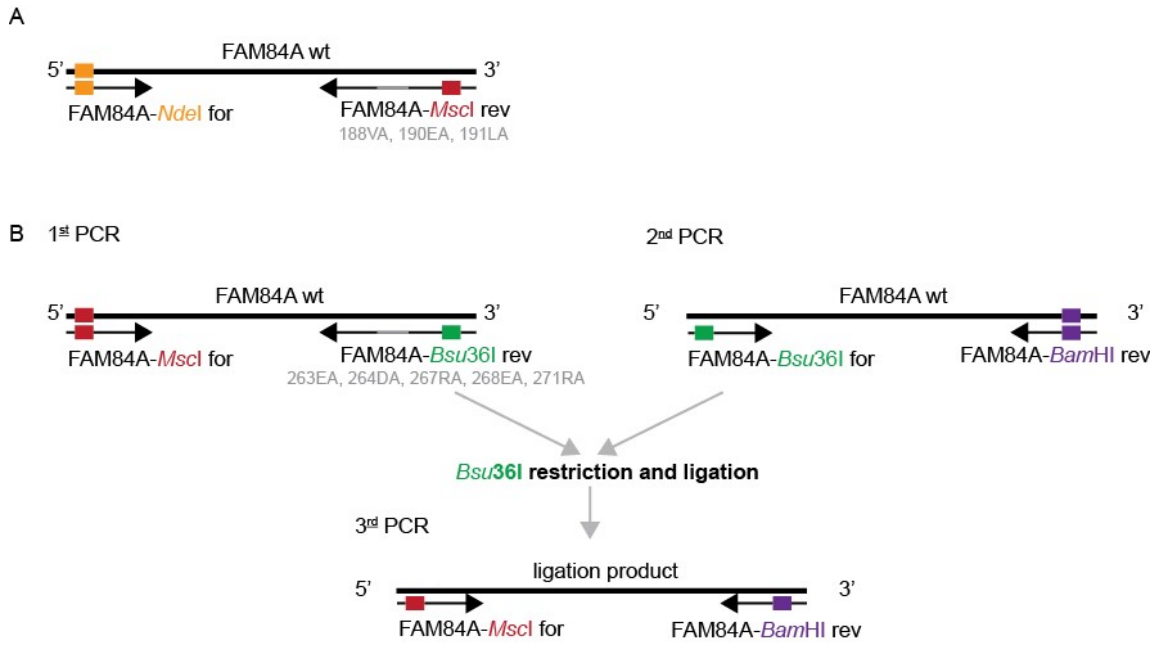

Figure 2-3: Cloning Strategy for FAM84A Mutagenesis.

Mutations at AA188, 190 and 191 were introduced via PCR with the FAM84A-*Nde*I for Primer and FAM84A-*Msc*I rev Primers coding for the respective AA exchange (A). To introduce mutations at AA 263, 263, 267, 268, and 271, a two-step strategy was applied. AA exchanges were introduced in a first PCR on the FAM84A wild type (wt) sequence using FAM84A-*Msc*I for primers and FAM84A-*Bsu*36I rev primers that carry the nucleotide mismatches for the mutations. A second PCR using FAM84A-*Bsu*36I for and FAM84A-*Bam*HI rev primers introduced the *Bsu*36I restriction site. The two PCR products were digested with *Bsu*36I and then ligated. The ligation product was used as template for a third PCR with FAM84A-*Msc*I for and FAM84A-*Bam*HI rev primers. The resulting PCR products carrying single AA exchanges were digested with *Msc*I and *Bam*HI and replaced the wt FAM84A 3' end.

2.2.11.2 AKAP17A

AKAP17A (UniProt: Q02040-3) had previously been cloned [102] into the pQE30 vector via *Bam*HI and *Sal*I for prokaryotic expression. For expression in the HEK293E system, AKAP17A was equipped with a signal peptide, *Sac*II und *Bam*HI restriction sites and inserted into the pTT5-vector. Furthermore, AKAP17A was cloned in two variants with and without C-terminal V5-tag. Primer sequences are listed in Table 2-7.

2.2.11.3 $GABA_AR\alpha1ex$

In this study, the soluble extracellular domain of the $GABA_AR$ α1-subunit ($GABA_AR\alpha1ex$) was used. The nucleotide triplets coding for extracellularly localized AAs of the α1-subunit of the $GABA_A$-receptor (UniProt: P14867-1) were deduced. The sequence stretch entailing AA28-251 of the full length protein was selected for recombinant expression.

The transmembrane domain was replaced by C-terminal V5- and His_6-tags using PCR mutagenesis. The protein-coding sequence was further modified to carry a 5' *Nco*I restriction site

that allows directional insertion of the construct into the pET33b(+)-vector via *Nco*I and *Bam*HI restriction sites. The pET33b(+)-system allows prokaryotic expression. Primers to introduce specific restriction sites and tags in the $GABA_AR\alpha1$ex-sequence are listed in Table 2-8.

2.2.12 Transformation of chemically competent *E. coli*

Chemically competent *E. coli* strains OneShot® TOP10 and BL21 strain were transformed with protein-coding vectors by heat shock. Both bacterial strains were thawed on ice and incubated with 1-2 µl of plasmid for 30 min on ice. Subsequently, bacteria were heat shocked for 30 s at 42 °C and then quickly cooled. 250 µl of S.O.C. medium (Invitrogen) were added and bacteria incubated with horizontal shaking for 1 h at 37 °C. Cells were either plated on agar plates or directly used for pool expressions.

The TOP10 strain was used to propagate new constructs. This strain is characterized by high transformation efficiencies and suitability for replication of high-copy plasmids. This strain was also used to produce vast amounts of pTT5-vector constructs for eukaryotic expression (section 2.2.2). To recombinantly express proteins in *E. coli*, the BL21 strain was used, which has been specifically constructed for high protein expression rates.

2.3 Recombinant Protein Expression

Studying the specificity and reactivity spectrum of antibodies requires large amounts of IgG-molecules and their candidate antigens. Recombinant production of these molecules is one way to meet this requirement. The two main expression systems employed in this study were HEK293E and *E. coli* strain BL21.

2.3.1 Eukaryotic Protein Expression in HEK293EBNA Cells

HEK293EBNA cells have been specifically developed for large scale recombinant protein expression and secretion. This cell line is derived from human embryonic kidney cells, grows in suspension and has been adapted to serum-free medium. It is stably transfected with the pCEP5-vector and transiently transfected with pTT5-vector constructs for recombinant expression. The pTT5-vector is described in more detail in section 2.2.9. The “HEK293E Large Scale Transient Expression System“ and the original pTT5 vector construct are patented by Y. Durocher (NRC Biotechnology Research Institute, Ottawa, Ontario, CA) and provided by courtesy of D. Jenne (license holder, MPI of Neurobiology/Helmholtz Zentrum Munich, Germany).

2.3.1.1 Cell Culture Maintenance

Suspension cultures of HEK293E cells are kept in polycarbonate conical flask with vented caps (Corning) and incubated at 37 °C, 8 % CO_2, 70 % humidity and 90 rpm in a Multitron shaker. FreeStyle™ 293 Expression Medium was supplemented with 0.1 % Pluronic F68 non-ionic surfactant to reduce foam formation and thereby shear forces. Addition of geneticin to a final concentration of 25 µg/ml ensured that only cells that carry plasmids survive. Cell concentrations of 0.1-3 x 10^6 cells per ml ensure optimal growth and survival. Cell numbers were determined using Neubauer counting chambers, according to the manufacturer's instructions. Trypan blue allowed distinction of live and dead cells. Cells approximately doubled within 24 h and were used up to passage 25-30.

2.3.1.2 Transfection and Expression

One hour prior to transfection, the cell suspension was diluted to a final concentration of 1 x 10^6 cells/ml. Production scale for all constructs was 500 ml. For all transfections, the culture volume determined the total amount of transfected DNA. 1 µg DNA per 1 ml cell suspension was used. In case of antibody transfections, the same amount of H- and L-chain coding pTT5-plasmids was transfected. Plasmids and the transfection reagent polyethylene imine (PEI, 0.2 µg/ml final concentration) were each independently diluted in 0.01 % volume cell suspension OptiPro™ SFM (Invitrogen). PEI was then carefully added to the plasmid solution and incubated at RT for 30 min to allow formation of DNA-PEI-complexes that can be endocytosed by cells. The DNA-PEI-complexes are dropwise added to the cell suspension which is then further incubated with standard parameters. To ensure optimal expression of the recombinant protein, medium was supplemented with tryptic protein hydrolysates at 0.5 % final concentration at 3-24 h post transfection.Harvest and Purification

HEK293E productions were harvested 120 h after transfection by centrifugation of the cell suspension for 5 min at 300 g and 4 °C. The target proteins were either directly purified from cell culture supernatants (rAbs) or cell pellets (AKAP17A) were stored at -20 °C.

a) Full Antibodies and F_{ab}-Fragments

Full length antibodies and F_{ab}-fragments were secreted by the HEK293E-system and purified from the culture supernatant. The C-terminal His_6-tag of antibodies and F_{abs} enables purification of recombinant protein by immobilized metal ion affinity chromatography (IMAC).

After harvest, the culture supernatant is further cleared by centrifugation at 24 000 g and 4 °C for 30 min. The supernatant is adjusted to 10 mM imidazole, 1x PBS, pH 7.5 and a final concentration of 100 µM phenylmethanesulfonyl fluoride (PMSF) was added. Ni-NTA-Agarose (Qiagen) was packed to a final volume of 1/100 initial volume cell suspension and equilibrated with 10 mM Imidazole in PBS. The adjusted culture supernatant was loaded onto the column at 1.5 ml/min flow rate. The column was then connected to the "Amersham Pharmacia Biotech" FPLC-system that is controlled by the LCC-501 Plus and attached to the UV-detector (Uvicord

SD) that allows tracking of washing and elution steps at 277 nm wavelength. Loaded columns were washed with 10 CV of 20 mM imidazole in PBS. Elution of proteins is achieved by increasing the imidazole concentration to 200 mM. The eluate was collected in one ml fractions and stored at 4 °C until further processing. F_{ab}-fragments used in this study had previously been produced and purified by J. Bruder according to this protocol [102].

b) AKAP17A

AKAP17A was retained inside HEK293E cells. Thus, after harvesting the cell suspension, the supernatant is discarded and the cell pellet stored at -20 °C. Cell pellets were thawed and lysed directly prior to further experiments and described in the according sections.

2.3.2 Prokaryotic Protein Expression in *E. coli* BL21

In case of failure of expression in HEK293E, the *E. coli* BL21 prokaryotic expression system was used. The BL21 strain carries the T7 RNA polymerase, controlled by the lac-promotor and is thereby suited to express recombinant protein under the T7 promotor at high levels after induction with isopropyl-thio-β-galactoside (IPTG). Generally, prokaryotes perform distinct posttranslational modifications (PTM) that differ markedly from mammalian PTM-patterns. A major difference is the inability of E. coli to introduce glycosylations, thus prokaryotic expression was not the system of choice to recombinantly produce candidate antigens. However, a major advantage of this system is high production rates and easy handling. As the chosen system is not suited for secretion, products were purified from the cytoplasm.

2.3.2.1 Transformation and Expression

scF_v-MS2-s5/pET19b, FAM84A/pET33b(+) and $GABA_AR\alpha1ex$/pET33b(+) constructs were transformed into BL21 bacteria by heat shock (section 2.2.12). Single clones were picked and grown in kanamycin (50 µg/ml) supplemented LB-medium at 37 °C overnight. FAM84A-transformed bacteria were further supplemented with 1 % (w/v) glucose during overnight culture. Overnight cultures were centrifuged for 10 min at 3 000 g and resuspended in the original volume of non-supplemented LB-medium. In case of the scF_v, the washed overnight cultures were further diluted 1:20 and 1:10 in pure LB medium respectively. To induce protein expression, 2 mM final concentration of IPTG was added once the bacteria had reached an optical density (OD) of 0.4. FAM84A-expressing bacteria were allowed to grow for 1.5 h in pure LB medium prior to induction. Induced bacterial cultures were incubated for 4 h at 37 °C before cells were harvested by centrifugation at 4 °C for 20 min at 3 000 g. Pellets were instantly frozen after harvest and stored at -20 °C until used for protein purification.

2.3.2.2 Harvest and Purification

Recombinant production in *E. coli* strains mainly yields two forms of the desired product: natively folded protein and clusters of protein aggregates, so called inclusion bodies (IB). To account for the different aggregate conditions that the target proteins will adopt, the purification strategy is different as described in the following sections.

a) Inclusion body Purification of scF_V-MS2-s5 and $GABA_AR\alpha1ex$

The IB purification protocol used here is adapted from Palmer and Wingfield [129] all steps are carried out at 4 °C if not stated otherwise.

IBs of scF_V-MS2-s5 or GABAα1ex were purified from BL21 bacteria. Per gram bacterial pellet, 8 ml of 100 mM Tris-Cl, pH7.0 with protease inhibitor tablet (Roche) were added and resuspended. Lysozyme was added to a final concentration of 200 µg/ml and incubated at RT for 20 min. Samples were sonified for 5 min with stirring and then centrifuged for 30 min at 18 000 g (Eppendorf, 5417R). The supernatant is discarded and the pellet thoroughly washed with 4 ml of 100 mM Tris, pH7.0 with 2 M urea and 2 % Triton X-100 per gram initial weight. The suspension was centrifuged at 18 000 g for 16 min, the supernatant discarded and the washing procedure was repeated twice. In a final washing step, the pellet was washed with 4 ml of 100 mM Tris, pH7.0. IBs are extracted by resuspending the pellet in 2 ml of 8 M guanidine hydrochloride with 5 mM EDTA in 50 mM Tris, pH7.0 per gram initial weight. To ensure complete solution of aggregates, the IB preparation is rotated for 1 h at RT prior to final centrifugationn at 18 000 g for 3 h. Purification yielded 1-5 mg scF_V-MS2-s5 and about 20 mg GABAα1ex per gram bacterial pellet. Solubilized IBs were either directly refolded as described in section 2.3.3 or stored at 4 °C.

b) Native Protein Purification of FAM84A from E. coli Cytosol

FAM84A was expressed in a natively folded state by E. coli BL21. To recover the folded target protein, bacteria were lysed and the released protein purified by IMAC.

Bacterial pellets (section 2.3.2) was thawed on ice and resuspended in 10 ml lysis buffer (300 mM sodium chloride, 50 mM sodium phosphate, 10 mM imidazole, 0.1 % Tween-20, pH8.0 and protease inhibitor tablet) per gram initial wet weight. Lysozyme at a final concentration of 1 mg/ml was added and incubated on ice for 30 min. To ensure complete lysis of cells, the suspension was sonified for 2 min on ice. Cell debris was removed by centrifuging at 4 °C for 10 min at 10 000 g and subsequently for 60 min at 150 000 g. Ni-NTA agarose is equilibrated with lysis buffer without Tween-20 and packed into a column to form a CV of 1/10 of the lysis volume. The supernatant is loaded onto the column with a flow rate of 1.5 ml/min. As described in section 2.3.1.3, the column is connected to the FPLC system and washed with 8 CV lysis buffer, containing 20 mM imidazole, and then with 2 CV lysis buffer containing 50 mM imidazole. Recombinant protein is eluted from the column by an imidazole gradient from 50-270 mM imidazole in 40 ml. Eluted protein was collected in 2 ml fractions and further subjected to ultrafiltration and dialysis as described in section 2.3.4.

2.3.3 Protein Refolding

scF_v-MS2-s5 and GABAα1ex were produced as IB in *E. coli* BL21 and therefore not natively folded. For further experiments, natively folded protein is required, especially with regard to the scF_v-fragment, as antibody-antigen-recognition may be conformation dependent. By means of rapid dilution, many unfolded proteins fold in their native conformation by rapidly removing the denaturing agent. Yields may vary depending on the efficiency of the refolding reaction. The scF_v-MS2-s5 IB preparation in 8 M guanindine-chloride solution (section 2.3.2.2) was rapidly diluted by dropwise infusing it into 100-fold sample volume of PBS at RT while stirring. The highly diluted protein solution was stirred for 1 h after rapid dilution and then left at 4 °C overnight without stirring. The GABAα1ex preparation was treated accordingly, but diluted 1:1 000 in PBS. The final concentration was 15 µg/ml. scF_v-MS2-s5 was further concentrated by ultrafiltration and dialyzed as described in section 2.3.4. The final concentration was 70 µg/ml. To determine their secondary structure, all refolded proteins were analyzed by CD-spectroscopy as described in section 2.4.3. Refolded proteins were directly employed in ELISA assays.

2.3.4 Ultrafiltration

To concentrate proteins, either from elution fractions or after refolding, Amicon® centrifugal filters (Merck) were used. The exclusion size was adapted to the MW of the target protein. For good recovery, the exclusion size is generally chosen to be 20 % smaller than the protein of interest. Therefore Amicons with MW cutoff of 30 kDa, 10 kDa and 3 kDa were used according to the manufacturer's instructions.

To finalize protein purification, the retentate is dialyzed twice against PBS overnight at 4 °C. The finalized products were stored at 4 °C.

2.4 General Protein Analysis

Prior to the application of in-house productions of candidate antigens and antibodies in experiments, careful assessment of biochemical characteristics is warranted to ensure the identity and quality of the product in use.

2.4.1 Protein Determination

Determination of total protein concentration of a sample is most useful when handling pure preparations of proteins. In this case, the total protein concentration approximates the concentration of the protein of interest. Protein purification procedures described in sections 2.3.1.3 and 2.3.2.2 yield pure recombinant protein preparations and therefore allow the use of the two methods of protein determination described below.

2.4.1.1 Lowry's method

Determination of total protein concentrations by "Lowry's method" is most widely used. In this study modifications of the original protocol by Peterson were applied. In a first step, copper ions

(Cu(II)) form complexes with peptide bonds of the protein in an alkaline environment. Subsequently, Folin-Ciocalteu phenol reagent is reduced, resulting in a purple color [130]. Unknown samples or BSA standard dilutions were mixed with the same volume of cupric tartrate reagent (0.8 M sodium hydroxide, 10 % SDS, 2 % cupric sulfate, 4 % sodium tartrate, 20 % sodium carbonate) and incubated for 10 min at RT. Then, half the initial sample volume of Folin-Ciocalteu phenol reagent is added and further incubated at RT for 30 min. Resulting absorbance is measured using the Victor2 1420 Multilabel Counter (Perkin Elmer) at 650 nm. Using the calibration curve that is calculated from BSA standard dilutions (20–140 µg/ml), the concentration of the unknown samples was determined.

2.4.1.2 UV-Absorbance

The absorbance of aromatic AA at 280 nm wavelength can be used to determine the total protein concentration of a sample. In this case, the extinction coefficient that takes into account the AA-composition of the protein of interest is factored into the calculation. All measurements were done using the ND1000 spectrophotometer.

2.4.2 Sodiumdodecylsulfate polyacrylamide Gelelectrophoresis (SDS-PAGE)

SDS-PAGE is the method of choice to analytically separate different proteins of a sample based on their MW [131].

Gels may be run under reducing or non-reducing conditions. Reducing conditions are generally preferred as this will yield more defined protein bands. To this end, samples were complemented with reducing loading dye, including 2 % β-mercaptoethanol, and heated to 95 °C for 5 min before loaded to the gel. When analyzing the integrity of full length antibodies, however, using non-reducing conditions is inevitable as this treatment preserves disulfide bonds that interconnect H- and L-chains. Irrespective of reducing or non-reducing conditions, loading buffer was added to samples before loading them to either Tris-Glycine gels (4-20 %, Invitrogen) or Bis-Tris gels (12 %, Invitrogen). All gels were run with the appropriate running buffer for 90 min at 130 V.

2.4.2.1 Coomassie Staining

To visualize total protein of SDS-PAGE separated samples, Coomassie Brilliant Blue was used. This allows detection of minimal protein amounts of approximately 500 ng. Gels were soaked with Coomassie solution (0.1 % (w/v) Coomassie Brilliant Blue R-250, 40 % methanol, 10 % acetic acid) for 20-30 min, followed by destaining (50 % methanol, 7 % acetic acid) to remove excess Coomassie and to achieve the desired staining intensity. By washing with 5 % acetic acid overnight, unspecific background staining is reduced and the gel returns to its original size.

2.4.2.2 Silver Staining

Weak protein bands, representing protein amounts in low ng ranges, can be detected using silver staining protocols. To retain the option to later analyze protein bands by mass spectrometry, the Shevchenko protocol for silver staining was applied [132].

Proteins are fixed by soaking the gel with fixing solution (50 % methanol, 5 % acetic acid in water) for 10 min. Fixing solution is washed off and sensitizing solution (0.02 % (w/v) sodium thiosulfate in water) is added and incubated with gentle shaking for 1 min before it is washed off with water. Repeating this step for a total of three-times will allow for a more sensitive staining. Subsequently, staining solution (0.1 % (w/v) silver nitrate in water, pre-chilled) is added and incubated for 20 min at 4 °C with gentle shaking. The gel was washed with water twice before adding developing solution (0.04 % formaldehyde, 2 % (w/v) sodium carbonate in water). Gels were incubated with developing solution until the desired staining intensity was reached, refreshing the solution in case of discoloring. To end the reaction, stop solution (5 % acetic acid in water) was added.

2.4.3 Circular Dichroism Spectroscopy

The secondary structure of proteins can be studied using circular dichroism spectroscopy. This method takes advantage of differential optical activity of the chiral C_α-atom in the peptide backbone and distinct structural features of a folded protein. The C_α-atoms of AA in α-helices and β-sheets have different extinction coefficients. Experimentally, the absorption of circular polarized light of different wavelengths is measured. The difference between the absorbance of right-handed circularly polarized and left-handed circularly polarized light is calculated and determines the molar ellipticity θ at a certain wavelength. Plotting the ellipticity values and according wavelengths yields a spectrum that may be translated into structural features of the protein. CD-measurements were done with Elisabeth Weyher-Stingl and Reinhard Mentele using the J-715 spectrometer at the “Microchemistry Core Facility” of the MPI for biochemistry. Spectra were taken at wavelengths between 195 and 250 nm at RT and read at 50 nm/min acquisition speed. All spectra were acquired in multiple runs and averaged for analysis. PBS or the according sample buffer was used as blank value that was subtracted prior to data analysis. Protein concentrations of 0.1 - 0.2 mg/ml were used for measurements. Using the “Spectra Manager CDPro Analysis” program, the experimental measurements were compared to a set of 56 reference proteins (Contin SMP56) and the proportions of secondary structures deduced from these [133].

2.4.4 Mass Spectrometry

To confirm the identity of recombinantly produced proteins, mass spectrometry was applied as this method is suited to rapidly identify proteins based on characteristic peptides. In this study, proteins were digested by trypsin and applied to matrix-assisted laser/desorption/ionization (MALDI) mass spectrometry.

Mass spectrometric measurements were done in cooperation with Reinhard Mentele and Monica Zobawa (MPI for Biochemistry, Department for Proteinanalytics, Prof. Lottspeich, Martinsried, Germany). Mass spectra were acquired using either the „4700 Proteomics MALDI-TOF/TOF Analyzer“ or “4800 Proteomics MALDI-TOF/TOF Analyzer”. Mass spectra were analyzed using

“Data Explorer“ software (Applied Biosystems, Darmstadt, Germany) and generated peak list run through the NCBI protein database.

2.4.5 Secondary Structure Predictions

To evaluate CD-spectroscopy data on proteins that had not previously been studied by X-ray diffraction or nuclear magnet resonance spectroscopy, predictions on the secondary structure of the specific proteins were consulted. Predictions were based on the “psipred” propgram [134] that distinguishes between α- helices, β-sheets and disordered regions. The “Spectra Manager CDPro Analysis” program used to analyze CD-spectra differentiates each of the three structure categories α-helix, β-sheet and disorders into two subclasses which were summed up to compare to the prediction results.

2.4.6 Sequence Alignment

Some candidate antigens were compared with respect to AA-sequence homology. The Clustal Omega program [135] is a multiple sequence alignment tool that is used to determine the overall similarity of multiple protein sequences. The program was run using default settings and results were fed to the ESPript 3.0 program [136] that was used to prepare alignment illustrations.

For pairwise global sequence alignments the EMBOSS Needle tool, based on the Needlemann-Wunsch-algorithm, was used to identify the best overall alignment for two sequences. The EMBOSS water tool uses the Smith-Waterman-algorithm to find the best local alignment and to identify homologous regions within small stretches of two sequences [137].

2.4.7 Helical Wheel Projections

The arrangement of AAs in an α-helix is illustrated in a wheel projection. The wheel depicts a full turn every 3.6 AAs and provides a way to easily identify the residues that face the same direction of a helix. Helical wheel projections of AA-sequences of candidate antigens were generated by the projection program created by Don Armstrong and Raphael Zidovetzki using default settings. Version: Id: wheel.pl,v 1.4 2009-10-20 21:23:36 don Exp.

2.5 Immunological Methods

Identification and validation of candidate antigens was based on immunological methods. These allow specific detection of target molecules in low concentrations ranging from pico- to nanogram. If not stated otherwise, the antibody concentrations applied to the individual assays are listed in Table 2-13 and Table 2-14.

2.5.1 Flow Cytometry

The general functionality of recombinantly produced OCB-derived antibodies was tested using flow cytometry. This method allows detecting fluorescence-labeled antibodies that recognize their antigen on the cell surface. Thus, a previously established TE671-cell line (provided by K. Dornmair, [138]), which expresses the extracellular domain (AA30 –150) of MOG, was used to verify the binding reactivity of r8-18C5 to its antigen.

10^5 cells were incubated with 10 µg/ml of r8-18C5 or rOCB-MS3-s1 as isotype control for 30 min on ice. The original mouse 8-18C5 antibody served as positive control. The positive control antibody along with its isotype control X40 was run in parallel using the above parameters. All dilutions and washing steps were in PBS with 2 % BSA. Cells were centrifuged in between washing steps for 5 min at 300 g and 4 °C. After three washing steps, secondary AlexaFluor647-coupled goat-anti-human IgG H+L-chain antibody was diluted 1:150 and incubated for 30 min on ice. In case of the original 8-18C5 antibody, secondary AlexaFluor647-coupled goat-anti-mouse IgG H+L-chain was used. Following three final washes, cells were taken up in 150 µl of PBS with propidiumiodide at a final concentration of 2 µg/ml. 10^4 cells of each condition were analyzed using the FACSverse and data was analyzed with “FlowJo”© software V10 (Tree Star, Ashland, OR, USA).

2.5.2 Protein Microarray

To screen OCB-antibodies for reactivity to proteins, “ProtoArrays®” (v5.0 Human Protein Microarrays, Invitrogen, PAH0525101, Lots HA20259 and HA20302) were used. Each array consists of 48 subarrays, made up of 22 columns by 22 rows that contain more than 9 000 proteins. Most proteins originate from the “Invitrogen human Ultimate ORF™ collection”. Additionally, the tested proteins are enriched for kinases and proteins that have been related to various disease processes, including 20 established antigens of autoimmune diseases. All proteins were purified from an insect cell system, printed in duplicates on nitrocellulose-coated glass slides and screened simultaneously for reactivity with one of the rAbs. All rAbs, along with the humanized, MOG-specific r8-18C5 [127], were assayed in their full length format with V5-tag. Arrays were treated according to the manufacturer’s statement and all procedures were carried out at 4 °C , arrays were gently agitated during incubation times.

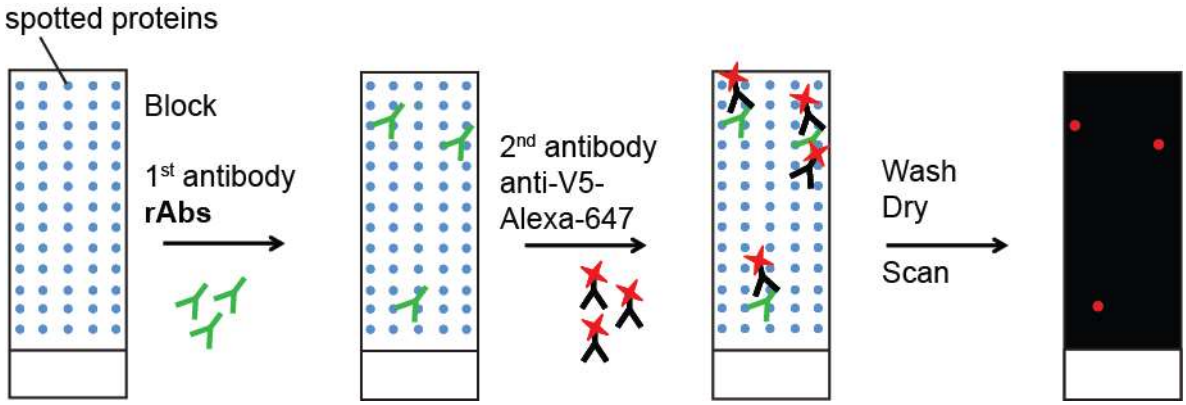

Figure 2-4: Schematic Illustration of the Protein Microarray Workflow.

The glass slide with ~9400 spotted proteins is incubated with recombinant antibodies that are detected with an AlexaFluor647-coupled anti-V5 secondary antibody. Arrays were washed and dried before fluorescence signals were detected. The illustration is modified from [102]

Arrays were blocked using blocking buffer (LifeTechnologies, PA055) with synthetic block (LifeTechnologies, PA017) for 1 h. Recombinant OCB-antibodies were added at a concentration of 10 µg/ml in wash buffer (synthetic block in PBS, 0,05 % Tween-20) and incubated for 90 min. As only limited amounts of the rOCB-MS2-s5 were available, the antibody concentration was reduced to 5 µg/ml in this case. Arrays were washed five times for 5 min before the secondary α-V5 antibody conjugated with Alexa647 (LifeTechnologies, 45-1098) was added at 1 µg/ml concentration in wash buffer and incubated for 90 min. The washing procedure was repeated, the array dried by centrifuging at 200 g for 2 min and stored in the dark at 4 °C until analyzed with the Microarray Scanner GenePix 4000B (Axon Instruments) at 635 nm wavelength using different photomultiplier (PMT) settings. Signals were analyzed using the PPI option of the "Protoarray™ Prospector 5.2.1" program (LifeTechnologies) as described earlier by J. Bruder [102]. For quality control, the mean signal of internal negative controls and the overall mean array signal were determined. Besides the internal array controls, one array was probed with only the secondary antibody and used as negative control, the array probed with r8-18C5 served as isotype control. To analyze the r8-18C5 probed array, rOCB-MS3-s1 was chosen as isotype control. The specific background signal measured at every spot was subtracted from the signal prior to analysis. Signals were considered that were 3x enriched compared to both the signal intensity of the negative control as well as the one of the isotype control (r8-18C5 or rOCB-MS3-s1) and 5x enriched compared to the background signal. In case of rOCB-MS2-s5, only signals that were also recognized by the Prospector software as "hits" were selected. "Hits" are defined by the program as proteins with Z-score above 3, CIP-value below $1*10^{-4}$ and Z-factor above 0.05 with a coefficient of variation below 0.5. This additional selection was necessary to account for the increased number of candidate antigens caused by unspecific reactivity due to lower concentration and purity of rOCB-MS2-s5. Proteins were only considered as candidate antigens when duplicate signals were detected. For analysis, data acquired using PMT700 was used and all hits were visually confirmed.

Results from protein microarrays were confirmed with independent techniques to verify the reactivity found in the screening approach. From the pool of candidate antigens ($f \geq 3$) only proteins with enrichment factors above 100 were selected for further experiments. Those methods included immunoprecipitation, Western blotting, and ELISA and are described in detail in the following sections. Further, candidate antigens used in these validation experiments were produced in organisms other than insect cells, to confirm that array reactivity was not directed at insect cell specific modifications. Such validation experiments were carried out for selected antigen candidates, the selection of these candidates is described in the results (section 3.3.1).

2.5.3 Immunoprecipitation

One of the methods used here to verify the binding of the OCB-derived antibodies to candidate antigens was immunoprecipitation. Two general approaches were applied for precipitation. First antibody-antigen-complexes were allowed to form in solution and were subsequently incubated with the bead matrix that binds IgG-molecules. Second, antibodies were coupled to the bead matrix and the samples were then added. Thus, the complexes form directly at the matrix.

2.5.3.1 Immunoprecipitation of HEK-derived MKNK1

MKNK1 purified from HEK-cells (amsbio) was used to validate the reactivity of rOCB-MS2-s5 by immunoprecipitation.

Tosyl-activated magnetic beads (Thermo Fisher Scientific) were coupled with rscF$_v$-MS2-s5, control F$_{ab}$-fragments rFab-MS3-s1, rFab8-18C5 and positive control antibody ab56425 (abcam) to MKNK1. Tosyl-activated beads covalently bind primary amine or sulphydryl groups and were therefore best suited for this experiment. 20 µg of antibodies were coupled to 1 mg of beads according to the manufacturer's recommendations. Beads were then blocked in 1 % BSA in PBS-T for 1 h at RT. 0.7 µg of MKNK1 were added and incubated for 30 min at RT. Beads were washed three times with 1 % BSA in PBS-T and twice with PBS-T. Bound antigens were eluted with 60 µl reducing SDS-PAGE loading buffer at RT for 10 min and analyzed by Western blotting.

2.5.3.2 Immunoprecipitation of HEK-derived FAM84A

FAM84A was validated as candidate antigen of rOCB-MS1-s8 by immunoprecipitation. To this end, purified HEK-derived protein FAM84A (amsbio) was used.

Protein G Dynabeads (LifeTechnologies) were washed in PBS and then incubated with 1 % BSA in PBS-T rotating for 1 h at RT. Simultaneously, 2 µg of purified HEK-derived FAM84A were individually incubated with 25 µg of each of the antibodies rOCB-MS3-s1, rOCB-MS1-s2, rOCB-MS1-s8 and r8-18C5. ab58330 served as positive control. Following 30 min of incubation with rotation at RT, 3 mg of blocked Protein G beads were resuspended in each of the individual tubes and incubated for another 10 min at RT with agitation. Beads were washed five times with PBS-T and complexes eluted from the matrix by incubation with 60 µl reducing SDS-PAGE loading

buffer for 10 min at 95 °C. The eluate was analyzed using Western blotting as described in section 2.5.4.

2.5.3.3 Immunoprecipitation of HEK293-derived AKAP17A

AKAP17A was precipitated from crude HEK293E cell lysate, validating the Protoarray findings with rOCB-MS1-s2. HEK293E cells were transfected with the AKAP17A/pTT5 construct without V5-tag, grown and harvested as described in section 2.3.1 and stored at -20 °C until lysis.

Protein G Dynabeads were covalently coupled with individual antibodies using the amine cross-linker bis(sulfosuccinimidyl)suberate (BS^3, Pierce). Coupling was carried out according to the manufacturer's instructions. In short, an excess of recombinantly produced OCB-antibodies and beads were mixed and incubated for 1 h. Antibody attached to Protein G is covalently coupled by adding 5 mM BS^3 in 20 mM Na_2HPO_4, 150 mM NaCl, pH8.6 and rotating for 30 min. The cross-linking reaction is repeated once with fresh BS^3 reagent and then stopped by adding 5 % (v/v) quenching buffer (1 M Tris pH 7.5) and further rotating incubation for 15 min. Coupled Dynabeads were stored in PBS at 4 °C until deployed in immunoprecipitation.

Cells were thawed, resuspended in lysis buffer (300 mM NaCl, 150 mM NaH_2PO_4 in 1x PBS pH 7.5) and sonified for 5 min on ice. The lysate was cleared from cell debris by centrifuging for 10 min at 3 400 g, 4 °C and 10 min at 12 000 g, 4 °C. The supernatant was immediately subjected to immunoprecipitation using Protein G Dynabeads with covalently coupled antibodies.

Prior to the immunoprecipitation, pre-coupled and fresh Dynabeads were blocked using synthetic buffer (Life Technologies) in PBS for 1 h. Pre-blocked, uncoupled Protein G Dynabeads were incubated with the lysate for 15 min to minimize background resulting from unspecific interactions with the bead matrix. Pre-cleared lysate was then incubated with Protein G Dynabeads pre-coupled with recombinant OCB-antibodies rOCB-MS3-s1, -MS1-s2, -MS1-s8, r8-18C5 and polyclonal α-AKAP17A (MBS711914) antibody for 30 min. All incubation steps were carried out at RT. Bound molecules were eluted in reducing SDS-PAGE loading buffer for 10 min at RT and analyzed by Western blotting (2.5.4).

2.5.3.4 Immunoprecipitation of HEK-derived MAPK7, CRIP2 and CSRP2

To verify reactivity of Ab-Ip2 to MAPK7, CRIP2 and CSRP2, commercially available HEK-derived proteins (all Origene) were applied to immunoprecipitation experiments.

rAb-Ip2 and control antibodies r8-18C5 and rAb-MS3-s1 were covalently coupled to Protein G beads as described above and then incubated with 2 µg of MAPK7. Beads were washed six times with PBS-T and eluted in 200 µl 1x SDS-loading dye for 10 min at 95 °C.

For immunoprecipitation of CRIP2 and CSRP2, Protein G beads were blocked in synthetic buffer in PBS-T with 0.5 mM DTT for 1 h at RT. Simultaneously, 2 µg of purified CRIP2 or CSRP2 protein were incubated with 8 µg of antibodies Ab-Ip2, rOCB-MS3-s1, and r8-18C5 in synthetic

buffer in PBS with 0.3 mM DTT for 30 min at RT. After complex-formation, 30 µl of Protein G beads were added to each of the antibody-antigen solutions and incubated for 10 min at RT with shaking. The supernatant was discarded and beads washed five times with 100 µl of PBS-T with 0.5 mM DTT. Complexes were eluted from the bead matrix by incubation with 1x SDS-loading dye for 10 min at 95 °C. Eluates were analyzed by SDS-PAGE and Western blotting.

2.5.4 Western Blot

Low amounts of defined proteins may be specifically detected by Western blotting. This method was used to analyze eluate fractions from immunoprecipitation experiments. In case of antibodies that recognize linear epitopes, antibody-antigen-recognition can be directly detected by Western blotting.

Proteins separated by SDS-PAGE were electrotransferred to polyvinylidene fluoride (PVDF, GE Healthcare) membranes in a semi-dry manner for 3 h at 35 mA per membrane. Membranes were blocked in 5 % milk powder in PBS-T by incubation at RT for 1 h or overnight at 4 °C to prevent unspecific binding. Primary antibodies were diluted in 5 % milk powder in PBS-T and diluted as stated in Table 2-13. Membranes were incubated with primary antibodies at RT for 1 h with shaking and then washed off using PBS-T three times for 5 min. HRP-coupled secondary antibodies were also diluted in 5 % milk powder in PBS-T as stated in Table 2-14 and incubated with shaking at RT for 1 h. The washing procedure described above was repeated.

Enhanced chemiluminescence (ECL)-substrate solution to detect antibody reactivity is prepared freshly by mixing 10 ml of ECL A with 100 µl of ECL B and 3.1 µl 30 % hydrogen peroxide. The membrane was covered with ECL-substrate solution for 1 min and signals were then captured on radiographic films and visualized using the OPTIMAX x-ray developer. Signals were also directly detected using digital imaging systems “Odyssey Fc” and “ImageQuant LAS4000”. Exposure times varied from seconds to maximally 20 min, depending on the signal strength.

A modification of the described Western blotting technique is dot blots. In this case the sample is directly spotted onto a nitrocellulose membrane, where the target protein is immobilized in a denatured state. After complete drying, the membrane is treated as described above for classical Western blots.

To exemplarily verify the capability of r8-18C5 to bind its antigen, 1 µg and 0.5 µg of recombinant human MOG (HEK293-derived, provided by D. Jenne) as well as sample buffer without protein were spotted. After drying, the membrane was blocked with synthetic block in PBS-T for 1 h at RT. r8-18C5 antibody was added at a final concentration of 1 µg/ml in blocking buffer and incubated for 1 h at RT. The primary antibody was washed off and HRP-coupled anti-V5 antibody was added and incubated for 1 h at RT. This was followed by developing the membrane using ECL, as described above.

For additional validation experiments with r8-18C5, human MOG (HEK293-derived, provided by E. Meinl) and candidate antigens FAM20B (in-vitro translation, Abnova) and CHD2 (CHO-derived, R&D) were used. 0.5 µg of each of the proteins was loaded to a SDS-gel and transferred to a PVDF-membrane. To detect reactivity to linear epitopes on these candidate antigens, 1.5 µg/ml of r8-18C5 in 5 % milk powder in PBS-T were used as primary antibody.

2.5.5 Enzyme-linked immunosorbent Assay (ELISA)

For ELISA, the target protein is directly coated to the assay plate. In sandwich-ELISAs, an antigen specific capture antibody is coated. The capture antibody immobilizes the antigen of interest and allows thorough washing throughout the procedure. In both cases, binding of the tested sample to the target antigen is detected by adding a detection antibody coupled to horseradish peroxidase (HRP). The subsequently added 3,3′,5,5′-Tetramethylbenzidin (TMB) substrate is oxidized by HRP thereby creating a blue-colored product. The reaction is stopped by adding sulfuric acid which quenches the reaction and turns oxidized TMB into a yellow-colored product that is read out at 450 nm wavelength. Measuring the absorbance at 540 nm allows correction of the measurements for uneven background signal. TMB substrate solution (eBioscience, San Diego, CA, USA) was used according to the manufacturer's statement.

2.5.5.1 ELISA for Reactivity to MKNK1

Based on Protoarray findings, MKNK1 was identified as candidate antigen for rOCB-MS2-s5. To validate this result, an ELISA using commercial HEK-derived MKNK1 (amsbio) was established. scF_v-MS2-s5 and F_{ab}-fragments of control antibodies were used in this experiment. This accounts for the different binding characteristics of scF_v-Fragment and full length antibodies due to the different number of antigen binding sites.

a) Validation

MKNK1 was directly coated to Costar half-area assay plates at a concentration of 16 µg/ml in PBS at 4 °C overnight. All other dilution and washing steps were carried out using 0.5 % BSA in PBS. Unless stated otherwise, further incubation was carried out at 37 °C. The plate was washed once with 1 % BSA in PBS and subsequently incubated in this blocking buffer for 2 h. Monoclonal OCB-derived F_{ab}-fragments, scF_v-MS2-s5 (section 2.3.2.2) and the commercial polyclonal antibody PA5-13951 were added at concentrations ranging from 0.5 µg/ml to 150 µg/ml and incubated for 40 min. After washing off excess antibody, HRP-coupled detection antibodies to human IgG H- and L-chains, rabbit IgG Fc-region and V5-tag were added and incubated for 20 min. The final washing steps were done using PBS-T. Procedures of TMB substrate reaction, OD measurements and data analysis have been adopted as described in section 2.5.5. Developing time for the TMB reaction in this experimental setup is 4-5 min at RT.

b) Patient Screening

To screen patient CSF for reactivity to MKNK1, the above described MKNK1-ELISA was employed. Each of the samples was employed at 25 µl per well of undiluted CSF. Positive

controls PA5-13951 and scF_v-MS2-s5 were applied in concentrations of 100 µg/ml and 50 µg/ml respectively.

In total, 28 CSF samples were screened for MKNK1-reactivity. The main focus of this screening approach was CSF samples of other MS patients (20 samples). For control reasons, non-inflammatory neurological disorders (NIND, 8 samples) were screened in parallel. The NIND cohort consists generally of neurological symptoms with unclear etiology such as tension headache. The respective clinical findings of these patient samples are listed in Table 2-1.

2.5.5.2 ELISA for Reactivity to FAM84A

Reactivity of rOCB-MS1-s2 to FAM84A, as suggested by the Protoarray data, was further confirmed by ELISA. The assay described in the following section was also applied to screen CSF samples of a larger patient cohort and to examine more closely the epitope recognized by rOCB-MS1-s2 by analyzing alanine-mutants.

a) Validation

Costar half-area assay plates were coated with a final concentration of 10 µg/ml α-V5 capture antibody in PBS at 4 °C overnight. Plates were washed once and then incubated with 2 % bovine serum albumin (BSA) in PBS-T at 37 °C for 2 h. All dilution and washing steps were carried out with 0.5 % BSA in PBS-T. Unless stated otherwise, further incubation was carried out at 37 °C.

FAM84A purified from *E. coli* (see Section 2.3.2) was diluted to a final concentration of 16 µg/ml, added to the blocked assay plate and incubated for 30 min. Recombinant FAM84A is bound by the capture antibody via its C-terminal V5-tag sequence (GKPIPNPLLGLDST). This sequence not only allows strong attachment of the target protein to the plate surface, but also adds an extra purification step to the experimental setup. Unbound impurities and excess FAM84A is washed off the plate and OCB-derived monoclonal antibodies are added at concentrations ranging from 5 µg/ml to 2 mg/ml. Besides rOCB-MS1-s2, that had recognized FAM84A on the Protoarray, rOCB-MS3-s1, rOCB-MS1-s8 and r8-18C5 were used to control for unspecific isotype reactivity. The commercial monoclonal antibody to human FAM84A (ab58330) served as positive control at concentrations ranging from 2.5 ng/ml to 330 ng/ml. Monoclonal antibodies and the positive control were incubated for 40 min. Recombinant monoclonal antibodies bound to FAM84A were detected using HRP-coupled polyclonal rabbit α-human IgG at 1:100 000 dilution. The commercial α-FAM84A antibody was detected by HRP-coupled rabbit α-mouse diluted 1:5000. Detection antibodies were incubated for 20 min. After thorough washing of the plate and a final washing step with pure PBS, 25 µl of TMB substrate solution (eBioscience) were added and incubated at RT for 15-20 min. Following incubation time, the reaction was stopped by addition of 13 µl of 1 M H_2SO_4 solution.

The signal intensity was read out using the Victor2 1420 Multilabel Counter at 450 nm. Additionally, the OD at 540 nm was determined to account for optical imperfections. The OD

values at 540 nm were subtracted from those at 450 nm using Microsoft Excel and the corrected values were further analyzed using Prism Graphpad software.

b) Patient screening

To determine if other MS patients have antibodies reactive to FAM84A, the above described ELISA was applied to matching CSF and serum samples of a larger patient cohort. In total, 66 samples were measured in a blinded manner. rOCB-MS1-s8 is derived from an antibody species expanded in the CNS of a MS patient. Thus, the main focus of this screening approach was CSF samples of other MS patients (20 samples). Additionally, samples from patients with other neurological disorders were employed for control purposes, these included neuroborreliosis (NB, 13 samples), other inflammatory disorders (OID, 7 samples), cranial nerve palsies (CNP, 9 samples) and non-inflammatory neurological disorders (NIND, 17 samples). CNP samples contained facialis paresis and cranial palsies and the NIND cohort consists generally of neurological symptoms with unclear etiology such as tension headache. Overall, the groups represent acute inflammatory settings (NB and OID) and chronic or non-inflammatory settings (MS, CNP and NIND). The clinical findings of these patient samples are listed in Table 2-1.

The above described monoclonal OCB-derived antibodies as well as the original CSF sample of patient MS1 were run in parallel to the unknown samples as controls. rOCB were used at a final concentration of 50 µg/ml, the positive control antibody ab58330 was used at 10 µg/ml. CSF samples were applied without dilution, irrespective of their *a priori* unknown protein or IgG-concentration. The matching serum samples were diluted 1:400 in PBS to lower the IgG-content to levels comparable to CSF IgG-concentrations. All other experimental details were retained. For a total of four CSF samples the matching serum sample was not available.

c) Screening of mutated FAM84A

In order to obtain a closer insight into the epitope that is recognized by rOCB-MS1-s2, FAM84A-mutants were expressed and applied to the above described FAM84A validation assay (section 2.5.5.1). Mutants were applied to the assay at a final concentration of 16 µg/ml. In contrast, only a reduced number of different monoclonal antibodies, namely rOCB-MS1-s2, r8-18C5 and the commercial α-FAM84A, were used in this setting.

2.5.5.3 ELISA for Reactivity to $GABA_AR$ α1-subunit

Costar half-area assay plates were coated with the refolded extracellular domain of the $GABA_AR$ α1-subunit (section 2.3.3). Final concentration of the $GABA_AR$-fragment was 15 µg/ml. The protein was allowed to attach to the assay plate for 2 h at 37 °C. All following dilution and washing steps were carried out using 0.5 % BSA in PBS. Unless stated otherwise, incubation was carried out at 37 °C. The plate was washed once with 1 % BSA in PBS and then blocked in the same buffer for 1 h. rAb-Ip2, one MS-OCB-derived control (rOCB-MS3-s1) and r8-18C5, along with the positive control anti-V5 antibody, were applied at a final concentration of 50 µg/ml and incubated for 1 h. Unbound antibody was washed off thoroughly. HRP-coupled antibodies to

human and rabbit IgG H- and L-chains at concentrations of 1:50 000 and 1:10 000 were used as secondary antibodies respectively. Secondary antibodies were incubated for 20 min and excess was washed off. A final washing step with pure PBS was included. Reactivity was detected using TMB chemistry as described above (section 2.5.5) and the results analyzed using Graphpad Prism software as described (section 2.1.9). Developing time for the TMB reaction in this experimental setup was 20-30 min at RT.

2.5.6 Immunofluorescence

To test whether OCB-derived antibodies recognized target antigens in a cellular setting, HEK293E-cells were stained with OCB-derived antibodies and appropriate controls. HEK293E-cells endogenously express the candidate antigens FAM84A and AKAP17A. Cells transfected with the individual candidate antigens were stained in parallel.

Antigen-transfected and non-transfected HEK293E-cells were washed in PBS once. 1 x 10^5 cells were allowed to settle for 1 h at RT on poly-L-Lysin coated slides. Cells were again washed once with PBS and fixed in ice-cold ethanol with 5 % acetic acid for 10 min. Fixed cells were washed twice in PBS and permeabilized with PBS-T for 20 min. Unspecific binding sites were blocked with 2 % BSA in PBS-T for 1 h. rOCBs were added at 5 µg/ml final concentration. Positive control antibodies PA5-30705 and ab56425 were diluted 1:400, MBS711914 was diluted 1:100. After incubation for 1 h at RT, cells were washed three times in PBS-T. AlexaFluor594-coupled secondary antibodies A11005 to mouse IgG and A11037 to rabbit IgG were diluted 1:1000. The DyLight488-coupled secondary antibody 109-485-088 to human IgG was diluted 1:400. Secondary antibodies were incubated for 1 h. All antibodies were diluted in 1 % BSA in PBS-T. Cells were washed as described above with DAPI present in the final washing step. Stainings were analyzed using AxioVert 200M fluorescence microscope and MetaMorph software. For each of the antigens, the exposure times were kept constant for the different conditions.

2.6 Statistical Analysis

For statistical analysis, Prism software (GraphPad Software, La Jolla, Ca, USA) was used. Student's unpaired t-tests were used to identify statistical differences. All data is presented as mean ± standard deviation. p-values ≤0.1 were considered significant.

3 Results

The present study aimed at the identification of target antigens of expanded antibody species from patients with inflammatory neurologic diseases. The antibodies used here derive from MS patients and one $GABA_AR$-encephalitis case. Table 2-17 lists the rAbs used in this study and their source.

An approach established by B. Obermeier (Figure 1-8, [100]) allows the identification of matching H- and L-chains. In this previous study, H- and L-chain pairs of a total of six MS-OCB-derived antibodies were cloned and expressed in form of F_{ab}-fragments by B. Obermeier. F_{ab}-fragments were applied in primary antigen search experiments [100, 102]. Due to a lack of consistency of results, the established F_{ab}-fragments were re-cloned into full length IgG-constructs to be used in the study described here.

Ab-Ip2 was characterized from CSF of the $GABA_AR$-encephalitis patient Ip2 by E. Beltrán (unpublished data). Next generation sequencing of the B-cell repertoire identified a monoclonal expansion of this antibody.

Here, the experimental findings leading to the unambiguous identification and validation of target antigens of OCB-derived antibodies from MS patients and two target structures of rAb-Ip2 from a $GABA_AR$-encephalitis patient are described. To this end, candidate antigens were identified by protein microarrays and independent methods were used to confirm the antigen-antibody-interaction. Further, the epitope recognized by one of the OCB-derived antibodies is explored in greater depth and the reactivity profile of a larger patient cohort towards this antigen is presented.

3.1 Expression and Characterization of recombinant MS-OCB Antibodies

The full length IgG1 H-chains were cloned into the pTT5-vector, co-transfected with L-chains into HEK293E-cells, and purified from the cell culture supernatant. MS-OCBs were expressed as divalent antibodies because two antigen binding sites may allow the formation of more stable complexes with the antigen compared to F_{ab}-fragments. This may facilitate the identification of target antigens. The L-chain constructs are the same for F_{ab}-fragments and full length antibodies. Full length antibodies were expressed in two formats, with and without V5-tag. All antibodies carried the His_6-tag which was used for purification.

3.1.1 Biochemical Analysis of recombinant full length Antibodies derived from MS-OCB

All antibodies, except rOCB-MS2-s5 (see section 3.1.2), were expressed at sufficient levels, secreted to the medium and purified by affinity chromatography. Figure 3-1 shows the individual recombinantly expressed and purified V5-tagged OCB-antibodies separated by SDS-PAGE under reducing and non-reducing conditions. Disulfide bridges in between the two H-chains and the H- and L-chain pairs break under reducing conditions, thereby disintegrate the molecule into its components. Thus, SDS-PAGE run under reducing conditions shows two distinct bands for each

antibody representing the L-chains at 25 kDa and the H-chains at approximately 55 kDa. Loading the samples under non-reducing conditions preserves the heterodimeric molecule hence only a single protein band at around 160 kDa is present after Coomassie staining. No other proteins were detected, demonstrating sufficient purity of the recombinantly produced antibodies (Figure 3-2A). The final yield of an expression preparation was 2-4 mg/l of purified antibody.

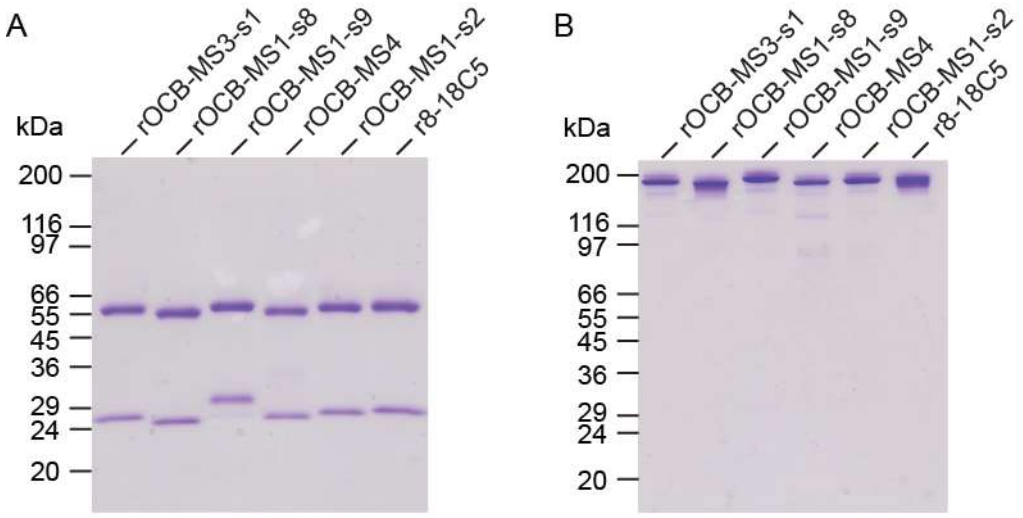

Figure 3-1: Recombinant full length monoclonal antibodies derived from MS-OCBs.

V5-tagged antibodies were expressed in HEK293E, purified by affinity chromatography, separated by SDS-PAGE under reducing (A) and non-reducing (B) conditions and stained with Coomassie Brilliant Blue. Antibodies treated with reducing agent show two protein bands at 25 and 55 kDa, representing disassembled heavy and light chains (A). Antibodies under non-reducing conditions are visualized as a single band at approximately 160 kDa (B). The preparations show no additional bands.

Western blotting to human IgG H- and L-chains confirmed the identity of the protein bands (Figure 3-2B). The secondary structure of the full length rAbs was determined using CD-spectroscopy. The CD-measurements corresponded to the expected large proportion of β-sheets, representing more than 40 % of the protein's secondary structure. Low levels of α-helical structures were detected within the limits of error. Approximately 20 % of the protein consist of turns, whereas the remainder is disordered stretches of AAs (Figure 3-2C and D). These results agree with antibody secondary structures described in the literature [139]. Mass spectrometry allowed the detection of unique peptides that unambiguously demonstrated the presence of the two distinct chains of a specific rAb (Figure 3-2E). These analyses were done in parallel for all full length rAbs. Figure 3-2 shows exemplary data from the humanized r8-18C5 antibody.

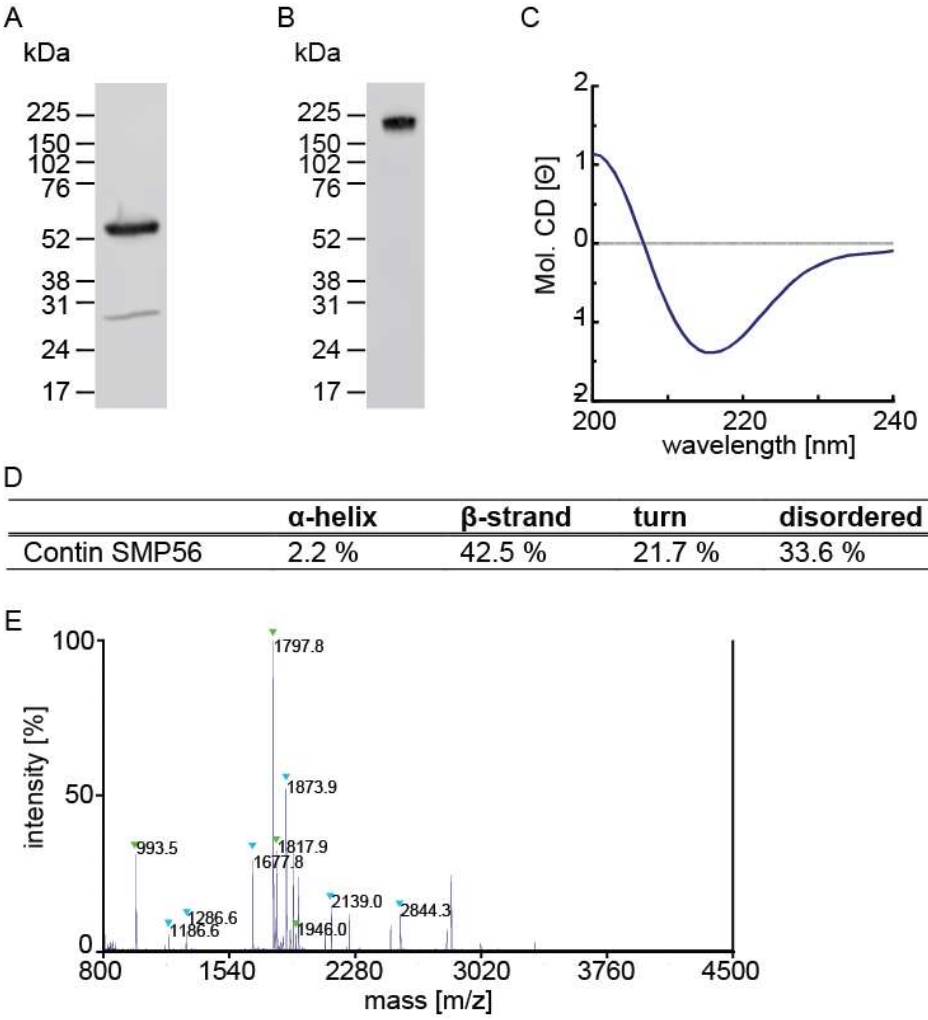

D

	α-helix	β-strand	turn	disordered
Contin SMP56	2.2 %	42.5 %	21.7 %	33.6 %

Figure 3-2: Detailed biochemical analysis of the humanized r8-18C5 antibody.

Western blotting of reduced (A) and non-reduced (B) samples of the r8-18C5 antibody demonstrated that all protein bands detected in Coomassie staining represent a human IgG-molecule or either of the individual chains (A and B). The CD-spectrum revealed a high content of β-sheets, some turns and disordered stretches, and only marginal amounts of α-helical structures. The IgG1-molecule is made up of Ig-domains that mainly consist of β-sheets interconnected by turns or disordered sequences (C). The correct assembly of the heterodimer was demonstrated by mass spectrometry. Green triangles indicate peptides derived from the light chain and blue triangles indicate heavy chain derived peptides (D) The illustration is modified from [101].

3.1.2 Single chain variable Fragment of rOCB-MS2-s5

rOCB-MS2-s5 could be purified from the cell culture supernatant in the same quality described for the other OCB-derived antibodies, but only in very low amounts. Pooling of 1.5 l total expression volume yielded approximately 15 µg (0.01 mg/l) of purified antibody. For comparison, the yields for the other MS-OCB antibodies are 2 – 4 mg recombinant protein per l of culture.

The pooled antibody preparation was analyzed by SDS-PAGE under non-reducing conditions to ensure that H- and L-chains have assembled to a heterodimer (data not shown). Due to low yields, the full length rOCB-MS2-s5 was not analyzed in depth. The recovered amounts of antibody secreted by HEK293E cells were sufficient for screening for antigens using protein microarrays, but were not sufficient for subsequent validation studies. Due to the low expression

in the HEK-system, recombinant production of the rOCB-MS2-s5 in alternative expression systems was evaluated.

Expression screenings in 58-, LTK-, CHO-, 3T3-cells and *in vitro* translation failed to produce sufficient amounts of rOCB-MS2-s5 in feasible culture volumes (data not shown). Therefore, the scF_v-variant of the antibody was produced in *E. coli* BL21. The scF_v-fragment was constructed and cloned into the pET19 vector and expressed in large amounts by this expression system.

3.1.2.1 Refolding of the single chain variable Fragment of rOCB-MS2-s5

The protein formed inclusion bodies (IBs) in *E. coli* BL21. The protein aggregates were purified in Tris buffer supplemented with low concentrations of urea and a detergent and then solubilized in high concentrations of guanidine hydrochloride, yielding 1-5 mg protein per gram wet weight bacterial pellet. To obtain natively folded protein, the solubilized protein is rapidly diluted in PBS, concentrated and dialyzed against PBS to remove residual denaturing agent. The refolding yield was approximately 70 µg/ml of soluble scF_v.

3.1.2.2 Biochemical Analysis of scF_v-PT

The scF_v-MS2-s5 construct carried V5- and His_6-tags but these were not used for affinity purification as the IB-preparation was of sufficient purity. The expected MW of approximately 28 kDa and sufficient purity was verified by SDS-PAGE (Figure 3-3A). Western blotting confirmed that the protein band observed by Coomassie staining represents the recombinant protein with V5-tag.

Folding of scF_v-MS2-s5 into a native state was verified by CD-spectroscopy (Figure 3-3C and D). The secondary structure determined by CD-spectroscopy consists mainly of β-strands (40 %) with little contribution of α-helices (10 %). The other half of the protein contains approximately 20 % of turns and 30 % disordered segments. Whereas the proportions of turns and disordered segments mirror the secondary structure of full length antibodies, the α-helix and β-strand proportions are shifted towards α-helices. This is represented by the more pronounced shoulder at 220-230 nm wavelength and a slight shift of the extremum that has been observed with single-chain constructs before [139, 140]. The identity of the scF_v was further demonstrated by detection of characteristic peptides by mass spectrometry (Figure 3-3E).

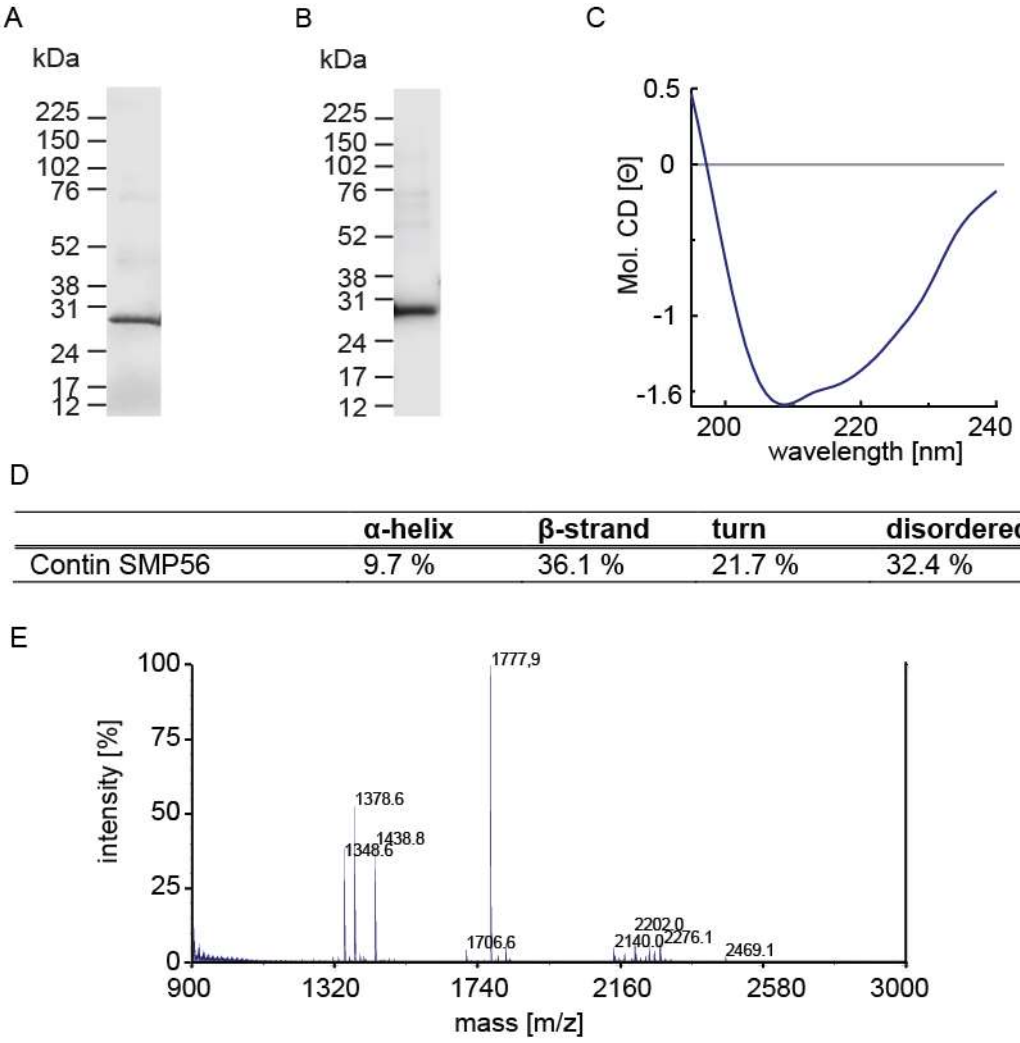

Figure 3-3: Characterization of scF$_v$-MS2-s5.

Size and purity of refolded scF$_v$-MS2-s5 were determined by SDS-PAGE and Coomassie staining showing a strong band at 29 kDa that represents the scF$_v$ (A). Western Blot detection of the V5-tag revealed a band at the same size confirming the identity of the protein band (B). CD-spectroscopy revealed high percentages of β-sheets and disordered stretches in the refolded protein, as expected (C and D). The identity of the refolded protein was demonstrated by mass spectrometry that detected scF$_v$-MS2-s5 specific peptides (E).

3.1.3 Recognition of MOG by r8-18C5

Functionality of the recombinant antibodies was verified using r8-18C5. Binding 8-18C5 produced in mouse hybridoma to MOG is well established and recombinant MOG-fragments were used in three individual experimental setups to ensure the rAbs' capacity to recognize the antigen.

The recombinant extracellular domain of human MOG, spotted onto a nitrocellulose membrane, was recognized by the humanized full length r8-18C5 (Figure 3-4A). The recombinant full length antibody had the capacity of binding the target antigen and carried the V5-tag, which was detectable by Western blotting.

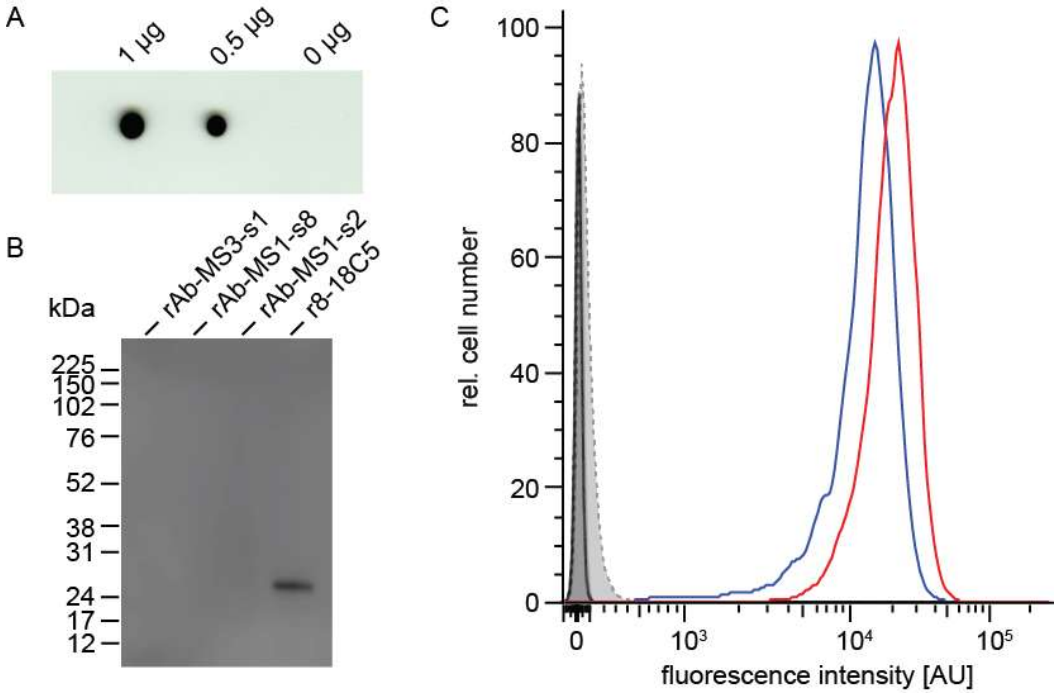

Figure 3-4: Reactivity of r8-18C5 to recombinant human MOG-fragment.

The extracellular domain of human MOG was spotted on a nitrocellulose membrane and detected by r8-18C5 and a secondary antibody to the V5-tag of the rAb. The antibody recognized its antigen in a dose-dependent manner (A). The soluble extracellular domain of MOG was bound by r8-18C5 in an immunoprecipitation experiment, while control antibodies did not show any reactivity (B). The extracellular domain of MOG present on the surface of TE671-cells was detected by r8-18C5 (blue) and the original mouse 8-18C5 (red). Non-transfected TE671-cells were not recognized (grey). Isotype controls rOCB-MS3-s1 and 349040 and secondary antibodies (A21455 and A21236) alone did not recognize MOG (grey) (C). Figure C is modified from [101].

Binding of r8-18C5 to natively folded MOG was demonstrated by immunoprecipitation of the soluble extracellular domain of MOG and FACS analysis with membrane-bound MOG on TE671 cells. The extracellular domain of MOG produced in HEK293E cells was subjected to immunoprecipitation. Control antibodies rOCB-MS3-s1, rOCB-MS1-s8 and -s2 did not show any reactivity whereas r8-18C5 yielded a single band at the expected MW by Western blot detection (Figure 3-4B). TE671-cells, that carry the extracellular loop of MOG [138], were stained with r8-18C5 (blue) and the original mouse IgG 8-18C5 (red), as expected both antibodies strongly reacted to the MOG-positive cells. Isotype controls and secondary antibodies did not show reactivity (Figure 3-4C).

3.2 Identification of MS Candidate Antigens using Protein Microarrays

Previous studies by B. Obermeier and J. Bruder tested for reactivity of MS-OCB derived F_{ab}-fragments to brain homogenate in 2D-Western blots, glycolipids, infectious agents and various proteins on microarrays [100, 102]. In this study, screening of protein microarrays to identify candidate antigens was repeated with full length antibodies. Chances of target antigen identification are enhanced by using full length antibodies due to increased avidity compared to F_{ab}-fragments. Since array hybridization is known to often yield false positive or negative results, potential antigen candidates were later validated by independent experiments (see section 3.3 below).

Commercial Protoarrays® (Invitrogen) were used that contain about 9 400 proteins. These protein microarrays were used as identification tool. Each of the MS-OCB-derived rAbs and r8-18C5 were incubated with one protein microarray and detected by a secondary anti-V5-tag antibody. The secondary antibody was also tested independently in the absence of any primary antibody. Proteins were defined as candidate antigens only if duplicate signals were detected. Further, duplicates with mean signal 3x enriched compared to both the signal intensity of the negative control and the isotype control and 5x enriched to the specific background signal were considered.

Analysis of the individual arrays yielded multiple candidate antigens for each of the monoclonal antibodies except for rOCB-MS3-s1 and rOCB-MS1-s9. The numbers of candidate antigens, the mean signal of the internal negative controls, as well as the mean signal of the specific array for each of the tested MS-OCB-derived antibodies are listed in Table 3-1. The secondary antibody alone and rOCB-MS3-s1 did not yield any duplicate signal as required for a candidate. Galectin 7 was the only protein bound by rOCB-MS1-s9 according to the selection criteria. The low mean signal of internal negative controls indicates generally low unspecific reactivity of the antibodies to proteins on the array and efficient washing procedures. The mean array signal is calculated from all proteins on a particular array. This value is similar for all tested antibodies and further confirms similar background reactivity of the individual rAbs.

Table 3-1: Protein Microarray Results from MS-OCB Antibodies.

For each of the MS-OCB-antibodies, background signal corresponds to the arithmetic mean of all signals from internal negative controls. The second column gives the mean array signal that is calculated from all human protein features on the array. The right column gives the number of candidate antigens according to the selection criteria described in section 2.5.2.

antibody	Mean array signal internal negative controls [AU]	mean array signal [AU]	# of candidate antigens
rOCB-MS3-s1	30	430	0
rOCB-MS1-s8	34	542	8
rOCB-MS1-s9	19	519	1
rOCB-MS4	23	521	4
rOCB-MS1-s2	24	518	9
rOCB-MS2-s5	32	444	13
r8-18C5	18	536	5
Sec. Ab	19	323	0

3.2.1 Recognition of Candidate Antigens by r8-18C5

Hybridization of r8-18C5 to a microarray was used as a positive control for the assay and is depicted in Figure 3-5. The generated signals range from 0 to 65,635 AU and are represented by a color scale from black over red to white. The zoomed area (Figure 3-5B) comprises block 26 with the MOG-protein. The position of the MOG duplicate (green box, C) and features representing internal array controls (red and white boxes) are highlighted in this illustration.

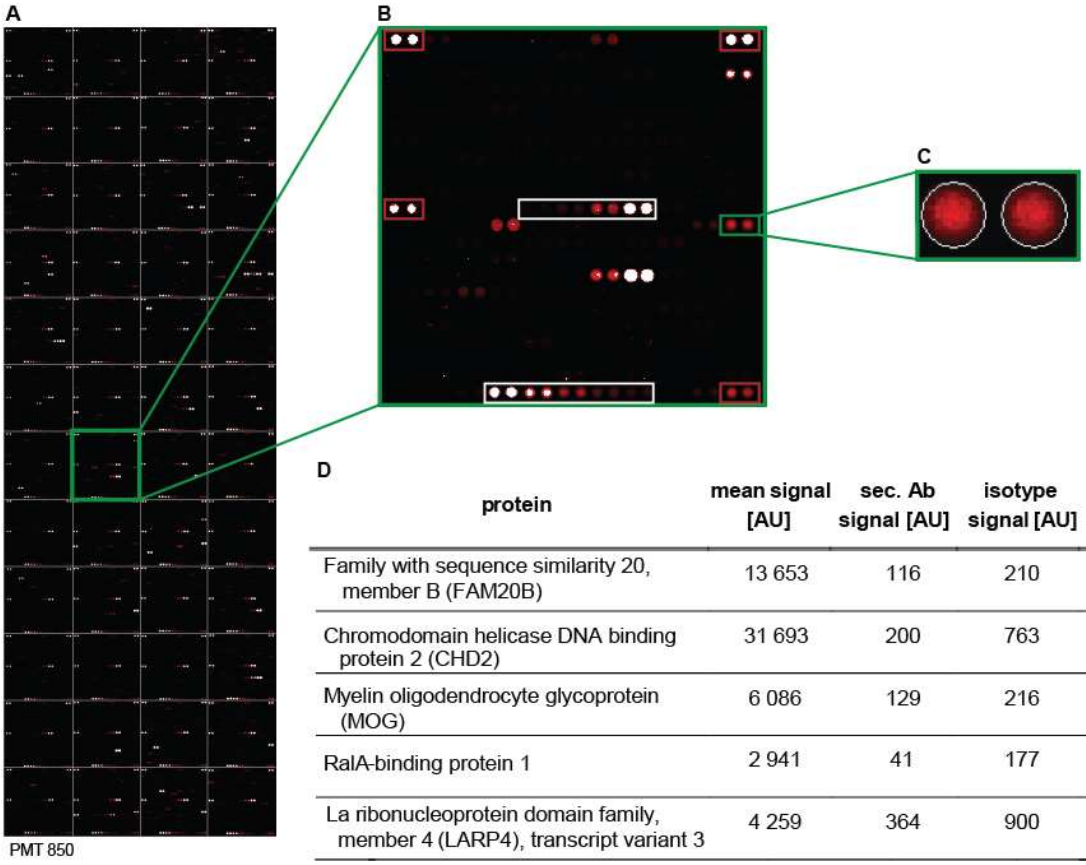

D

protein	mean signal [AU]	sec. Ab signal [AU]	isotype signal [AU]	enriched to isotype
Family with sequence similarity 20, member B (FAM20B)	13 653	116	210	65
Chromodomain helicase DNA binding protein 2 (CHD2)	31 693	200	763	42
Myelin oligodendrocyte glycoprotein (MOG)	6 086	129	216	28
RalA-binding protein 1	2 941	41	177	17
La ribonucleoprotein domain family, member 4 (LARP4), transcript variant 3	4 259	364	900	5

Figure 3-5: Exemplary Protein Microarray probed with r8-18C5.

The left panel depicts the entire array, including all 48 subarrays (A). The green box highlights the subarray of block 26. The enlarged area features positive control signals at the corners that originate from the spotted fluorophore-coupled proteins (red boxes), a gradient of anti-human IgG antibody (upper white box) and a V5-protein gradient (lower white box) (B). The final enlargement shows columns 21 and 22 in row 12 of block 26, the position of the MOG duplicate. The array is shown in PMT850 settings (C). The candidate antigens identified using r8-18C5 are listed (left column, D). Mean signal intensities of the duplicates, their respective secondary and isotype controls (middle columns) and the resulting enrichment factors (right column) are shown (D).

r8-18C5 bound to five proteins on the microarray, four of these produced enrichment factors above 10, including MOG. Interestingly, two proteins on the protein microarray were recognized by this antibody that produced higher signals than MOG. The recombinant FAM20B and CHD2 proteins and the extracellular domain of human MOG were tested for reactivity with r8-18C5 in an independent approach shown in Figure 3-6.

It was shown earlier, that binding of 8-18C5 relies on a linear epitope of MOG [141] that is present in native and denatured conformations. Both may be detected by Western blotting and FACS analysis allows detection of natively folded MOG (compare to Figure 3-4). Thus, MOG and the two other candidates were used in a Western blotting experiment to determine whether the same linear epitope is recognized by r8-18C5. Human MOG was recognized by the antibody on the protein microarray as was the extracellular domain of the human MOG-protein in the Western blotting experiment. The two candidates each yielded bands at the expected MW of 44 kDa (FAM20B) and 81 kDa (CHD2) in SDS-PAGE (Figure 3-6A), but were not detected by r8-18C5 by Western blotting (Figure 3-6B). The only protein detectable with r8-18C5 in this experimental setup was the extracellular domain of MOG with an approximate MW of 21 kDa.

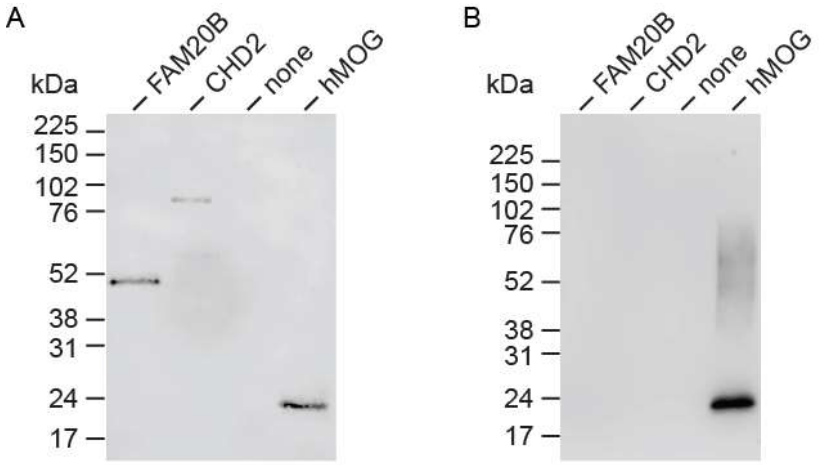

Figure 3-6: Independent Approach to validate Reactivity of r8-18C5 to FAM20B and CHD2.

Commercially obtained FAM20B and CHD2 and the extracellular domain of human MOG each yielded a defined band at the expected MW on SDS-PAGE (A). Except the hMOG-fragment, none of the proteins were detectable with r8-18C5 in the Western blotting approach (B).

Possibly, another epitope is recognized on these two candidate antigens that are only present in natively folded CHD2 and/or FAM20B. These findings underscored the need for validation studies on candidate antigens identified by protein microarrays.

3.2.2 Reactivity Profiles of OCB-derived Antibodies on Protein Microarrays

For all candidate antigens that conform to the selection criteria (section 2.5.2), enrichment compared to the isotype control was determined. Enrichment factors were assumed to correlate with the affinity of the antibody to the candidate antigen. Table 3-2 lists all antigens identified for MS-OCB-antibodies, including mean signal intensity, mean secondary antibody and isotype control signals, and the resulting enrichment factor.

Table 3-2: Candidate Antigens identified by Protein Microarrays using full length rAbs.

All candidate antigens identified with MS-OCB antibodies are listed with the nomenclature used in the Protoarray. The mean signals of the MS-OCB antibody, secondary antibody and isotype control for the specified protein are given in AU. The enrichment factor compared to the isotype control is listed in the right column. Antigens employed in validation assays are highlighted in green, for details on the selection criteria see section 3.3.1.

rAb	protein	mean signal [AU]	sec. Ab signal [AU]	isotype signal [AU]	enriched to isotype
MS1-s8	Family with sequence similarity 84, member A (FAM84A)	65 446	71	163	402
	Alcohol dehydrogenase 5 (class III), chi polypeptide (ADH5)	10 652	22	136	78
	EGF-like domain-containing protein 7	11 541	211	306	38
	NECAP endocytosis associated 1 (NECAP1)	4 499	103	140	32
	Stress-induced-phosphoprotein 1 (Hsp70/Hsp90-organizing protein) (STIP1)	3 464	50	156	22
	GTPase, IMAP family member 4 (GIMAP4)	3 898	114	374	10
	Betaine-homocysteine methyltransferase 2 (BHMT2)	5 299	48	704	8
	STIP1 homology and U box-containing protein 1	4 516	28	1 133	4
MS1-s2	Splicing factor, arginine/serine-rich 17A (SFRS17A)	46 830	74	458	102
	Alcohol dehydrogenase 5 (class III), chi polypeptide (ADH5)	9 867	22	136	73
	Immunoglobulin lambda constant 1 (Mcg marker) (IGLC1)	5 634	66	174	32
	cDNA clone MGC:31936 IMAGE:4765518, complete cds	3 699	113	238	16
	Immunoglobulin lambda locus (IGL@)	2 618	166	299	9
	Ig lambda chain C regions	3 146	144	410	8
	Recombinant human CTLA-4/Fc	6 921	859	1 252	6
	Serine/threonine-protein kinase VRK2	4 940	231	816	6
	WD repeat domain 5B (WDR5B)	6 226	232	1 450	4
MS1-s9	Lectin, galactoside-binding, soluble, 7 (galectin 7) (LGALS7)	3 782	118	397	10
MS2-s5	Cytochrome b5 reductase 3 (CYB5R3), transcript variant M	65 423	177	127	515
	MAP kinase interacting serine/threonine kinase 1 (MKNK1), transcript variant 1	65 453	133	264	248
	EF-hand calcium binding domain 4A (EFCAB4A)	46 759	126	263	178

rAb	protein	mean signal [AU]	sec. Ab signal [AU]	isotype signal [AU]	enriched to isotype
	Chromogranin B (secretogranin 1) (CHGB)	34 038	156	216	158
	MAP kinase-interacting serine/threonine-protein kinase 1	65 438	228	530	123
	Regulatory factor X, 5 (influences HLA class II expression) (RFX5), transcript variant 1	28 355	131	301	94
	MAP kinase-interacting serine/threonine-protein kinase 2	21 412	66	298	72
	PDS5, regulator of cohesion maintenance, homolog A (S. cerevisiae) (SCC-112)	28 348	203	497	57
	FCH domain only 1 (FCHO1)	12 660	117	226	56
	TCF3 fusion partner	14 801	325	732	20
	Melanoma antigen family B, 1 (MAGEB1), transcript variant 1	52 313	409	4 111	13
	Melanoma antigen family H, 1 (MAGEH1)	15 161	2 459	2 829	5
	Twinfilin, actin-binding protein, homolog 1 (Drosophila) (TWF1)	14 203	1 371	3 573	4
MS4	Splicing factor 45	4 525	106	790	6
	STIP1 homology and U box-containing protein 1	6 008	28	1 133	5
	Cortactin (CTTN), transcript variant 2	9 588	118	2 200	4
	Chromatin modifying protein 6 (CHMP6)	9 418	1 846	2 628	4

Each candidate antigen was only detected with one MS-OCB antibody except the “STIP homology and U-box containing protein 1” and the “alcohol dehydrogenase 5 chi polypeptide”, which were recognized by rOCB-MS1-s8 and -MS4 or -MS1-s2 respectively. Antibodies rOCB-MS1-s9 and MS4 generated only enrichment factors of 10 or less. For comparison, the top hits produced by the other OCB-derived antibodies reached factors greater than 100. From the MS-OCB-derived rAbs, rOCB-MS2-s5 recognized the largest number of candidate antigens.

Common molecular patterns or functional similarities were not observed. Yet, about half of the candidate antigens are strictly intracellular. Some candidates are membrane associated and locate to various cell organelles, others may be found at multiple locations, or are secreted proteins. Besides various localizations, a wide range of biological functions and biochemical characteristics are represented by the candidates.

For detailed validation studies, candidate antigens were selected based on enrichment factor, reproducibility from F_{ab}-fragment experiments and recurring protein families or motifs. The particular selection criteria for the individual candidate antigens are described in detail in section 3.3.1. The proteins selected for validation studies are highlighted in green in Table 3-2.

3.3 Validation of Candidate Antigens

Two features of Protoarrays® may have a critical influence on antibody-antigen recognition and may cause false-positive or -negative results: First, all proteins coated on the ProtoArrays® are derived from insect cells. Although the insect cell system is capable of introducing posttranslational modifications (PTMs), those still differ from the human PTM patterns and potentially influence the antibody binding. To exclude reactivity to insect cell specific PTMs introduced by the expression system, validation experiments were done using recombinant protein produced in an expression system other than insect cells. Preferably, proteins expressed in HEK-cells were chosen as these resemble best the human protein that may be encountered by the OCB antibodies *in vivo*. Additionally, the *E. coli* BL21 prokaryotic system was used for recombinant expression. This system is not capable of introducing glycosylation, a major PTM that may influence the antigen recognition. Second, printing the proteins onto a solid phase can affect the protein's secondary structure with unpredictable impact on antibody-reactivity. Consequently, besides recombinant protein derived from an alternative expression system, an independent validation method is required.

Therefore, candidate antigens were independently validated by immunoprecipitation or in ELISA using protein produced in either HEK-cells or *E. coli*. To enable validation experiments, the candidate antigens were either cloned and recombinantly expressed or obtained commercially.

3.3.1 Selection of Candidate Antigens from MS-OCB Antibodies

Three candidate antigens were selected from the pool of candidate antigens identified by protein microarray for detailed validation. Candidates with enrichment factors above 100 were considered. To further confine the selection, previous identification of the candidate antigen with the F_{ab}-fragment and recurring appearance of protein motifs and families was considered. Thus, validation studies were carried out with candidate antigens FAM84A, AKAP17A, and the MKNK-family using rOCB-MS1-s8, rOCB-MS1-s2 and rscF_v-MS2-s5 respectively. Figure 3-7 depicts duplicate signals (left panel) of each of the candidate antigens selected for validation along with the according secondary antibody controls (right panel). MKNK1, MKNK1_1 and FAM84A reached signal intensities at saturation (represented by white color). The signal produced by AKAP17A (SF17A)-recognition did not reach the maximum, but showed strong reactivity. MKNK2 elicited only medium signal (represented by red color). In all cases, the secondary antibody control did not yield any signal with the selected candidate antigens. The following sections substantiate the selection of the candidate antigens for validation from the pool of candidates and outline their key characteristics.

Information on basic structural and functional features of the candidate antigens studied in detail in validation experiments was retrieved from the UniProt data base [142] and the Proteinatlas [143] and is summarized in Figure 3-7B.

A

Antibody	Protein	Sec. Ab
rOCB-MS2-s1	MKNK1	
	MKNK1_1	
	MKNK2_1	
rOCB-MS1-s8	FAM84A	
rOCB-MS1-s2	SF17A	

PMT 850

B

Protoarray description	UniProt-ID	Name	Localization	Function
MAP kinase interacting serine/ threonine kinase 1 (MKNK1)	Q9BUB5-1	MAP kinase interacting kinase 1	cytoplasmic, potentially nuclear	translational regulation
Family with sequence similarity 84, member A (FAM84A)	Q96KN4-1	Family with sequence similarity 84 A	cytoplasmic/nuclear?	NA
Splicing factor, arginine/serine-rich 17A (SFRS17A)	Q02040-3	A-kinase anchoring protein 17A	nuclear speckles	regulation of pre-mRNA splicing

Figure 3-7: Details of Candidate Antigens identified by Protein Microarray Analysis.

The illustration shows details from microarrays scanned with PMT850 setting (A). Protein name and ID from the UniProt database and a description of the proteins localization and function are given (B). Of note, MKNK1 and MKNK1_1 spotted on the array at different locations represent the same isoform of the protein, despite differential naming by the manufacturer. The figure is modified from [101].

Candidate Antigen MKNK1

MAP kinase interacting kinase 1 (MKNK1) was recognized by rOCB-MS2-s5. Three out of 13 candidates identified for this antibody belonged to the MKNK-families 1 and 2, providing strong evidence for actual reactivity of rOCB-MS2-s5. MKNK1 was selected for validation experiments.

MKNK1 and MKNK1_1, that both reached signal intensities at saturation, represent the same protein. MKNK1 and MKNK2 are homologous proteins that share 51 % sequence identity. The two family members differ in their C-terminus and a central 41 AA-stretch that is absent in MKNK2 thus creating a 47 kDa large protein, while the MW of MKNK1 is 51 kDa (see Figure 3-8).

For MKNK1, data on protein expression levels is not available, but RNA data suggests expression of the protein in the majority of tissues. The candidate antigen recognized by rOCB-MS2-s5 with the highest enrichment factor was cytochrome b5 reductase, transcript variant m (f=515, CYB5BR3). CYB5R3 was not selected as primary candidate of rOCB-MS2-s5 because the MKNK-family was highly overrepresented.

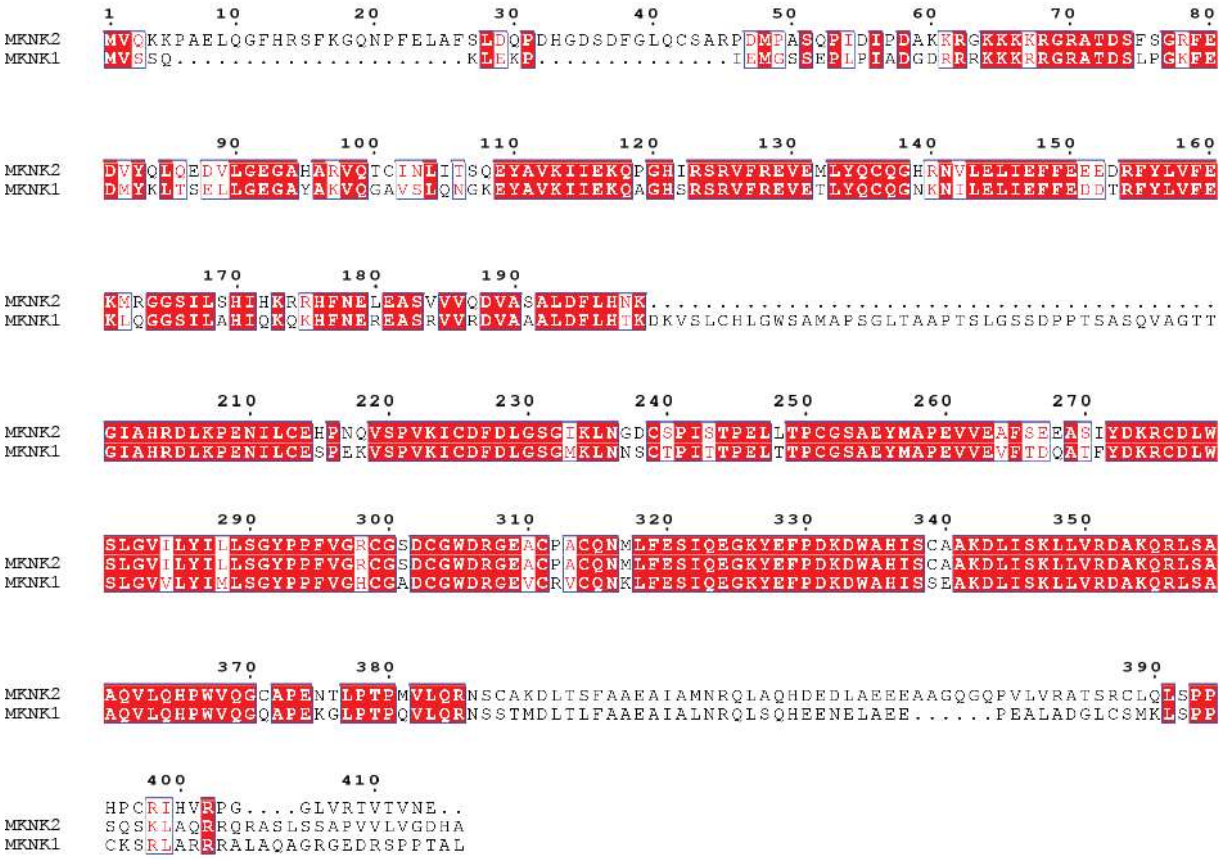

Figure 3-8: Sequence Alignment of MKNK-isoforms.

The three aligned MKNK-isoforms share high overall similarity. The N-terminal region of MKNK2 (upper row) is longer compared to MKNK1 (bottom row). MKNK2 is missing a 41-AA stretch that is found in MKNK1. White letters in red boxes represent residues identical in all three proteins. Homologous residues are depicted as red letters in white boxes. Letters without boxing indicate non-conservative exchanges or insertions/deletions in one of the sequences. Periods represent gaps.

Candidate Antigen FAM84A

Very high signal intensities (f=402) were recorded for reactivity of rOCB-MS1-s8 to “family with sequence similarity 84A-protein” (FAM84A). For comparison, the signals produced by other candidates of rOCB-MS1-s8 were at least five-fold less. Even though enrichment factors of 70-80 were reached, these candidates were deferred.

FAM84A is a 32 kDa protein that is localized in the cytoplasm.

Candidate Antigen AKAP17A

AKAP17A, termed SF17A in the ProtoArray®, has consistently been identified with the full length antibody rOCB-MS1-s2 and the corresponding F_{ab}-fragment. Additionally, this protein elicited by far the highest signal that was detected for rOCB-MS1-s2. AKAP17A is present on the array in its 52 kDa isoform, i.e. isoform 3, which was selected for subsequent experiments. The protein is mainly found in nuclear speckles and a minor fraction of the protein is localized in the cytoplasm.

3.3.2 Recognition of MKNK1 by rOCB-MS2-s5

rOCB-MS2-s5 had shown strong reactivity to multiple MKNK-family members on the protein microarray. MKNK1-protein used for validation studies was recombinantly produced in HEK293-cells (amsbio).

3.3.2.1 Immunoprecipitation of MKNK1

To verify that the OCB-derived antibody rOCB-MS2-s5 specifically binds to MKNK1, recombinant candidate antigen derived from HEK-cells was subjected to immunoprecipitation and subsequent Western blot analysis.

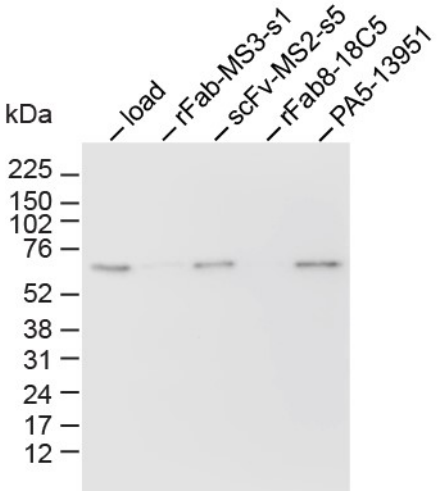

Figure 3-9: Immunoprecipitation of MKNK1.

Only rscF$_v$-MS2-s5 and PA5-13951 specifically recognized MKNK1, while control antibodies did not yield signals. rscF$_v$-MS2-s5 and the commercial PA5-13951 to MKNK1 precipitated a single protein band at approximately 60 kDa with similar intensity to the loading control. The exemplary blot is representative of three individual experiments. The figure is modified from [101].

rscF$_v$-MS2-s5 specifically precipitated MKNK1 which was detected by Western blotting as a single band at approximately 60 kDa MW. The positive control antibody PA5-13951 yielded a slightly stronger band with the same size. The expected molecular weight of MKNK1 is 51 kDa. The control F_{ab}-fragments rFab-MS3-s1 and rFab8-18C5 did not yield any signal.

3.3.2.2 ELISA of MKNK1

Commercial MKNK1 was directly applied to an ELISA plate. In contrast to the other validation experiments described here, MKNK1 was validated using the scF$_v$-fragment of rOCB-MS2-s5. F_{ab}-fragments of other MS-OCB antibodies served as negative controls. Because the scF$_v$-fragment possesses only a single antigen binding site, F_{ab}-fragments were used to mirror the binding characteristics of scF$_v$-MS2-s5.

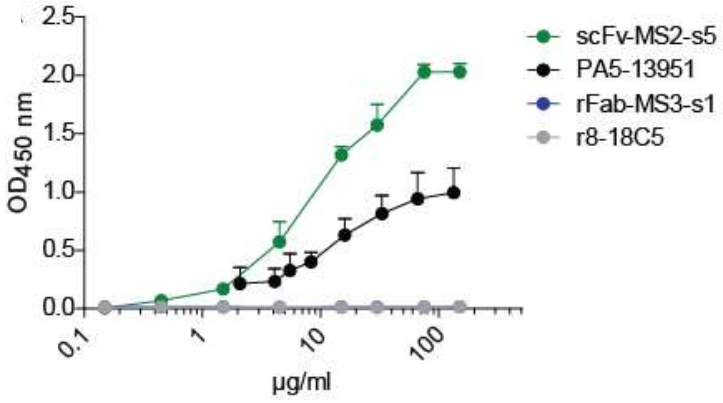

Figure 3-10: Titration of scF$_v$-MS2-s5 Reactivity to MKNK1 by ELISA.

scF$_v$-MS2-s5 specifically recognized recombinant MKNK1 in a dose dependent manner, while none of the control antibodies yielded signals above background. The commercial antibody PA5-13951 recognized MKNK1 with slightly higher affinity than the OCB-derived scF$_v$-MS2-s5. Data represents four independent experiments. The figure is modified from [101].

ELISA on MKNK1 clearly confirmed that MKNK1 is recognized by scF$_v$-MS2-s5 in a dose dependent manner, as illustrated in Figure 3-10. PA5-13951 recognized MKNK1 with slightly higher affinity. OCB-derived F$_{ab}$-fragments as well as secondary antibodies to either human IgG H- and L-chains, rabbit IgG, or V5-tag alone showed background reactivity. After multiple freeze-thaw cycles, MKNK was denatured and was no longer recognized by scF$_v$-MS2-s5 (data not shown). Thus, scF$_v$-MS2-s5 recognizes a conformational epitope of MKNK1.

To test whether the reactivity can be detected in cells, HEK293E-cells, either transfected with MKNK1 or non-transfected, were stained with scF$_v$-MS2-s5. scF$_v$-MS2-s5 did not show any reactivity in neither transfected nor non-transfected cells (data not shown). Although MKNK1 is expressed in HEK293E-cells, the positive control antibody PA5-30705 only recognized transfected cells but not non-transfected cells.

3.3.2.3 MKNK1-reactivity in a larger Patient Cohort

To test whether other MS patients were reactive to MKNK1, CSF samples were screened for reactivity in the MKNK1-ELISA described above. Screening revealed no difference between the MS- and NIND-cohort. Both groups showed only background reactivity with single values slightly above the group mean (Figure 3-11).

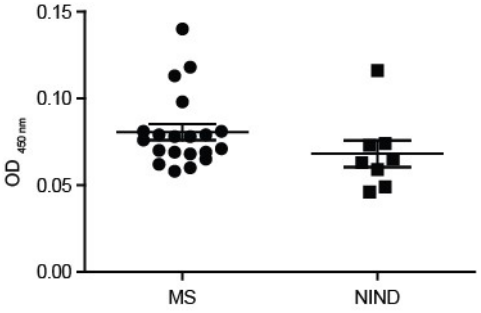

Figure 3-11: Screening of CSF Samples from MS and NIND patients for Reactivity to MKNK1.

CSF samples from patients from MS- and NIND-cohorts were tested for reactivity to MKNK1 by ELISA. Reactivity of the MS-group was not different from the reactivity detected for NIND-samples. Individual samples had slightly increased reactivity in both groups.

3.3.3 Recognition of FAM84A by rOCB-MS1-s8

Recombinant FAM84A was used in two formats: First, commercially obtained FAM84A produced in HEK293-cells was used for initial verification of reactivity with rOCB-MS1-s8. Attempts to express and purify this protein in HEK293E-cells did not yield sufficient amounts of secreted protein. FAM84A-transfected HEK293E-cells were used for further verification of rOCB-MS1-s8 reactivity. Second, FAM84A was recombinantly expressed and purified from *E. coli*. Recombinant *E. coli*-derived protein was used in ELISA to verify the reactivity of rOCB-MS1-s8 to FAM84A and to test a larger patient cohort for such reactivity.

3.3.3.1 Expression of recombinant FAM84A

FAM84A was cloned into the pTT5 vector, carrying V5- and His_6-tags and the same signal sequence applied for antibodies. Using standard expression conditions in HEK293E-cells, the protein was produced, but insufficiently secreted (data not shown).

Therefore, the FAM84A-gene with tags was transferred to the pET33b(+)-vector for prokaryotic expression. The protein was soluble inside *E. coli* BL21 bacteria and purified by IMAC using its His_6-tag. Expression yields were approximately 5 – 6 mg of natively folded protein per liter bacterial culture. The expected MW of the recombinant product was 32 kDa, the purified protein migrated at around 38 kDa on SDS-gels. Coomassie staining revealed the presence of one major band at 38 kDa and three additional bands at lower MWs (Figure 3-12A). Comparing Coomassie staining to Western blotting results demonstrated that all three protein bands at MW of 38 kDa, 35 kDa and 32 kDa correspond to the FAM84A protein (Figure 3-12B). These bands result from proteolysis and represent an N-terminally truncated FAM84A-fragment as demonstrated by Edman-degradation (data not shown). The protein band at around 25 kDa seen in Coomassie staining, but not with Western blotting, may either be an unrelated contamination or a proteolytic FAM84A-product that is no longer detectable by anti-V5 Western blotting. The preparation was analyzed by CD-spectroscopy to determine the secondary structure. The spectrum reveals evenly distributed secondary structures with a slightly higher prevalence of β-sheets (Figure 3-12C and D), these data coincide with the predicted secondary structure (section 2.4.5).

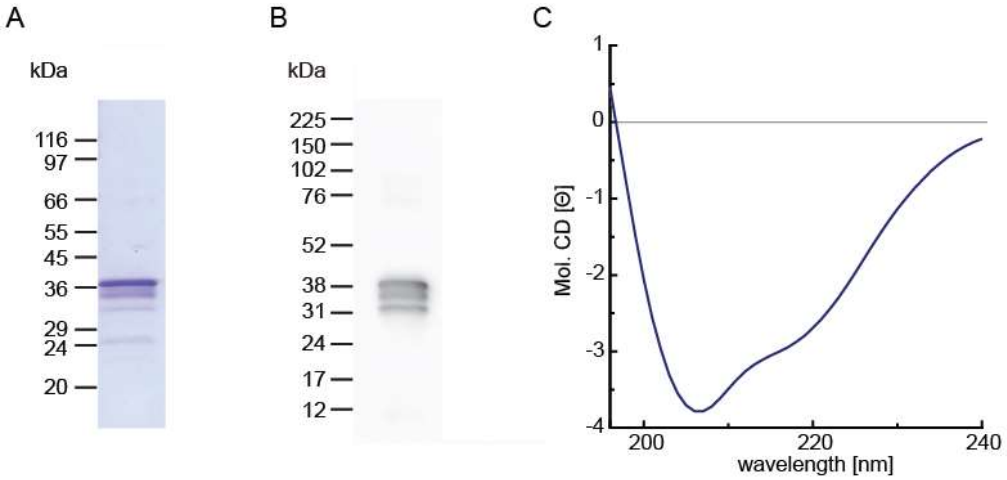

D

	α-helix	β-strand	turn	disordered
Contin SMP56	20.5 %	25.4 %	22.8 %	31.3 %

Figure 3-12: Characterization of recombinant FAM84A purified from *E. coli*.

Staining with Commassie brilliant blue of FAM84A separated by SDS-PAGE reveals the presence of three distinct bands at MW of 30-38 kDa. The uppermost band represents the majority of the sample's protein content and corresponds to FAM84A. The recombinant protein has an expected MW of 32 kDa (A). Western blotting, detecting the C-terminal V5-tag of the protein revealed that all three bands with approximately the correct size are FAM84A (B). The conformational state of FAM84A was determined by circular dichroism spectroscopy. FAM84A is predicted to have α-helix, β-sheet and disordered regions as reflected by the CD-spectrum (C and D).

3.3.3.2 Immunoprecipitation of FAM84A

To verify that the OCB-derived antibody rOCB-MS1-s8 specifically binds to FAM84A, HEK derived FAM84A (amsbio) was subjected to immunoprecipitation and subsequent Western blot analysis.

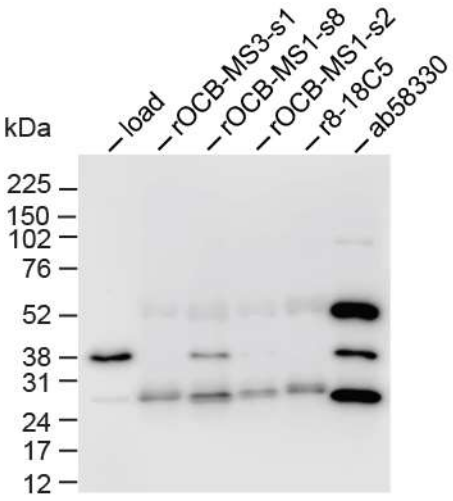

Figure 3-13: Immunoprecipitation of FAM84A.

rOCB-MS1-s8 and the commercial antibody ab58330 to FAM84A recognized a protein band at 38 kDa. The expected MW of FAM84A was 31 kDa. Only rOCB-MS1-s8 and the commercial anti-FAM84A antibodies specifically recognized FAM84A, while the control antibodies did not yield signals. Additional bands at 52 kDa and 26 kDa correspond to H- and L-chains of the antibodies that are cross-reactive with the secondary antibody. The exemplary blot is representative of three individual experiments. The figure is modified from [101].

FAM84A was individually incubated with rOCB-MS1-s8, two other OCB-derived antibodies rOCB-MS3-s1 and rOCB-MS1-s2, r8-18C5, and the monoclonal antibody ab58330 to FAM84A as positive control. As shown in Figure 3-13, rOCB-MS1-s8 is the only of the OCB-derived antibodies that bound detectable amounts of FAM84A, migrating at approximately 38 kDa. The other two OCB-derived antibodies and r8-18C5, which served as negative controls, did not

precipitate the candidate antigen. ab58330 had precipitated FAM84A. Additional bands at 52 kDa and 26 kDa correspond to the H- and L-chains of the antibodies used for precipitation.

3.3.3.3 Immunofluorescence Staining of FAM84A

The reactivity of rOCB-MS1-s8 to FAM84A was further confirmed by immunofluorescence staining of HEK293E-cells. These cells endogenously express low levels of FAM84A [143], thus FAM84A transfected as well as non-transfected cells were stained.

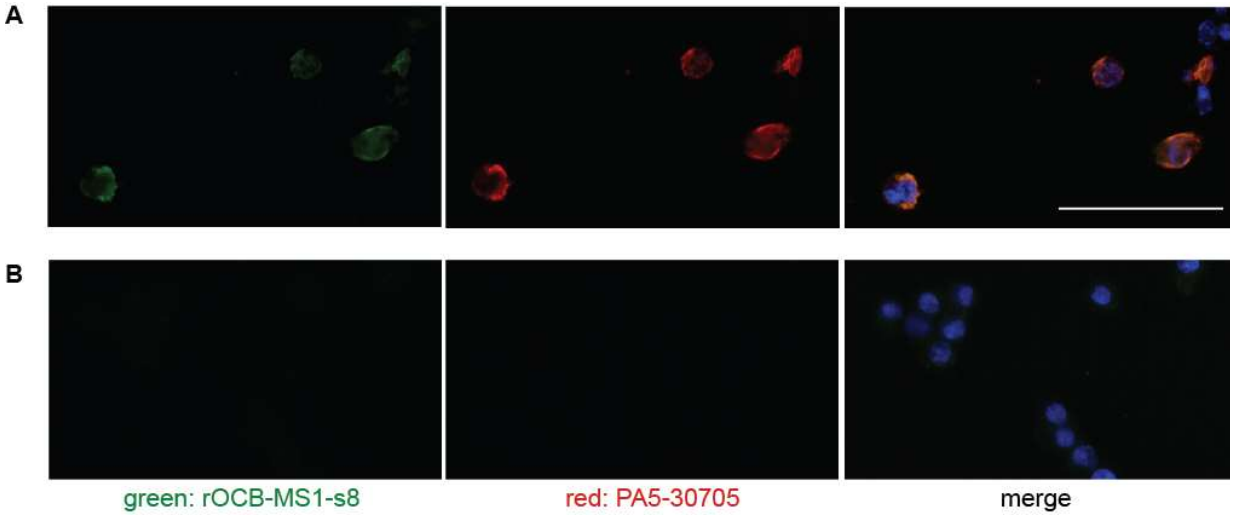

Figure 3-14: Immunfluorescence Staining of HEK293E-cells with rOCB-MS1-s8.

FAM84A-transfected (A) and non-transfected (B) HEK293E-cells were stained with rOCB-MS1-s8 (green) and PA5-30705 (red) as positive control. Both rOCB-MS1-s8 and PA5-30705 stained transfected cells in perinuclear regions but did not yield any signal with non-transfected cells. Scale bar: 50 µm.

As shown in Figure 3-14, rOCB-MS1-s8 and PA5-30705 both stained FAM84A transfected cells in perinuclear regions. Detected signals had higher intensity at their outer boundaries and were less intense in the center. Merging the channels revealed good overlap of signals. In contrast, non-transfected cells were neither recognized by rOCB-MS1-s8 nor by PA5-30705.

3.3.3.4 ELISA of FAM84A

An ELISA was developed to enable screening of biological material of a larger patient cohort for reactivity to FAM84A. FAM84A was bound to the assay plate in an oriented manner via its V5-tag. The OCB-derived monoclonal antibodies were incubated with the target antigen and then detected using an HRP-coupled polyclonal antibody against human IgG.

The ELISA confirmed the reactivity of rOCB-MS1-s8 to FAM84A and substantiated the results of the immunoprecipitation. rOCB-MS1-s8 recognized FAM84A in a dose-dependent manner and control antibodies showed signals on background level. At extreme IgG-concentrations, minor reactivity of the control antibodies was detected. The signal of the commercial antibody ab58330 to FAM84A showed much stronger reactivity (Figure 3-15).

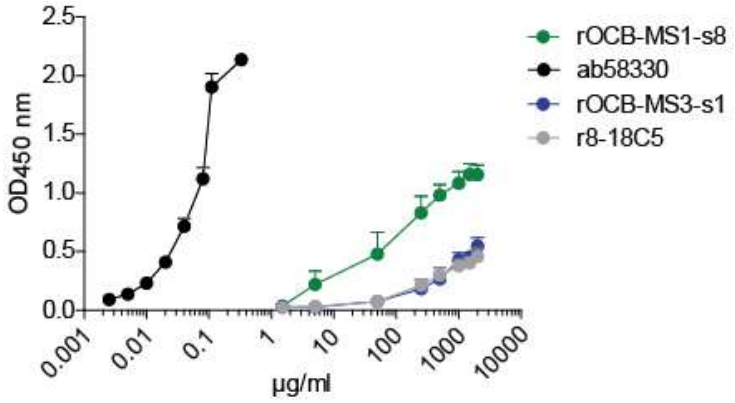

Figure 3-15: ELISA validating the Reactivity of rOCB-MS1-s8 to FAM84A.

rOCB-MS1-s8 recognized FAM84A in a dose dependent manner as determined by ELISA. The commercial antibody ab58330 to FAM84A showed very high signals at low concentrations. Control antibodies yielded background signal and minor reactivity at extreme IgG-concentrations. The secondary antibody controls did not show any signal. Data represents four independent experiments. The figure is modified from [101].

Two proteolytic forms of FAM84A (see section 3.3.3.1) that occupy α-V5 binding sites but are not recognized by rOCB-MS1-s8 are present. The comparably lower signal from rOCB-MS1-s8 may in part be due to the reduced total number of molecules available for specific recognition.

3.3.3.5 FAM84A-reactivity in a larger Patient Cohort

Increased reactivity to FAM84A in serum and CSF has previously been described in the context of the autoimmune disease inflammatory bowel disease and multiple sclerosis [95, 144]. To determine whether other MS patients recognized FAM84A, the FAM84A-ELISA was employed to screen CSF and serum samples of larger patient cohorts including various controls. The individual samples were used in the ELISA without prior knowledge of their classification to one of the groups of neurologic disorders in study.

a) CSF Samples

A total of 65 CSF samples was analyzed representing multiple sclerosis (MS), neuroborreliosis (NB), other inflammatory diseases (OID), cranial nerve palsies (CNP) and non-inflammatory neurologic diseases (NIND) cases. Analysis revealed no difference in reactivity to FAM84A between CSF from MS patients compared to NIND-samples (Figure 3-16A). However, CSF of patient MS1, from which rOCB-MS1-s8 was derived, shows increased reactivity reaching the level of the monoclonal rAb used to validate the ELISA assay (compare to Figure 3-15). Samples of the CNP group were found to have slightly increased mean reactivity to FAM84A. In contrast, samples from patients with NB and OID showed significantly increased reactivity against FAM84A in comparison to NIND-samples. Besides increased mean reactivity of the samples from inflammatory conditions, these samples also showed higher variance within the group than the non-inflammatory CSF samples. These groups contain the samples producing highest signals, but also some with signals ranging around the control levels (Figure 3-16A).

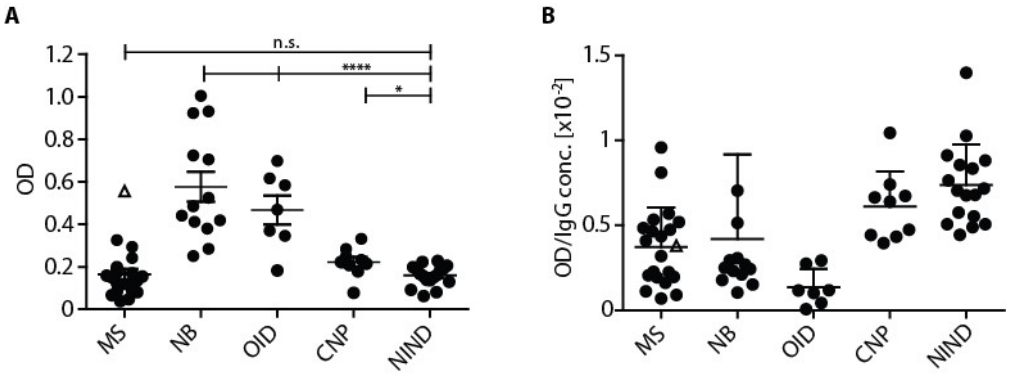

Figure 3-16: Reactivity against FAM84A in CSF samples of Patient Cohorts by ELISA.

CSF samples were applied without dilution to the FAM84A-ELISA. The mean reactivity in the MS-group was not different from the control NIND-group. However, CSF from MS1 (depicted as Δ), from which rOCB-MS1-s8 was cloned, did show increased reactivity. The NB- and OID-groups showed significantly increased reactivity to FAM84A compared to the NIND-group. CNP-samples had slightly increased reactivity compared to the NIND-samples (A). To account for different IgG-concentrations, OD values were corrected for IgG-concentration. After corrections, the increased reactivity of MS1 was no longer present. Increased mean reactivity of the NB- and OID-groups was also removed (B). ****=p≤0.0001, *=p≤0.1, and n.s. = not significant. Data are representative of two independent experiments. The figure is modified from [101].

NB and OID are acute inflammatory diseases of the CNS. Therefore, IgG-concentrations in these samples are strongly increased as compared to NIND samples. IgG titers of MS-samples were moderately increased in comparison to NIND-samples. NIND- and CNP-samples showed normal IgG-concentrations. To test whether increased total IgG in the NB- and OID-samples account for the FAM84A-reactivity in the assay, OD-values were corrected for IgG-concentration (Figure 3-16B). After correction, reactivity of NB- and OID-samples was no longer different from the other groups. Also, the reactivity of CSF of patient MS1 did not exceed the mean reactivity of the MS-group.

In summary, CSF samples from patients with infectious conditions showed reactivity to FAM84A whereas samples from MS patients did not show enhanced reactivity except the CSF of patient MS1. This effect is mainly due to increased IgG-levels in inflammatory samples.

b) Serum Samples

Matching serum samples were analyzed in parallel to CSF samples. Analysis did not reveal any significant difference between mean reactivity of the groups. In both the MS and NB cohort, two patient samples evidently exceeded the mean signal of the group, one in the MS-group being the MS1 sample (Figure 3-17A). NB and OID mean signals did not differ significantly from the other groups, in contrast to the findings with the respective CSF-samples.

The IgG-titers from all patient serum samples were similar as compared to CSF samples. As above (Figure 3-16B), OD values were corrected for IgG-concentration of the sample (Figure 3-17B). After corrections, two MS-samples and one NB-sample were still different from the respective group mean.

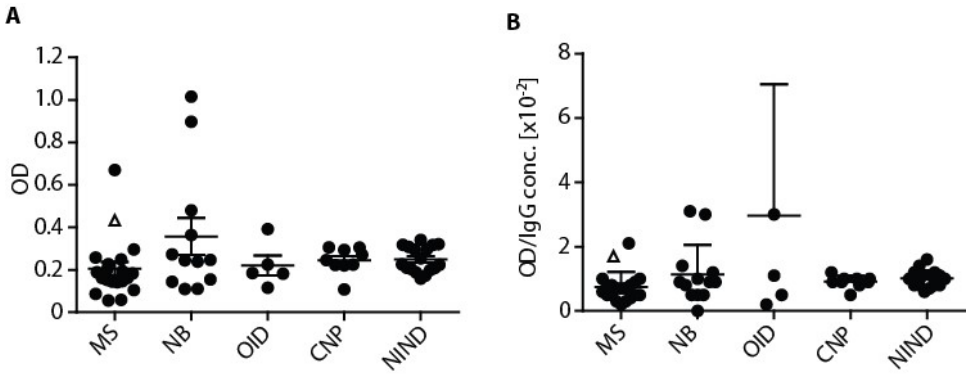

Figure 3-17: Reactivity against FAM84A in Serum Samples of Patient Cohorts by ELISA.

Serum samples diluted 1:400 were applied to the FAM84A-ELISA. In the MS-group, two samples exhibited increased signal intensities. One of these is serum MS1 (depicted as Δ). Also, two samples in the NB-cohort and one in the OID-cohort showed increased reactivity. The mean reactivity to FAM84A was similar for all groups (A). After corrections for IgG-concentration, the same samples of the MS-group showed increased reactivity. From the NB-cohort, only one sample showed consistent reactivity independent of its IgG-concentration. The increased reactivity of one sample in the OID-group was no longer present. IgG-concentrations were comparable between the groups (B). Data are representative of two independent experiments. The figure is modified from [101].

3.3.4 Recognition of AKAP17A by rOCB-MS1-s2

AKAP17A was cloned and recombinantly produced in the cytosol of HEK-cells. The recombinant protein was used for immunoprecipitations to verify the reactivity of rOCB-MS1-s2 to AKAP17A.

3.3.4.1 Expression of recombinant AKAP17A

The AKAP17A-coding sequence, including a secretory signal peptide and C-terminal His_6-tag, was cloned into the pTT5 vector and expressed in HEK293E-cells. As observed before with FAM84A, the amount of secreted AKAP17A in the cell culture supernatant was only marginal (data not shown), despite fair expression in the cell pellet. Various other expression systems, including wheat germ extract and CHO-cells, were tested for AKAP17A production, but none of the systems secreted sufficient amounts of AKAP17A (data not shown). Thus, protein extraction from cell pellets was explored as an alternative approach.

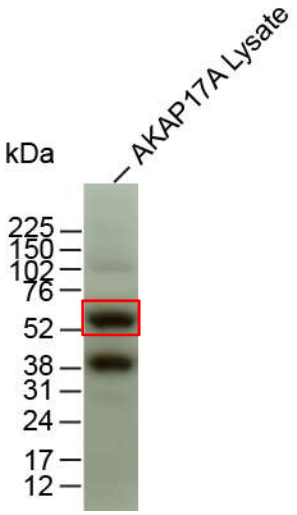

Figure 3-18: AKAP17A in HEK293E lysates.

The crude lysate of AKAP17A-transfected HEK-cells contains large amounts of the recombinant target protein with a MW of 52 kDa. An additional band with comparable signal strength is observed at 40 kDa. Weak bands at 31 and 102 kDa are present as well. Additional bands may represent either proteolytic products or aggregates or derive from endogenous AKAP17A-variants.

AKAP17A-transfected HEK293E-cells were lysed using a high-salt buffer. The lysate contained a plethora of different proteins (data not shown), but also contained considerable amounts of AKAP17A as determined by Western blotting detection with a monoclonal antibody to AKAP17A (Figure 3-18). The originally transfected construct at approximately 52 kDa size was present along with a second, smaller fragment of around 40 kDa MW. This may represent a proteolytic product. Data reveals the presence of AKAP17A in the soluble fraction of crude HEK293E-cell lysate. AKAP17A is potentially associated with lipid structures because the protein is no longer detectable after ultracentrifugation (data not shown). AKAP17A was not detectable in non-transfected cell lysates (data not shown).

A variety of different detergents and high salt conditions were tested, but failed to identify suitable purification conditions (data not shown). Additional purification steps were therefore deferred and detailed characterization of the target protein was precluded by the insufficient purity of the preparation. Validation experiments were carried out using the crude HEK293E-cell lysate.

3.3.4.2 Immunoprecipitation of AKAP17A

Immunoprecipitation of AKAP17A from crude HEK293E-cell lysate validated the reactivity of rOCB-MS1-s2 identified in the protein microarray screening. The crude lysate was first pre-cleared with uncoupled Protein G beads and then incubated with rAbs covalently coupled to Protein G beads. The eluted molecules were analyzed by Western blotting using the monoclonal MCA4225Z antibody to human AKAP17A.

The immunoprecipitation experiment confirmed binding of rOCB-MS1-s2 to AKAP17A. Both, rOCB-MS1-s2 and MBS711914, a polyclonal antibody to AKAP17A, precipitated a band at 52 kDa (Figure 3-19). In contrast to rOCB-MS3-s1 and r8-18C5, which did not show reactivity to AKAP17A, the rOCB-MS1-s8 unexpectedly recognized AKAP17A. Of note, this antibody was previously found to bind FAM84A (section 3.3.3.2). Additional bands at larger MW that were present in the loading control were not detected in the precipitates.

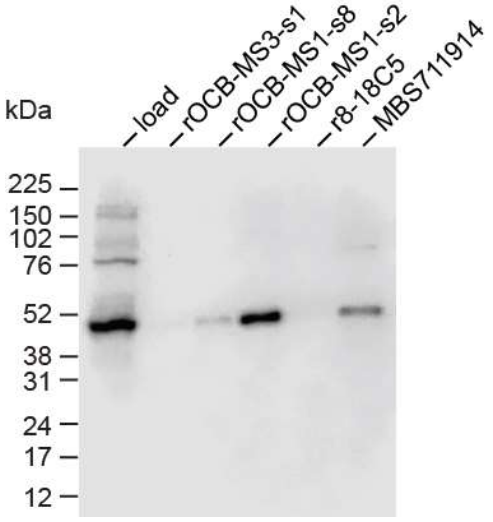

Figure 3-19: Immunoprecipitation of AKAP17A.

Recombinant AKAP17A was precipitated from crude HEK293-cell lysate by the positive control antibody MBS711914 and the OCB-derived antibodies rOCB-MS1-s8 and rOCB-MS1-s2. The expected MW of AKAP17A is 52 kDa. Additional bands in the loading control were not detected in the precipitates. Other control antibodies rOCB-MS3-s1 and r8-18C5 did not show reactivity to AKAP17A.

3.3.4.3 Immunofluorescence Staining of AKAP17A

To demonstrate that rOCB-MS1-s2 recognizes AKAP17A in cells as well, HEK293E-cells were stained. Since AKAP17A is expressed in these cells, however in low levels [143], antigen transfected and non-transfected cells were used.

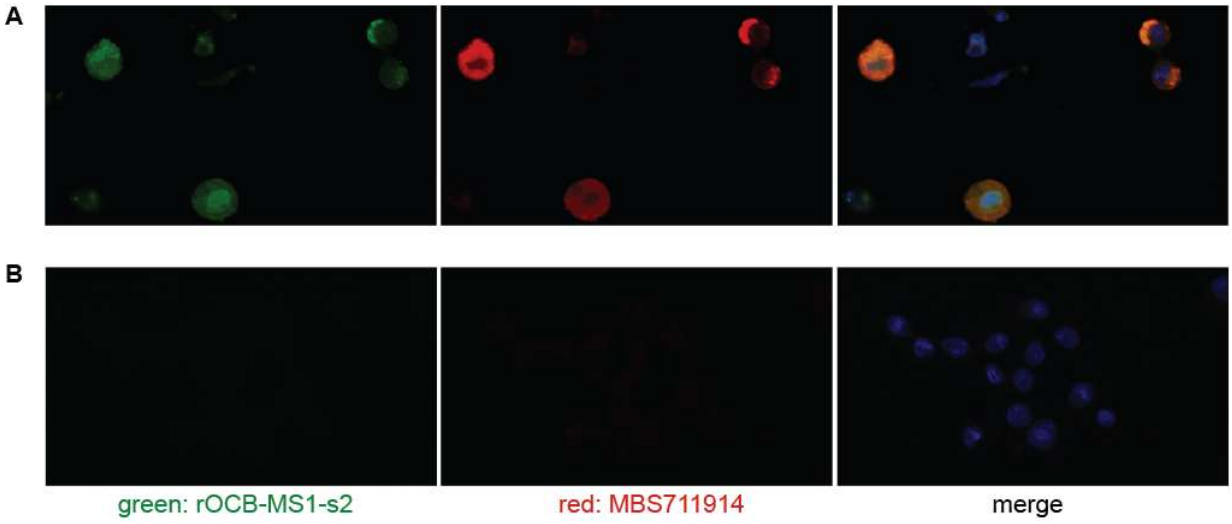

Figure 3-20: Immunfluorescence Staining of HEK293E-cells with rOCB-MS1-s2.

AKAP17A-transfected (A) and non-transfected (B) HEK293E-cells were stained with rOCB-MS1-s2 (green) and MBS711914 (red) as positive control. Both rOCB-MS1-s2 and MBS711914 stained transfected cells in perinuclear regions, but did not yield any signal with non-transfected cells. See Figure 3-14 for scale bar.

Immunofluorescence staining of AKAP17A transfected HEK293E-cells with rOCB-MS1-s2 and MBS711914 further confirmed AKAP17A as target antigen. rOCB-MS1-s2, like the positive control, stained perinuclear regions of transfected cells. In part of the stained cells, the signal was locally enriched. In contrast, neither of the antibodies yielded any signal in non-transfected cells even though HEK293E-cells endogenously express AKAP17A [143].

3.4 Cross-reactivity of rOCB-MS1-s8 to FAM84A and AKAP17A

Validation studies for AKAP17A revealed that rOCB-MS1-s8, besides binding FAM84A, also recognized AKAP17A. The major hypothesis to explain this finding is that both antigens share a structural characteristic that allows rOCB-MS1-s8 to bind to both proteins. This may be a similar AA-sequence or a secondary structure that forms similar epitopes. Therefore, the AA-sequences of both target antigens AKAP17A and FAM84A were aligned to detect sequence stretches with high similarity and secondary structure predictions were analyzed to find structural characteristics that may cause the observed cross-reactivity.

3.4.1 Identification of potentially cross-reactive Epitopes

Global alignment of the two AA-sequences did not disclose highly similar regions, but local alignments of 20 AA-stretches of FAM84A to the complete AKAP17A sequence revealed two sections that are similar in the two proteins (Figure 3-21).

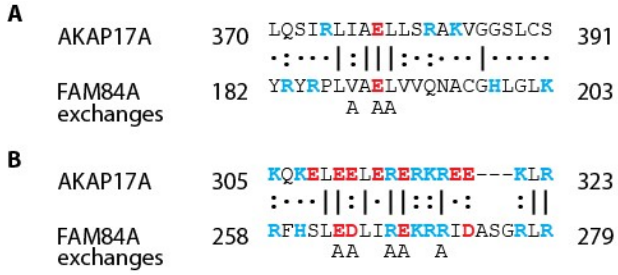

Figure 3-21: Potential Epitopes of AKAP17A and FAM84A for rOCB-MS1-s8 Recognition.

AKAP17A AA370-391 (A) and AA305-323 (B) are shown in comparison to FAM84A AA182-203 and AA258-279 respectively. The two AA-stretches were selected based on their high AA-sequence similarity. The AA370-391 stretch in AKAP17A shares high homology with AA182-203 of FAM84A (A). Even higher homology is seen between the AA305-323 in AKAP17A and AA258-279 in FAM84A (B). Blue characters indicate positively charged AA. Red characters represent negatively charged residues. Identical residues are represented by a vertical line, colon depicts highly similar residues and periods weakly similar residues, dashes represent gaps. The figure is modified from [101].

First, FAM84A AA182-203 comprises six AA that closely resemble AA370-391 of AKAP17A. There are four identical and two highly similar AA in close proximity surrounded by non-homologous sequences (Figure 3-21A). This stretch carries hydrophobic AA interspersed with few charged ones. Second, FAM84A AA258-279 encompasses a ten AA-stretch with six identical and three highly similar residues to AKAP17A AA305-323 (Figure 3-21B). The FAM84A sequence, and even more so the corresponding AKAP17A sequence, is characterized by a sequence of charged AAs only interrupted by few hydrophobic residues. Such stretches of charged residues are frequently located on the surface of proteins in their native state, because this is thermodynamically favorable.

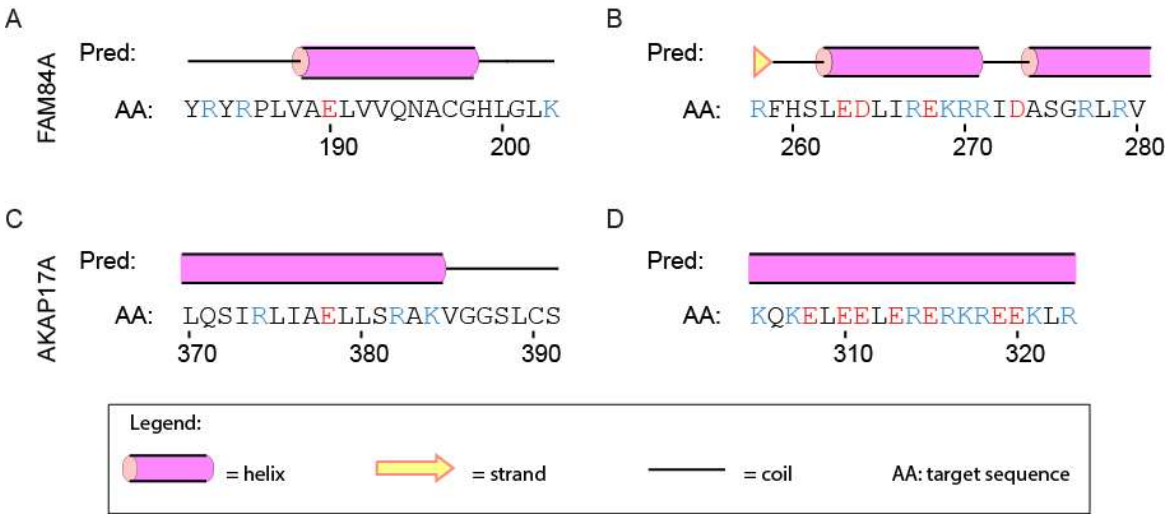

Figure 3-22: Detail of Secondary Structure Predictions of FAM84A and AKAP17A.

Secondary structure predictions revealed that the potentially cross-reactive epitope between FAM84A (A and B) and AKAP17A (C and D) is located to an α-helical structure (pink barrel) in both proteins. Two homologous candidate epitopes are depicted that encompass AA182-203 (A) and AA370-391 (C), and AA258-279 (B) and AA305-323 (D). For each AA-stretch, the secondary structure prediction is depicted on top of the AA-sequence. Charged AAs are color-coded: red letters indicate negatively charged residues, blue indicates positively charged residues.

ELISA and Western blot experiments using FAM84A and AKAP17A showed that the epitopes are not recognized when denatured (data not shown). Therefore, a secondary structure is necessary

to form the epitope recognized by rOCB-MS1-s8. Hence, the highly similar AA-sequences identified above are not sufficient for rOCB-MS1-s8 to recognize both proteins, but the secondary structure plays a crucial role. Secondary structure predictions [134] revealed that the two corresponding sequence stretches, described above, are most probably embedded in α-helical structures in the respective protein's native conformation (Figure 3-22).

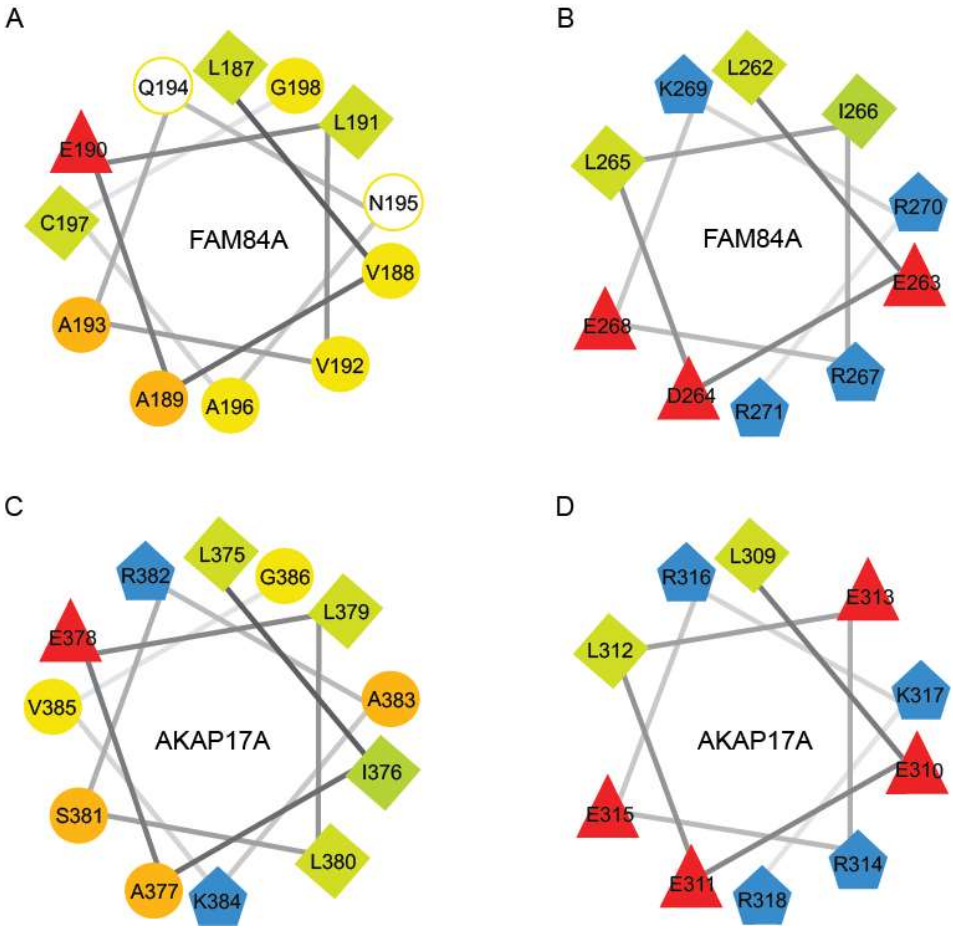

Figure 3-23: Helical Wheel Projections of FAM84A and AKAP17A Epitopes.

Epitopes AA182-203 and AA258-279 of FAM84A (A and B) and the respective corresponding sequences of AKAP17A (C and D) are depicted. The projection approximates the arrangement of AAs in an α-helical structure. Hydrophobicity is color-coded and represented by shapes: blue pentagons are positively charged residues, red triangles represent negative charges. Hydrophobicity decreases from green to yellow. Hydrophobic residues that are depicted as diamonds. Circles represent hydrophobic AAs. Empty circles represent large neutral, hydrophilic residues. The corresponding sequences in A and C share a similar distribution of hydrophilic and hydrophobic residues. The helical wheels shown in B and D share higher similarity. Charged residues are concentrated at the bottom half of the wheel and are exactly matched by its counterpart.

A full α-helical turn of 3.6 AAs translates into every third to fourth AA facing the same direction of the helix as illustrated in Figure 3-23. As a consequence, only some AAs of a sequence stretch may be involved in the binding reaction. Resulting from the high sequence similarity, AA-distributions of AA258-279 and AA209-318 in the helix prediction are highly similar (Figure 3-23B and D). The similarity of the other candidate epitope (Figure 3-23A and C) is clearly lower, but still features regions with distinct similarity. In summary, sequence analysis and secondary structure predictions revealed two candidate epitopes that share similarity between the two antigens, are predicted to form similar secondary structures, and are probably located on the protein surface.

3.4.2 Mutant Screening of FAM84A with site directed AA-exchange

To clarify whether these candidate epitopes are involved in antigen recognition by rOCB-MS1-s8, alanine mutants of FAM84A were produced. In each mutant, a single AA of the original FAM84A sequence is replaced with alanine. As depicted in Figure 3-21, three AAs were exchanged in candidate epitope AA182-203 and five AAs in candidate epitope AA258-279. All mutants were expressed in and purified from *E. coli* (data not shown) and subsequently analyzed for reactivity with rOCB-MS1-s8 using the FAM84A-ELISA.

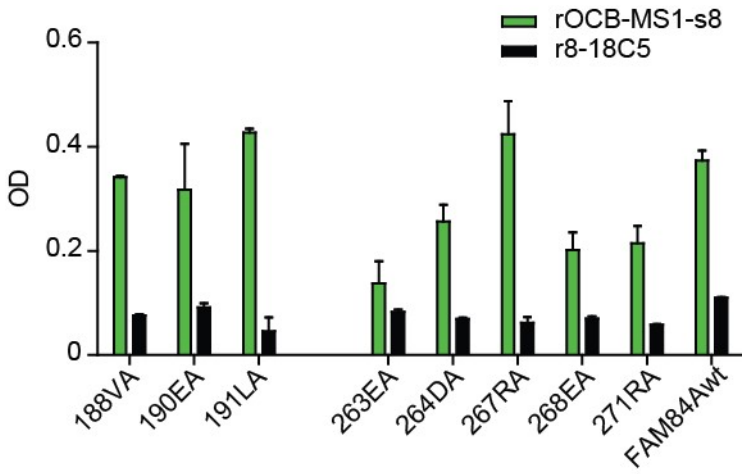

Figure 3-24: ELISA FAM84A-Mutant Screening.

Individual AAs of the putative epitopes were exchanged to alanine. AA-exchanges at positions AA188, AA190, and AA191 in FAM84A did not change the antigen recognition by rOCB-MS1-s8. Substitutions at positions AA263, AA264, AA268, and AA271 considerably reduced binding of the antibody as compared to wild type FAM84A. Exchanging the glutamic acid at position AA267 did not influence the binding. The control r8-18C5 did not react with any of the mutants. Data is representative of four independent experiments. Error bars indicate standard deviation. The figure is modified from [101].

FAM84A-ELISA screening revealed that the candidate epitope AA182-203 does not influence the recognition by rOCB-MS1-s8, while some AAs of the AA258-279 candidate epitope did change the binding capacity of the antibody to its antigen. Alanine substitution at positions AA263, AA268 and AA271 markedly reduced the reactivity detected by ELISA. Position AA264 may also play a role in antigen recognition in this case. None of the single alanine exchanges completely abolished the binding of rOCB-MS1-s8. The final preparation was free of contaminants detectable on SDS-PAGE. The positions of the mutations were selected based on homologous regions of the AKAP17A and FAM84A proteins. The secondary structure in this segment was predicted to form an α-helix and the helical wheel projection of the individual residues revealed that all mutated positions locate to the same side of the helix. As all of these residues are charged, it is conceivable that this side of the helix faces the solvent in the natively folded protein. AAs identified to be of relevance, locate to the same side of the helix (compare Figure 3-23) however AA267 also faces the same direction, but does not influence the interaction. Overall, the findings confirm the concept of a conformation dependent epitope located in an α-helical structure at AA258-279 in FAM84A that is targeted by the rOCB-MS1-s8 and shares strong homology with its counterpart in AKAP17A.

3.5 Antigen Recognition of the encephalitogenic rAb-Ip2

In contrast to MS, where chronic inflammation is a hallmark of pathogenesis, there is a broad spectrum of CNS diseases with acute neuroinflammation.

Analysis of CSF from patient Ip2, who had a severe form of acute encephalitis, revealed monoclonal expansion of a single antibody species. Using next generation sequencing of CSF B-cells, E. Beltrán identified and cloned the expanded antibody species (unpublished data). The V(D)J-regions of the H- and L-chains of Ab-Ip2 were cloned into the pTT5 H- and L-chain cassette vectors and expressed in HEK293E-cells as full length IgG1-molecules.

The recombinant antibody, termed rAb-Ip2, was biochemically analyzed as previously described for the OCB-derived antibodies (see section 3.1.1). The antibody formed a heterodimer that disintegrated upon treatment with a reducing agent and secondary structure proportions determined by CD-spectroscopy conform to the other rAbs.

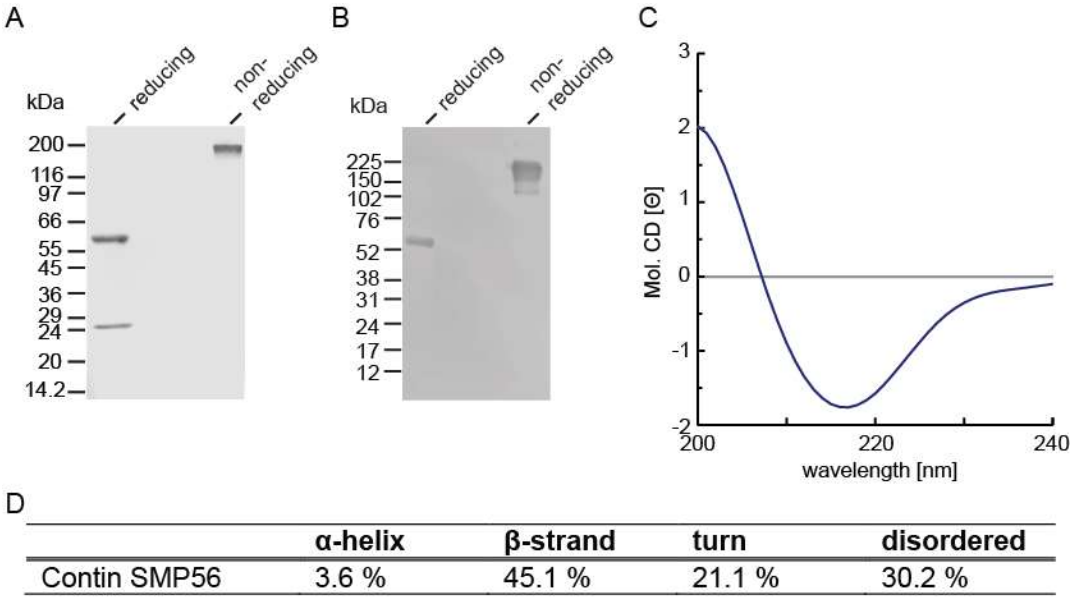

D

	α-helix	β-strand	turn	disordered
Contin SMP56	3.6 %	45.1 %	21.1 %	30.2 %

Figure 3-25: Characterization of rAb-Ip2.

rAb-Ip2 separated by SDS-PAGE under reducing and non-reduicng conditions and Commassie brilliant blue staining. Two protein bands at 25 kDa and 57 kDa were detected under reducing conditions, confirming the disassembly of the heterodimer. Under non-reducing conditions, a single protein band at 160 kDa was detected corresponding to the full length antibody (A). Western blotting, detecting the H-chain C-terminal V5-tag confirmed these findings (A and B). The conformation of rAb-Ip2 was determined by circular dichroism spectroscopy. Large parts of antibodies fold into ß-sheet interconnected by turns and disordered segments as reflected by the CD-spectrum (C and D).

3.5.1 Recognition of the $GABA_AR\alpha1ex$ by rAb-Ip2

It has been shown that CSF from patient Ip2 strongly reacts to the $GABA_AR$ α1-subunit [111]. Here, it was therefore tested whether rAb-Ip2 would also recognize the $GABA_AR$ α1-subunit. Since only the extracellular domain is accessible in intact cells, the extracellular domain of the $GABA_AR$ α1-subunit was cloned into the vector pET33b(+) and recombinantly expressed in *E. coli* BL21. The protein fragment formed IBs in the *E. coli* cytoplasm. These were purified and

solubilized in guanidine hydrochloride and yielded about 20 mg/g bacterial wet weight. Solubilized protein was refolded by rapid dilution in PBS. Attempts to subsequently concentrate the protein were not successful as the protein was lost due to aggregation or adsorption to the ultrafiltration membrane. Hence, the protein was used in the dilute solution of approximately 15 µg/ml. SDS-PAGE analysis demonstrated a single band at the expected MW of 31 kDa. CD-spectroscopic analysis was not possible due to the low concentration of refolded protein in solution.

$GABA_AR$α1ex-ELISA was employed to determine whether the isolated monoclonal rAb-Ip2 recognizes the extracellular domain of the $GABA_AR$ α1-subunit. The assay revealed significantly higher reactivity of rAb-Ip2 to $GABA_AR$α1ex as compared to the MS-OCB-derived control antibody 1039-s1 and the humanized r8-18C5 (****=p≤0.0001). The C-terminal V5-tag of the $GABA_AR$-fragment was used as positive control. Both secondary antibody controls alone did not yield any signal.

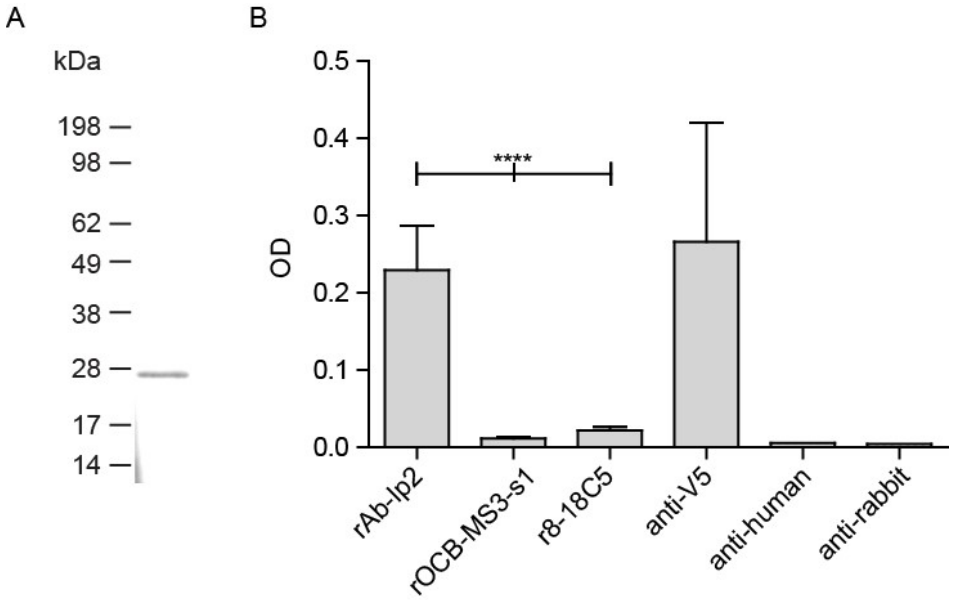

Figure 3-26: Recombinant $GABA_AR$α1ex and its Recognition by Ab-Ip2 in ELISA.

SDS-PAGE of the refolded extracellular domain of $GABA_AR$ α1-subunit yielded a single band at approximately 28 kDa. The calculated MW of the $GABA_AR$-fragment is 31 kDa (A). ELISA demonstrated binding of rAb-Ip2 to the extracellular domain of the $GABA_AR$ α1-subunit. rAb-Ip2 recognized the recombinant $GABA_AR$-fragment, while MS-OCB-derived control and r8-18C5 did not show any reactivity (****=p≤0.0001, n=5). Reactivity did not differ from the positive control antibody that detected the V5-tag of the recombinant protein (B).

3.5.2 Reactivity Profile of rAb-Ip2 on Protein Microarrays

To assess the hypothesis that the encephalitis of patient Ip2 might have a paraneoplastic background, reactivity of rAb-Ip2 to other protein antigens was analyzed. To this end, rAb-Ip2 was applied to a protein microarray to identify potential peripheral cross-reactive antigens that might have induced an immune response to the $GABA_AR$.

The array revealed reactivity to a total of 17 antigen candidates. The mean signal of the internal negative controls (18 [AU]) was comparably low, while the mean array signal (736 [AU]) was

increased compared to the MS-OCB-derived rAbs. The candidate antigens are listed along with the mean signal intensity of rAb-Ip2 and the controls as well as the enrichment factor in Table 3-3.

Table 3-3: Candidate Antigens identified for Ab-Ip2 using Protein Microarrays.

The mean signals of rAb-Ip2, secondary antibody and r8-18C5 (isotype control) for the specified protein are given in AU. The enrichment factor compared to the isotype control is listed in the right column. Antigens employed in validation assays are highlighted in green. Zinc-binding proteins are indicated by grey background. For details on the selection of these proteins see section 3.5.3.

Ab	Protein	Mean signal [AU]	Sec. Ab signal [AU]	Isotype signal [AU]	enriched to isotype
Ip2	Mitogen-activated protein kinase 7 (MAPK7), transcript variant 3	12 406	140	546	22.7
	Isovaleryl-CoA dehydrogenase, mitochondrial	15 077	3 656	1 323	11.3
	Zinc-finger protein 207 (ZNF207), transcript variant 2	6 149	452	602	10.2
	Cysteine- and glycine-rich protein 1 (CSRP1)	10 306	942	1 324	7.8
	Cysteine- and glycine-rich protein 2 (CSRP2)	49 741	7 145	8 908	5.6
	Putative E3 ubiquitin-protein ligase SH3RF2	7 806	352	1 501	5.2
	ATP-dependent RNA helicase DHX8	4°222	177	944	4.5
	STIP1 homology and U-box containing protein 1	4 982	28	1 133	4.4
	Outer dense fiber protein 3-like protein 2	5 118	264	1 259	4.1
	Sciellin (SCEL)	5 680	443	1 422	4
	Leukocyte receptor cluster (LRC) member 1 (LENG1)	3 721	175	966	3.9
	Cell cycle associated protein 1 (CAPRIN1), transcript variant 1	6 271	261	1 683	3.7
	Cortactin (CTTN), transcript variant 2	7 799	118	2 200	3.5
	DEAD (Asp-Glu-Ala-Asp) box polypeptide 17 (DDX17), transcript variant 2	6 745	421	1 905	3.5
	Cystein-rich protein 2 (CRIP2)	14 160	2 073	4 158	3.4
	Serine/threonine kinase 40 (STK40)	5 121	3 211	1 508	3.4
	C-C motif chemokine 21	4 598	354	1 411	3.3

Overall, the signal intensities of the candidate antigens measured in the isotype control (r8-18C5) treated array are increased compared to the MS-OCB-derived rAbs and this converts into low

enrichment factors. The cysteine- and glycine-rich protein 2 (CSRP2) was the only protein that elicited a very high signal approaching saturation. Due to the signal intensity of the isotype control the high signal did not translate into a high enrichment factor. The strongest enrichment was found for the mitogen-activated protein kinase 7 (MAPK7).

The STIP 1 protein, which had previously been identified as candidate antigens for rOCB-MS1-s8 and rOCB-MS4, was recognized by rAb-Ip2 at comparable levels. The pool of candidate antigens contains a total of six zinc-binding proteins, representing about one third of all candidates. Four of these carry a LIM-domain: CSRP1, CSRP2, CRIP1 and sciellin. The zinc-finger protein 207 and the putative E3 ubiquitin-protein ligase both are zinc-binding proteins but mediate this interaction via a different zinc-binding motif.

Several subunits and transcript variants of $GABA_AR$, including the $GABA_AR$-α1-subunit, are present on the array. None of these showed enhanced reactivity with rAb-Ip2 even though the reactivity to the extracellular domain of the $GABA_AR$-α1-subunit had previously been demonstrated by ELISA.

3.5.3 Selected Antigen Candidates for rAb-Ip2

From the list of candidate antigens identified for rAb-Ip2, two entities were selected for further validation. MAPK7 was selected because it had the highest enrichment factor. The LIM-domain proteins, especially CSRP-proteins, represented another focus, because multiple members of this gene family were identified as candidate antigens. CSRP2 elicited the highest signal intensity. CRIP2 and CSRP1 showed comparably lower signal intensities of about the level detected for MAPK7. Figure 3-27A depicts the signals for each of the candidate antigens selected for validation and the appropriate secondary antibody control spots. The protein name and UniProt-ID and basic information on localization and function of the protein are summarized in Figure 3-27B.

A

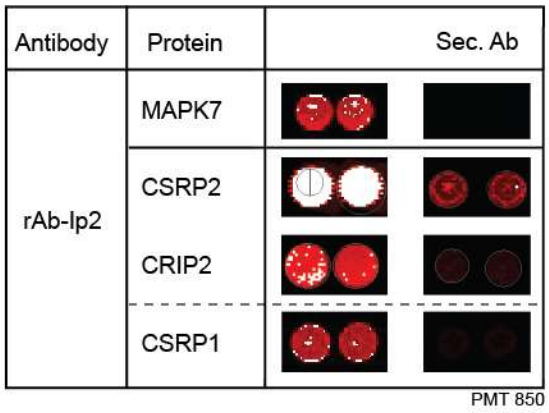

B

Protoarray description	UniProt-ID	Name	Localization	Function
Mitogen activated protein kinase 7, transcript variant 3 (MAPK7)	Q13164-1	Mitogen activated protein kinase 7	cytoplasmic/nuclear	transcriptional regulation
Cysteine- and glycine-rich protein 2 (CSRP2)	Q16527-1	Cysteine- and glycine -rich protein 2	cytoplasmic/nuclear	diverse regulatory roles
Cysteine-rich protein 2 (CRIP2)	P52943-1	Cysteine-rich protein 2	cytoplasmic/nuclear	diverse regulatory roles
Cysteine- and glycine-rich protein 1 (CSRP1)	P21291-1	Cysteine- and glycine -rich protein 1	nuclear	neuronal development

Figure 3-27: Details of the Protein Microarray developed with the Ab-Ip2.

The most enriched signal compared to controls was found with MAPK7 (uppermost panel). Three closely related LIM-domain proteins were recognized by rAb-Ip2. Highest signal intensity was elicited by CSRP2, CRIP2 and CSRP1 showed slightly lower signal intensities reaching similar levels like the MAPK7 (left panel). The secondary antibody control did show some signal for CSRP2 but strongly reduced in comparison to the signal produced by rAb-Ip2. The other secondary antibody controls did not elicit increased background signals (right panel). Increasing brightness of red represents stronger signals with strongest signals being depicted in white (A). Protein name and Uniprot-ID as well as localization and functional information of candidate antigens selected for validation (B).

Candidate Antigen MAPK7

Mitogen-activated protein kinase 7 (MAPK7) is a ubiquitously expressed protein that plays a role in cell survival, proliferation and differentiation in response to extracellular stimuli through transcriptional regulation. It is therefore also named extracellular signal regulated kinase 5. The 88 kDa protein localizes to the cytoplasm or nucleus, depending on its functional state.

Candidate Antigen LIM-proteins

CSRP2 is a 21 kDa protein that contains two zinc-binding LIM-domains. It is expressed in most cells and localizes to the cytoplasm or the nucleus. CSRP1 is highly similar to CSRP2 with ≈80 % sequence identity (Figure 3-28) and localizes to intracellular regions. The exact function of these proteins is not understood. Both proteins contain about 15 % of glycine and 8 % cysteine

residues which are essential for the zinc-binding activity. CSRP2 was selected for validation since this protein gave the highest array signals and shares fundamental similarity with CSRP1.

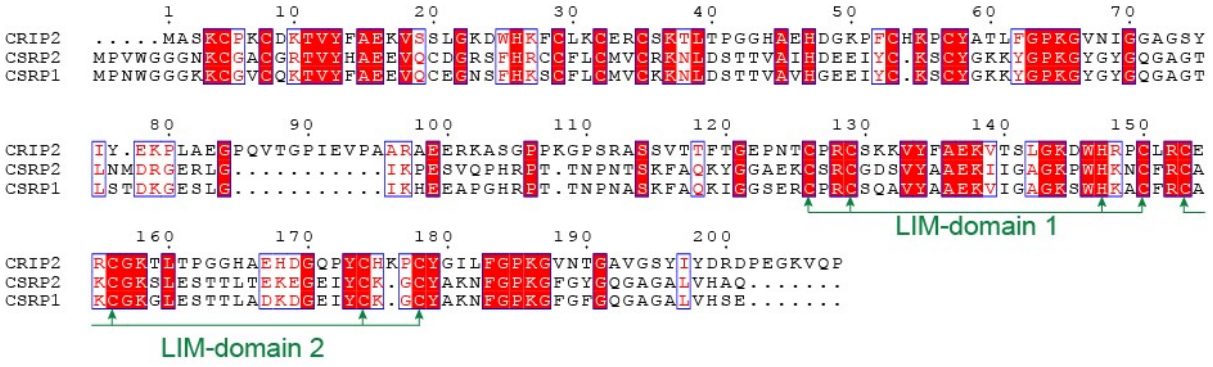

Figure 3-28: Sequence Alignment of Ab-Ip2 Candidate Antigens with LIM-domain.

The CRIP2-protein (upper row) shares similarities with both CSRP2 and CSRP1 (middle and bottom row), in particular the zinc-coordinating cysteine- and histidine-residues are conserved. The residues that form the LIM-domains and coordinate Zn^{2+}-ions are marked by arrows. AAs in between the zinc-binding LIM-domains show lesser conservation. The two CSRP-proteins share high homology even in the non-conserved regions. See legend Figure 3-8 for explanations of symbols.

CRIP2 also contains two zinc-binding LIM-domains, but only shares 34-39 % sequence identity with the CSRP-proteins (Figure 3-28). This protein is 208 AAs in length and has a slightly higher MW of 23 kDa as compared to the CSRPs. CRIP2 was selected for further validation as well. All three LIM-domain proteins carry a positive net charge due to the high number of lysine residues.

3.5.4 Recognition of CSRP2 by rAb-Ip2

The LIM-domain protein CSRP2 is strongly expressed in HEK293E cells, CSRP1 and MAPK7 are expressed at medium levels, and the expression of CRIP1 is not detectable in this cell line [143]. Therefore, non-transfected HEK293E-cells were stained with rAb-Ip2 for initial validation of reactivity. rAb-Ip2 stained perinuclear regions, while r8-18C5 and the secondary antibody did not yield any signal (Figure 3-29). The staining pattern corresponds to the expected cytoplasmic or nuclear localization of the proteins but does not allow conclusions on the identity of the stained structure.

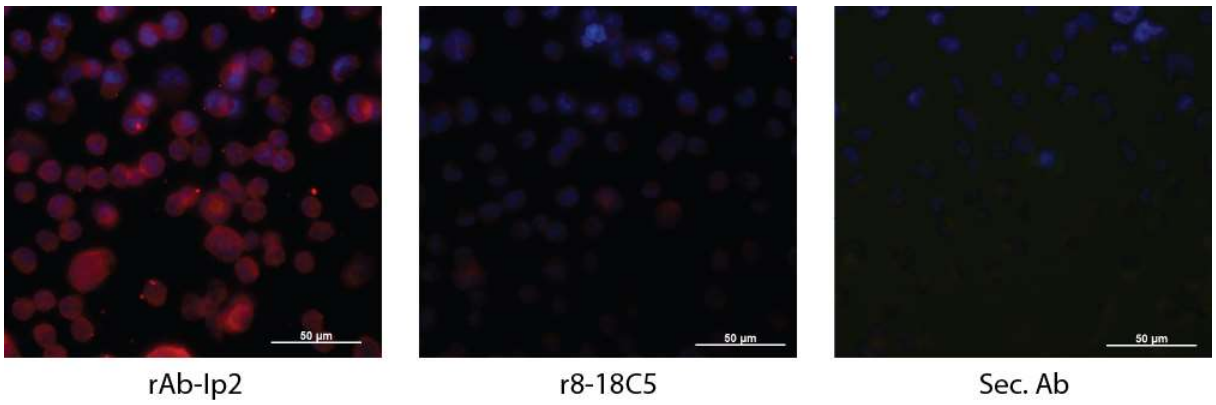

Figure 3-29: Immunofluorescence Staining of non-transfected HEK293E-cells.

Ab-Ip2 stained perinuclear regions in HEK293E cells (red). r8-18C5 and the secondary antibody did not show staining. Cell nuclei are depicted in blue. Pictures by courtesy of E. Beltrán.

Reactivity of rAb-Ip2 towards MAPK7, CSRP2 and CRIP1 was therefore analyzed in immunoprecipitation experiments with purified recombinant protein produced in HEK293-cells. Besides rAb-Ip2, the OCB-derived rOCB-MS3-s1 and r8-18C5 were used as controls. rAb-Ip2 precipitated CSRP2, while the other antibodies only showed background reactivity at the expected MW of 21 kDa. An additional band at 50 kDa was detected with rAb-Ip2 (Figure 3-30). Recognition of CSRP2 by rAb-Ip2 was lost upon repeated freeze-thaw cycles or prolonged storage of the recombinant protein at -80 °C (data not shown). The other LIM-domain protein, CRIP2, and MAPK7 did not show any reactivity in the immunoprecipitation assays.

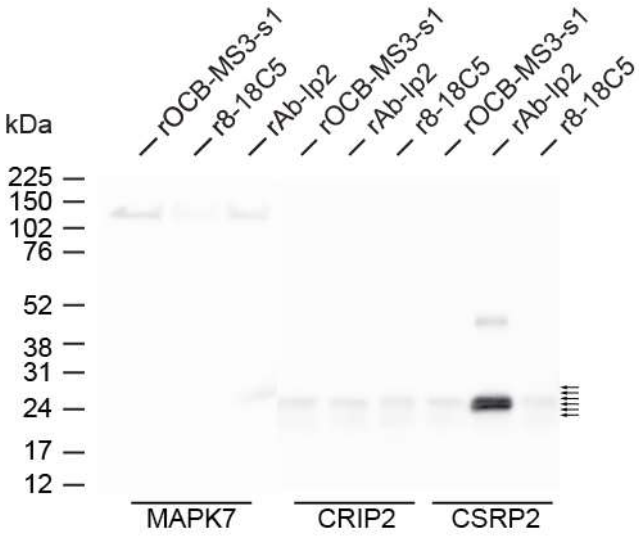

Figure 3-30: Immunoprecipitation of MAPK7 and two LIM-domain Proteins by rAb-Ip2

rAb-Ip2 precipitated recombinant CSPR2, yielding a band at 25 kDa, while the control antibodies rOCB-MS3-s1 and r8-18C5 showed background signal at this MW. An additional band at 48 kDa was detected for rAb-Ip2, but none of the control antibodies. Arrows indicate the position of gel slices cut for mass spectrometric analysis. Slices were cut from all three CSRP2-immunoprecipitations. The candidate antigens MAPK7 and CRIP2 did not elicit any specific reactivity in the immunoprecipitation assay. The blot is representative of two independent experiments.

CSRP2-precipitates were additionally analyzed by mass spectrometry. Six slices from each CSRP2-immunoprecipitation (rAb-MS3-s1, r8-18C5 and rAb-Ip2) were cut at the appropriate region between 20-25 kDa from the Coomassie-stained SDS-PAGE gel (see Figure 3-30) and the proteins were in-gel digested with trypsin. Mass spectrometric analysis revealed the presence of CSRP2-specific peptides in three of the six slices taken from the rAb-Ip2 loaded lane. None of the slices cut from the control antibody lanes carried CSRP2-specific peptides. The unspecific background at 25 kDa in control antibody lanes, detected by Western blotting, is attributable to the antibody light chains that dissociate during the elution process, since this band was also observed in control assays that omitted the CSRP2 completely (data not shown).

Figure 3-31 shows an enlargement of the spectra obtained with the three rAbs. Exemplarily, the 1099.5 peak is depicted that corresponds to the CGDSVYAAEK-peptide (carbamidomethylated cysteine) which is solely detected with rAb-Ip2. Because the antibody L-chain migrates at similar MW, non-CSRP2-specific peaks are detected as well.

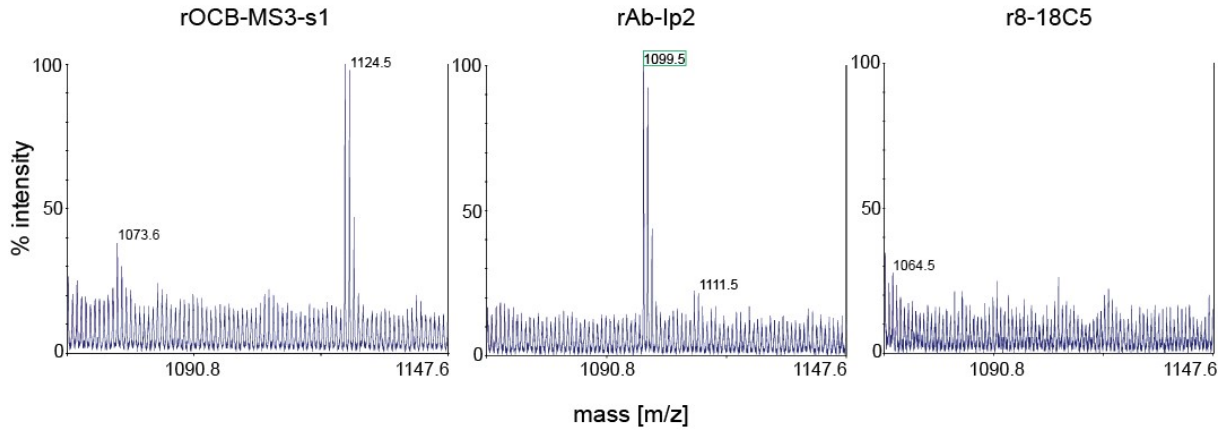

Figure 3-31: Detail from mass spectrometric Analysis of CSRP2 Immunoprecipitation.

The 1099.5 mass corresponds to the CSRP2-specific peptide sequence CGDSVYAAEK (carbamidomethylated cysteine) and was only detected in slices taken from the lane loaded with rAb-Ip2-eluate. Other strong signals not attributable to CSRP2, for example the peak at 1124.5 in rOCB-MS3-s1, correspond to antibody L-chain peptides. CSRP2-specific peptides were not found in lanes loaded with eluates from rOCB-MS3-s1 and r8-18C5.

4 Discussion

This study aimed at identifying the target antigens of OCB-antibodies from patients with neurologic diseases. In the first project target antigens of OCB-antibodies from patients with MS were identified. The OCB-antibodies had previously been identified using a newly developed strategy by B. Obermeier. This technique allows differentiating distinct expanded antibody species from the polyclonal background of IgG and from other OCBs in CSF samples. H- and L-chains were matched by combining proteome analysis and sequencing of the IgG-transcriptome (see Figure 1-8) [100]. This method allowed for the first time to characterize and recombinantly produce distinct OCB antibodies. As all previous studies that investigated target molecules of OCBs could not link the target antigens to distinct expanded antibody species (see section 1.2.3). Here, three target antigens of distinct OCB-antibodies were identified that showed a common pattern: all three are intracellular proteins, not specific for CNS-tissue.

The second project focused on the expanded antibody species from CSF of a patient with $GABA_AR$-encephalitis. CSF from this patient was found to react to the $GABA_AR$ α1-subunit and presumably causes neurologic symptoms [111]. Deep sequencing of the CSF IgG-repertoire revealed antibody rAb-lp2 as an expanded species. The pathogenesis of $GABA_AR$-encephalitis in this patient is unknown, but neurologic symptoms might possibly been caused by a cross-reactivity of an antibody to $GABA_AR$ and an unknown tumor antigen. Here, binding to the $GABA_AR$ α1-subunit was confirmed and a potential systemic target antigen of rAb-lp2, that might have initiated such a paraneoplastic process, was identified.

4.1 Recombinantly expressed rAbs

In previous experiments, OCB-derived F_{ab}-fragments were used for antigen searches but these did not yield conclusive results [100, 102]. Here, full length antibodies were recombinantly expressed which mirror the natural structure and avidity of antibodies. The presence of two antigen binding sites can stabilize complexes and may allow identification of low affinity interactions.

A total of eight antibodies were expressed as full length IgG1-molecules in HEK293E-cells. Six of the antibodies derived from MS-OCBs, one derived from the $GABA_AR$-encephalitis patient lp2 and one antibody represented the humanized MOG-specific r8-18C5, serving as a control. All antibodies were produced as heterodimers and all but rOCB-MS2-s5 yielded fair amounts of protein. The final preparations were of sufficient purity as demonstrated by Coomassie staining of SDS-gels. The identity of each of the antibodies was confirmed by Western blotting and mass spectrometry. CD-spectroscopy demonstrated that approximately 40 % of the protein had a β-sheet conformation and marginal amounts α-helical structures were detected. These findings correlate well with CD-spectra and x-ray diffraction studies on other antibodies [145].

Expression yields of the full length rOCB-MS2-s5 from HEK cell supernatant were approximately 100-fold lower than expected from the other rAbs. The marginal amounts of purified antibody allowed screening for antigen candidates with protein microarrays but no subsequent validation experiments. Thus, this antibody was cloned and expressed as scF_v in *E. coli*. Detailed biochemical analysis of the corresponding scF_v-fragment of rOCB-MS2-s5 confirmed that the scF_v matches the quality of the full length antibodies regarding purity and conformation and thus was suited for validation experiments.

4.1.1 Recognition of native and denatured Forms of MOG by r8-18C5

The general capability of the full length antibodies expressed in HEK293E-cells to bind their target antigen was shown exemplarily for r8-18C5. The reactivity of the original mouse 8-18C5 antibody to MOG is well established [127]. Reactivity of r8-18C5 to MOG was demonstrated in three setups: dot blot, immunoprecipitation and flow cytometry. For dot blotting, the target protein in applied to a nitrocellulose membrane, which often results in conformational changes and denaturation of the protein. In immunoprecipitation experiments and flow cytometric analysis using living cells, MOG is present in its native conformation. All three experimental setups showed specific recognition of MOG by r8-18C5. The interaction of r8-18C5 and MOG is insensitive to the conformational status of the target antigen.

These experiments also demonstrated that none of the MS-OCB-derived antibodies rOCB-MS1-s2, rOCB-MS1-s8, and rOCB-MS3-s1 recognized the extracellular domain of MOG, although components of the myelin sheath such as MOG [146], MAG [147], and MBP [148] are suspected MS-antigens [149] and it was suggested that OCB would recognize myelin antigens [96]. Additionally, these proteins play a prominent role in animal models of the disease [150] and are CNS-specific target structures that may be accessible to antibodies.

4.2 Proof of Concept - Neuroborreliosis

In a parallel project, CSF from NB patients was used in a study by M. Senel to demonstrate that OCB-antibodies in NB represent disease-related antibodies. NB is an inflammatory disease of the CNS caused by *borrelia*-infection [151]. NB patients have OCBs and show strong reactivity to whole *borrelia*-lysates in later disease stages, suggestive of anti-*borrelia* specificity of the expanded antibodies in CSF [152, 153]. Using the method to isolate and characterize OCB-antibodies, rOCB-NB1-s13 was identified. rOCB-NB1-s13 was cloned, recombinantly expressed and employed in clinical routine tests for reactivity against *borrelia*. These experiments revealed increased reactivity of rOCB-NB1-s13 to whole *borrelia* lysates and identified protein “p21”, representing a 21 kDa-fragment of BBK53 [154] from *B. burgdorferi,* as target antigen (M. Senel, [101]). Reactivity of OCB-antibodies from CSF of patients with CNS-infections to *borrelia* is long known [155]. Therefore, these findings confirmed that the OCB-derived rOCB-NB1-s13 is involved in the patient’s immune reaction against the causative agent and that the method to identify and clone distinct OCB-antibodies indeed yields functionally relevant antibodies.

4.3 Identification and Validation of Candidate Antigens of MS-OCBs

Despite intensive antigen searches, specific factors that initiate and promote MS pathology remain elusive. Besides components of the myelin sheath, numerous other antigens have been proposed, including viral and bacterial components [89, 156-159] as well as self-structures like DNA, intracellular proteins [74, 160], and lipids [86, 87, 94]. These previous studies used either unfractionated CSF samples of MS patients or antibodies derived from single CSF B-cells. Both approaches suffer major shortcomings: using full CSF for screening purposes is complicated by the low IgG-concentration in the samples and signals may be superimposed by the high polyspecific background of antibodies. In contrast, single cell derived antibodies do not necessarily represent a distinct OCB-antibody, but may represent polyclonal background antibodies in CSF [98].

To identify candidate antigens of OCB-derived antibodies rOCB-MS1-s2, -MS1-s8, -MS1-s9, -MS3-s1 and -MS4, B. Obermeier and J. Bruder applied the corresponding F_{ab}-fragments to different screening assays. Clinical routine tests were used to test for reactivity against viruses, including Epstein-Barr, measles and herpes simplex, chlamydia and intracellular components like nuclear and neutrophil cytoplasmic factors. Further, reactivity against DNA, insulin, lipids and human brain homogenates was tested. However, these experiments yielded negative or inconclusive results [100, 102].

J. Bruder used protein microarrays to screen a larger panel of protein antigens. Experiments using F_{ab}-fragments identified candidate antigens, which had not been verified so far [102]. In the present study, full length rAbs were used on protein microarrays. Full length rAbs have two antigen binding sites, thus higher avidity for the antigen as compared to the F_{ab}-fragment and therefore increase the chances of identifying candidate antigens.

4.3.1 Protoarray Screening as Tool for Antigen Identification

Protein microarrays are a tool to rapidly screen for reactivity of a monoclonal antibody to a large number of candidate antigens [161, 162]. Different microarrays have previously been used by others to analyze the antigen specificity of antibodies from full serum [163] or CSF samples [82, 164, 165] of MS patients. Here, Protoarrays® were used to assess the reactivity of OCB-derived antibodies to protein antigens. A protein binding profile of each of the antibodies was created and the field of potential antigens narrowed down.

More than 9 000 proteins are spotted in duplicates on the Protoarrays®. According to the manufacturer, all proteins are expressed in insect cells and present in their native conformation. This approach enables parallel testing of a variety of proteins representing distinct structural and functional properties on a lab scale. Further, the array displays sufficient amounts of compounds that may be beneath the detection limit on the cellular- or tissue-level or difficult to access. r8-18C5 was used as positive control since its cognate antigen (MOG) is also spotted on the array.

The use of protein microarrays has several shortcomings: First, as all proteins are expressed in an insect cell system, they may differ from their human original in their posttranslational modifications (PTMs) and thus the accessibility of epitopes [166]. Second, the coating process may influence individual proteins differently. While most proteins keep their conformation during coating, a number of others may lose their natively folded state. Antibody-antigen complexes that rely on conformational epitopes will not be formed. Conversely, denatured proteins may exhibit structures that may not appear naturally, generating misleading results [167]. All proteins underwent purification but the purity of the particular entity is not known. Thus, it is possible that reactivity measured at a distinct spot is not directed at the coated protein, but at some co-purified contaminant. Therefore validation of the results using an independent method and candidate antigens produced in another expression system is imperative. To this end, candidate antigens produced in either HEK293-cells or *E. coli* were subjected to validation studies using independent experimental setups.

4.3.1.1 F_{ab}-fragments versus full length OCB Antibodies on Protein Microarrays

The overall reactivity profiles of the OCB-derived full length antibodies were compared to the results of the corresponding F_{ab}-fragments.

Identification of target antigens depends on the stability of the antibody-antigen-complex, which is a function of the antibody's affinity. It may be assumed that somatic hypermutation (SHM) introduced during the maturation process confer considerable affinity to these antibodies, however, it is not known *a priori*. Increasing the number of binding sites, i.e. avidity, stabilizes complexes and may therefore improve the screening for candidate antigens.

The mean array signal is comparable in F_{ab}- and full length antibody-probed microarrays. The mean signal of the internal negative controls is clearly reduced in the full length antibody experiment compared to the F_{ab}-probed arrays. This may in part be explained by the differential experimental setup. Because F_{abs} have a single antigen binding site and bind weaker to their target, the total amount of F_{ab}-fragments had to be increased and the washing procedure minimized. Further, a secondary antibody to human IgG (H+L) was used, which might also recognize some epitopes on the array. In contrast, the antibody-probed arrays were developed using the V5-tag/anti-V5-system that is recommended for this assay, because it is much more specific. This may explain the clear reduction of internal negative control signals when using the full length antibodies.

Comparison of the F_{ab} and full length data further revealed a considerable increase in enrichment factors. Using F_{ab}-fragments a total of 34 antigen candidates was identified, six of these (≈18 %) showed signals that exceeded their corresponding controls by a factor of ten or more [102]. In contrast, using the respective full length antibodies, approximately half (13 out of 27) of all candidate antigens had enrichment factors larger than ten. This observation clearly underscores the benefit of the full length antibodies in this experiment as it indicates a better signal to noise

ratio. Generally, lot-to-lot differences may also account for minor changes in the identified reactivity profile.

From a functional point of view, both experiments yielded proteins classified as kinases, GTPases, transcription and regulatory factors. Thus, the vast part of candidate proteins localizes to intracellular compartments.

Apart from that, the overlap of results from the two protein microarray analyses using F_{ab}-fragments and full length antibodies is small. The only candidate antigen consistently recognized in both approaches is AKAP17A. This may be attributed to the improved discrimination of signals from background reactivity due to higher avidity of full length antibodies. This is also reflected by considerably increased enrichment factors.

Except FAM84A, which has been associated with MS in another study [95], none of the identified candidate antigens had previously been linked to MS. Overall, for validation experiments, candidate antigens identified with full length antibodies were selected.

4.3.1.2 r8-18C5 recognizes MOG on Protein Microarrays

A signal of intermediate intensity was detected on protein microarrays upon hybridization of r8-18C5 to MOG. The signal doubled as compared to the signal detected with F_{ab}-8-18C5. Surprisingly, the analysis revealed that two other proteins were recognized, producing higher signal intensities than MOG. F_{ab}-8-18C5 had bound multiple antigens in the previous microarray [102] as well. Possibly, the avidity of the full length antibody may allow complexation of antigens recognized with weak affinity that may be missed when F_{ab}-fragments are used. Two proteins, FAM20B and CHD2 that were identified by protein microarray hybridization were subjected to Western blotting experiments to verify reactivity of r8-18C5. In both cases validation failed. Therefore, no linear epitopes are recognized by r8-18C5 on those two proteins although r8-18C5 does recognize linear MOG epitopes. However, reactivity to a conformational epitope is not excluded by this experiment. Whether a conformational epitope is recognized and the molecular basis for this remains unclear. A previous study found 8-18C5 to recognize bovine butyrophilin [168], indicating the cross-reactive potential of this antibody. The corresponding human butyrophilin was present on the microarray, but was not recognized by r8-18C5. It is not clear whether this is due to the human sequence or the protein's conformation on the array.

This finding highlights that array data represent guidelines that help to confine potential antigens. For ultimate proof, candidate antigens must be validated by independent techniques.

4.3.2 Validation of Antigens recognized by MS-OCB Antibodies

Protein microarrays were used as an antigen identification tool and provided an overview of protein candidate antigens recognized by MS-OCB antibodies. Selected antigens were validated in independent experiments.

For three OCB-derived antibodies, target antigens were identified and confirmed. rOCB-MS2-s5 recognized MKNK1, antibodies rOCB-MS1-s8 and rOCB-MS1-s2 bound FAM84A and AKAP17A respectively. Three other antibodies did recognize protein antigens on microarrays with low signal intensities and therefore were not followed up on (Table 3-2). MS3-s1 did not recognize any of the proteins present on the microarray.

4.3.2.1 rOCB-MS2-s5 recognizes MKNK1

rOCB-MS2-s5 represents the monoclonally expanded antibody species from CSF of a newly diagnosed MS patient. This antibody is particularly interesting because it was present from the time of first clinical signs of the disease, it was the only expanded antibody species in the sample and the patient had an acute exacerbation at the time of sampling. Therefore, this antibody may hold clues for a target structure that plays a role very early in disease development and that may relate to disease severity.

rOCB-MS2-s5 recognized three different members of the MKNK-family on the protein microarray, putting a strong focus on this candidate antigen family. mRNA coding for MKNK1 is detectable in all human tissues. Primary data on protein expression is only available for MKNK2 and suggests ubiquitous expression of the protein and its nuclear localization (Proteinatlas, [143]). Although all family members are strictly intracellular, the individual isoforms may differ in their precise localization [169]. By phosphorylation of the eukaryotic translation initiation factor 4E (EIF4E), MKNK-proteins regulate protein translation [170]. MKNK-proteins are part of ERK- and p38 MAP-kinase pathways that allow integration of external stimuli and adaption to those in terms of proliferation, survival or production of certain factors. Thus, members of the MKNK-family may exert a broad influence on cellular systems [169]. Due to their regulatory function in gene expression, they have been associated with tumor development [171].

Reactivity of scF_v-MS2-s5 to MKNK1 was initially validated by immunoprecipitation. Dose dependent binding of scF_v-MS2-s5 to MKNK1 was further confirmed by ELISA. Recognition of MKNK1 by scF_v-MS2-s5 was conformation dependent, because reactivity was lost upon repeated freeze-thaw cycles.

Subsequent screening of a small cohort of MS and NIND patients did not show increased reactivity to MKNK1 by other MS patients. Thus, MKNK1 appears to be a private antigen to patient MS2. Testing of the original CSF sample was not possible because the existing sample had been used to identify rOCB-MS-s5 and was therefore depleted of IgG-molecules.

4.3.2.2 rOCB-MS1-s8 recognizes FAM84A

rOCB-MS1-s8 yielded the highest signal with FAM84A. FAM84A is a 32 kDa protein with only limited data available on its function. It is localized beneath the plasma membrane at regions where cells do not contact neighboring cells and has been associated with increased invasiveness of colon cancer [172]. FAM84A has so far been found to be expressed in a variety

of tissues, including central nervous system tissues and exhibits enhanced staining in striated muscle, respiratory epithelium and the exocrine pancreas (Proteinatlas, [143]). The general function of FAM84A in the various tissues remains elusive.

Immunoprecipitation of FAM84A unambiguously confirmed the specific reactivity of rOCB-MS1-s8. Like the MKNK-family, this protein is an intracellular protein with a number of cysteine residues and therefore sensitive to oxidation. This may explain the gradual loss of reactivity of rOCB-MS1-s8 to purified FAM84A over time.

rOCB-MS1-s8 also recognized FAM84A in mildly fixed antigen-transfected HEK293E-cells. This finding further confirms reactivity of rOCB-MS1-s8 to FAM84A. Non-transfected cells that endogenously express low levels of FAM84A were not recognized by the antibody. This may be due to the low expression rate of this protein that may not suffice to detect immunofluorescence staining. This is also in agreement with the fact that previous experiments staining brain tissue and 2D Western blots [100, 102] failed to demonstrate a distinct staining pattern.

FAM84A-reactivity of unfractionated CSF samples from MS patients and serum from inflammatory bowel disease (IBD) patients has previously been found in other antigen search studies using Protoarrays® [95, 144]. In the MS study, from a total of seven CSF samples, three showed clearly increased reactivity and three others showed reactivity around the cut-off value. Although the overall FAM84A-reactivity did not reach statistical significance, the data suggest enhanced FAM84A-reactivity in a subset of MS patients [95]. Therefore, an ELISA was established that allows rapid screening of larger patient cohorts for reactivity against FAM84A. Additionally, this assay required a minimal sample volume of 25 µl. This is a major advantage when using scarce patient material such as CSF. The use of unfractionated patient materials requires a highly specific technique to minimize background reactivity. The FAM84A preparation used for these experiments was of sufficient purity, as judged from SDS-PAGE. The specificity was further enhanced by coating anti-V5 antibody that specifically retains the recombinant *E. coli* protein and simultaneously prevents aggregation of FAM84A due to interactions with the hydrophobic assay plate surface. The findings of the protein microarray and the immunoprecipitation of FAM84A were confirmed with FAM84A-ELISA. rOCB-MS1-s8 specifically recognized FAM84A.

To clarify to what extend FAM84A is a target antigen in other MS patients, CSF and serum samples from different patient cohorts were tested using FAM84A-ELISA. From the MS-cohort, MS1, the patient from whom rOCB-MS1-s8 was isolated, was the only patient showing clearly increased CSF-reactivity to FAM84A. The finding suggests that FAM84A is a private antigen to this patient and other MS patients in this cohort do not share increased sensitivity to this protein.

In contrast, NB and OID CSF samples showed high reactivity to FAM84A. This may indicate that this protein is a preferred target in excessive humoral immune reactions. Infections initiate inflammatory processes that involve the production of antibodies at high titers. The IgG-

concentration in normal CSF is approximately 42 mg/l [173]. In this experiment, samples of the MS-, CNP- and NIND-cohort had normal to slightly increased IgG concentrations, but individual samples in NB- and OID-cohorts reached up to 1 300 mg/l. Within each of the groups, the IgG-concentrations were rather homogeneous.

After correcting for IgG-concentration, none of the CSF-samples from the NB- and OID-cohorts showed increased signal intensity. Similarly, the reactivity of the CSF sample of patient MS1 is eliminated by adjustments for IgG-concentration. This may indicate that the detection limit of the assay is not sufficient to detect FAM84A reactivity in CSF. Improving the assay sensitivity may help to clarify the reactivity of patient samples to FAM84A. Parallel reactivity in CSF and serum may be explained by related clones inside the CNS and the periphery that produce antibodies [68, 174].

The results are in accordance with two previous studies that analyzed the reactivity of patient material to FAM84A. Previously mentioned work by Querol et al. found a slight increase in CSF-reactivity to FAM84A in three out of seven MS patients [95]. This study focused on identifying antigens that discriminate MS patients from inflammatory and non-inflammatory controls, and FAM84A did not qualify. Here, only MS1 showed slightly increased reactivity to this protein. Accordingly, FAM84A is a private antigen to patient MS1.

Experiments by Vermeulen et al. revealed enhanced seroreactivity to FAM84A in IBD patients [144]. IBD is an immune-mediated disease that is characterized by chronic inflammation of the gastro-intestinal tract [175]. The disease has a higher prevalence in MS patients as in the general population [176] and may share etiological characteristics with MS [177]. Approximately 20 % of IBD patients had significantly higher seroreactivity to FAM84A than gastrointestinal controls [144]. This is in accordance with our findings that acute inflammatory reactions, e. g. viral or bacterial infections of the CNS, manifest high reactivity to FAM84A in CSF. FAM84A may be a highly immunogenic protein that rapidly elicits humoral responses, once available to the immune system. The general reactivity in serum was not increased in the individual cohorts, but in a small number of samples from the MS-, NB-, and OID-groups the signal was above the average.

4.3.2.3 rOCB-MS1-s2 recognizes AKAP17A

The A-kinase anchoring protein 17A (AKAP17A) was selected for validation because this candidate antigen had previously been detected in the F_{ab}-fragment protein microarray and had the highest enrichment factor of rOCB-MS1-s2 candidates. AKAP17A is also known as “splicing factor 17A”. AKAP17A forms complexes with proteinkinase A targeting it to splicing factor compartments in nuclear speckles [178]. Additionally, minor amounts of this protein localize to the cytoplasm [179]. AKAP17A also interacts with a number of other factors involved in pre-mRNA splicing, controlling splice site selection [179]. AKAP17A is ubiquitously transcribed which is in line with its universal function [178]. The protein has an overall positive charge with arginine being highly overrepresented. Due to the positive charges, the protein is well suited to interact non-

specifically with negatively charged molecules such as DNA or phospholipid bilayers. The observation that the *per se* soluble AKAP17A is lost upon high speed centrifugation of crude lysate may suggest that the protein associates with lipid-vesicles.

Immunocytochemistry using rOCB-MS1-s2 on AKAP17A-transfected HEK293E-cells revealed a perinuclear staining pattern. In contrast, non-transfected cells that endogenously express low levels of AKAP17A did not yield any signal. Thus, AKAP17A was confirmed as target antigen of rOCB-MS1-s2 by immunocytochemistry when present at high concentrations. This is in agreement with previous attempts to stain brain tissue and 2D-Western blots, that did not identify a specific staining pattern or antigen [100, 102]. The low endogenous expression levels of AKAP17A seem not to be sufficient for detection with these screening methods.

Membrane association of AKAP17A and the fact that it is an anchoring protein that binds to many other proteins make purification difficult. Different expression and purification strategies were found not to be effective. Thus, the method of choice to verify the binding of rOCB-MS1-s2 to this candidate antigen was immunoprecipitation from crude HEK-cell lysate in combination with Western blot detection. This allows the identification of a target protein in the presence of a variety of impurities. Additionally, immunoprecipitation is performed in solution, thus the antigen is accessible from all sides.

4.3.2.4 Cross-reactivity of rOCB-MS1-s8

AKAP17A was also recognized by rOCB-MS1-s8 in immunoprecipitation experiments. This antibody had previously been shown to recognize FAM84A, but had not displayed enhanced reactivity to AKAP17A in the protein microarrays. These seemingly contradictory findings may be explained by the differential experimental setup. Most probably, the epitope of AKAP17A recognized by rOCB-MS1-s8 is either not present on the protein microarray or not accessible to the antibody. This may be due to differential posttranslational modifications, (partial) misfolding or the protein's preferential orientation on microarrays.

To identify the molecular basis of the cross-reactivity, FAM84A-ELISA was applied to alanine-mutants of FAM84A. ELISA-technique allows handling a large number of parallel experiments, thus this method was chosen for the required screening experiments. The fact that AKAP17A could not be sufficiently purified precluded the use of an AKAP17A-ELISA, because OCB-derived antibodies may recognize co-purified contaminants. Therefore, the existing FAM84A-ELISA was employed to test rOCB-MS1-s8 for reactivity with FAM84A-mutants.

Mutations in the AA258-279 stretch resulted in differential recognition of FAM84A by rOCB-MS1-s8. This epitope is characterized by a high number of charged residues that locate to the same side of an α-helix. It is conceivable that this side of the helix faces the solvent in the natively folded protein. Interestingly, the AA exchange at position 267 to alanine did not change the binding although this position seems to be located in the center of the epitope.

In conclusion, the results revealed the α-helical structure of the AA-region 258-271 of FAM84A as epitope targeted by rOCB-MS1-s8. A homologous structure is present in the AA-region 305-323 of AKAP17A. The results suggest that the reactivity of rOCB-MS1-s8 to both FAM84A and AKAP17A may be due to the presence of this homologous sequence stretch that adopts a similar α-helical secondary structure. This finding does not exclude that rOCB-MS1-s8 also may bind to proteins other than those described here.

Identification of multiple antigens for a single monoclonal antibody is not surprising. Polyspecificity is defined as reactivity to LPS, DNA and insulin and is most pronounced in the naïve IgM-antibody repertoire [12]. Such classical polyreactivity was not observed with the OCB-derived antibodies studied here [102]. However, reactivity to multiple unrelated antigens is also found in affinity-matured IgG- and IgA-molecules [180]. Multispecificity of a monoclonal antibody may be attributed to distinct physical and chemical interactions that can be mediated by the binding pocket (Figure 1-5) [9]. Multispecific antibodies were shown to bind to numerous molecules in late apoptotic cells, activate complement and enhance phagocytosis of cell debris by macrophages [27].

Multispecificity of antibodies has been related to autoimmunity. It has been described in systemic lupus erythematosus (SLE). In the 1980s, Lafer et al. demonstrated that monoclonal antibodies derived from spleen cells of unimmunized MRL/1 mice, an animal model of SLE, reacted to DNA, the hallmark of SLE, but also recognized cardiolipin and phospholipids. They attributed this finding to the reactivity of such antibodies to the phosphate ester bonds in the different target structures [181]. This may, in part, explain the tremendous number of autoantigens described for this disease. Defective early maturation checkpoints may play a role [182], but the driving force behind the antibody production remains elusive [18].

4.3.3 Intracellular Proteins are Targets of expanded Antibody Species from MS-CSF

This study characterized three antigens of individual, unambiguously identified MS-OCB-antibodies. All are intracellular proteins that are ubiquitously transcribed and expressed in various tissues, including the CNS. One of these targets is recognized by a monoclonally expanded antibody species present in an early disease stage and may be particularly interesting with regard to early events in disease manifestation.

The array does not cover all human proteins, thus the possibility remains that the rAbs additionally recognize other molecules that were not identified in this study. A common pattern in their function could not be identified. Ubiquitous, intracellular proteins as targets of OCB-antibodies will not seem plausible at first, because these molecules reside inside cells, hidden from the immune system. Yet, a number of intracellular proteins were previously found to be specifically targeted by antibodies from MS samples, these include tubulin [183], transketolase [74] and GAPDH [160]. These antigens were identified using unfractionated serum and CSF, thus it is not clear whether this reactivity may be attributed to OCB-antibodies.

In an approach using antibodies derived from single CNS-resident B-cells from autopsy material, Willis et al. found expanded clones that virtually all recognized an intracellular structure, as demonstrated by intracellular flow cytometry. The same staining profiles were found with control antibodies from tumor tissue and inclusion body myositis [184], arguing against a primary pathogenic role of OCBs in MS. Another study based on single cell derived antibodies from MS-CSF found reactivity to areas of myelin degradation but rarely in healthy CNS-tissue [96]. Thus, these OCBs recognized structures, which were only accessible after tissue destruction. Similarly, Owens and Bennett et al. found that single cell derived antibodies weakly stained nucleic and cytoplasmic granules in brain tissue [97]. These findings, in accordance with the present data, support a role for intracellular molecules as target structures of OCB-antibodies.

In autoimmune-mediated connective tissue diseases like SLE [185] and systemic sclerosis [186], intracellular proteins are a major group of target antigens. In this context, different hypotheses were proposed to explain the origin of autoreactive antibodies against intracellular proteins. First, general dysregulation of the immune system may cause the production of irrelevant Igs, thereby creating autoimmunity [187]. The antibodies studied here, however, seem to have undergone antigen-driven affinity-maturation, demonstrated by extensive somatic hypermutation. This argues against random antibody expression. Second, antibodies raised in a previous immune response may be cross-reactive with an intracellular molecule by so called molecular mimicry [88]. However, if molecular mimicry induced cross-reactive antibodies, one might expect highly similar structures to be targeted. At least the antigens identified here do not share major properties except their intracellular localization. Third, apoptotic processes may deliberate intracellular molecules that had previously been hidden from the immune system. These newly appearing antigens then elicit an immune reaction, including the production of antibodies. This phenomenon has been described in apoptotic cells in breast cancer patients [188] and systemic autoimmune diseases [189, 190]. This concept also provides a potential functional role of these expanded antibody species in CSF of MS patients.

4.4 Potential Origins and Functions of OCB Antibodies in MS

The function and role of OCBs in MS etiology and pathogenesis is not understood. Although OCBs are thought to contribute to demyelination [191, 192] in a subgroup of patients, proof of a pathogenetic role of OCB-antibodies in MS is still lacking. OCB antibodies in MS may not recognize a causative agent but byproducts of a primary immune reaction or irrelevant structures [193].

OCB-antibodies carry somatic hypermutations and are of the IgG isotype, thus have obviously undergone an antigen-driven maturation process. The mere expansion of antibodies that show characteristic signs of antigen-experience points to a targeted humoral immune reaction in the CNS. Further, evidence of sustained intrathecal antibody production [68, 92] suggests a role of these antibodies in MS.

A number of early studies detected antibodies directed at MOG or other myelin antigens in MS patients [96, 146, 194]. In accordance with recent literature that suggests only minor reactivity to myelin in MS [149, 195] these classical MS antigens were not recognized by the six OCB-derived rAbs in this study. In general, a pathogenic role of OCBs, i.e. binding and inducing destruction of myelin and perpetuating a harmful immunologic response, does not seem to be the major function. OCB patterns remain stable over time [66]. However, affected patients live for years experiencing relapses and phases of remission. In contrast, conditions where pathogenic autoantibodies are present, mainly monophasic, fulminant disease courses are observed such as in paraneoplastic encephalitides [196].

The presence of affinity-matured and expanded antibody species [68, 69] indicates an underlying antigen-driven process and their persistence suggests a recurring stimulus that sustain the antibody production. Such a stimulus may be provided by a foreign invader or by a cryptic self-antigen. The concept of molecular mimicry describes the potential of an immune response initially targeted at foreign molecule to simultaneously recognize homologous self-structures [197]. This may be one way how pathogens may trigger autoimmunity and a number of autoimmune diseases are suspected to be associated with distinct infections [198]. Despite extensive research on infectious agents associated to MS pathology, conclusive data is lacking so far [199]. However, OCB-derived antibodies studied here did not react with commonly MS-associated viral (EBV, measles, rubella, varicella zoster) and bacterial (chlamydia) invaders [100, 101].

The release or presentation of intracellular components, originating from apoptotic processes, could be an alternative mechanism to induce autoreactive antibodies [200]. Antibodies may be formed in response to large amounts of cell debris that may occur naturally or due to a primary pathogenic condition inside the CNS. In this situation, antibodies may opsonize cellular debris including all types of molecules: DNA, lipids and intracellular proteins. This may simplify endocytosis by macrophages, help to clear the site of damage, and potentially enhances recovery processes. Such a process has been shown for SLE and may play a role in other autoimmune diseases [200, 201]. Interestingly, Willis et al. found reactivity to intracellular structures in virtually all expanded MS derived B-cell clones, control antibodies derived from tumors, and inclusion body myositis [184]. This finding may support the concept of expanded antibody species targeting a variety of intracellular molecules possibly in order to enhance clearance of excessive cell debris in a variety of conditions. In general, it is well accepted that the specificity of antibodies in MS ranges widely, possibly reflecting part of the heterogeneity of the disease [91, 202]. A role in cell debris removal may not only have implications on the origin of the expanded antibodies, but may also represent a function of OCB-antibodies. In early years of immunological research, the potential role of expanded antibodies in cell debris removal was proposed by Grabar. He hypothesized that antibodies may not only have a functional role in defense against foreign substances, but also may represent a physiological mechanism that allows “cleaning up” of cellular debris [203].

As discussed earlier, numerous studies have identified a wide variety of MS-antigens [91]. Based on three distinct OCB-derived antibodies, the present results support previous studies that failed to identify a single molecule that drives pathogenesis and/or disease progression to be targeted by OCB-antibodies. The three antigens studied here point to a rather heterogeneous humoral response in individual MS patients [91] and may suggest that the expanded antibodies possibly do not recognize a causative agent, but rather cryptic self-structures. This mechanism could help to efficiently remove cellular debris from the tissue after an initial insult. In the 1980s, macrophages present in MS lesions were found to take up cellular debris via an antibody-mediated endocytic process [191, 204]. This finding was associated with destructive demyelination, but may also entail beneficial clearance processes [205]. This is further supported by the fact that all rAbs described in this study derive from complement-fixing IgG1-molecules [100]. Antibodies of the IgG1-isotype are found in all OCB-positive MS patients and are the predominant Ig-subclass in OCBs [206, 207]. Opsonization of cell debris may be an important process to ensure rapid clearance of damaged cells to avoid more unspecific immunologic activation. This potential function would conform with the unchanged antibody profiles throughout the different disease states and has been associated with beneficial effects, like improved remyelination of damaged areas [208, 209].

4.5 Identification and Validation of a systemic Antigen of rAb-lp2

Although identical in regard of biochemical characteristics, the functional role of OCBs may differ. Three general modes of action could be differentiated: First, OCBs recognize infectious agents in infectious disorders. Thus, OCBs in NB recognize *borrelia* [153] and thereby help clearing the infection. Second, antibodies could help clearing cell debris produced by primary immune responses. This potential function of OCBs in MS, as proposed here, was previously shown to play a role in SLE [201]. Third, a number diseases is associated with clearly pathogenic antibodies such as NMDAR- [36] or AMPAR-encephalitis [105]. These pathogenic antibodies are found in serum and CSF and recognize a CNS-specific structure such as neuronal cell surface structures and synaptic receptors [196]. The functional difference of MS-OCBs and encephalitogenic antibodies is reflected by distinct disease courses. MS is usually characterized by a relapsing-remitting disease course [210] whereas encephalitis cases often display an acute, monophasic course [196].

4.5.1 rAb-lp2 recognizes the extracellular Domain of the $GABA_AR$ α1-subunit

Unfractionated CSF and serum of patient lp2 was used to first describe a severe form of encephalitis as $GABA_AR$-encephalitis [111]. Reactivity to the $GABA_AR$ α1-subunit was confirmed

in both serum and CSF of this patient by immunoprecipitation and immunostaining of rat brain [111].

So far, pathology of the $GABA_AR$-encephalitis remains to be elucidated. Here, patient Ip2 was studied who had severe encephalitis with seizures and psychic symptoms. Despite intensive search, an infectious cause was not identified [111]. A potential mechanism that was previously found to be involved in $GABA_BR$-encephalitis and similar conditions is an underlying paraneoplastic syndrome [211]. For most $GABA_AR$-encephalitis patients, an autoimmune process is assumed and patients presenting $GABA_AR$-encephalitis symptoms and a coexisting thymoma have been described [121]. The identification of a cross-reactive protein may be supportive of a paraneoplastic background in $GABA_AR$-encephalitis.

Since rAb-Ip2 represents the only expanded antibody species in the sample (E. Beltrán, unpublished data), it was hypothesized that it may be involved in $GABA_AR$ recognition. This hypothesis was confirmed here, as rAb-Ip2 recognized the extracellular domain of the $GABA_AR$ α1-subunit in an ELISA. Furthermore, application of rAb-Ip2 to hippocampal neuronal cultures [111] resulted in a staining pattern highly similar to the pattern observed with the unfractionated CSF sample (J. Dalmau, E. Beltrán, personal communication). These findings provide evidence for a pathologic role of rAb-Ip2 in patient Ip2.

Despite the fact that a number of GABA-receptor subunits were present on the Protoarray®, none of these were recognized by rAb-Ip2. The reason presumably is misfolding of the protein and resulting loss of conformational epitopes. Recombinant production and purification of membrane-associated proteins is difficult, as the insertion of hydrophobic residues into the membrane is crucial for overall folding. In the absence of a lipid-bilayer, the residues forming the transmembrane domain of the $GABA_AR$ α1-subunit will not be able to fold into their native conformation. This will interfere with the overall folding of the protein and thereby impede the conformation-sensitive antibody-antigen binding.

4.5.2 rAb-Ip2 recognizes CSRP2

To identify potential cross-reactive candidate antigens, rAb-Ip2 reactivity was analyzed on protein microarrays. In the protein microarray, rAb-Ip2 recognized a total of six different zinc-binding proteins (Table 3-3) and the majority the zinc-binding candidate antigens mediated this interaction via LIM-domains. rAb-Ip2 recognized three different LIM-domain proteins. The strongest overall signal was detected with CSRP2. The related proteins CSRP1 and CRIP2 showed lesser reactivity. The LIM-domain characterizes a distinct zinc-binding motif that makes up a large part of these LIM-domain proteins. LIM-domains serve as platform for protein-protein-interactions [212]. LIM-proteins are thought to mediate the organization of transcriptional protein-complexes [213] and thereby regulate gene expression [214]. In accordance with this, LIM-only proteins, which are closely related to CSRP2, have been associated with a variety of malignancies [215]. The highest enrichment factor was found with MAPK7, but immunoprecipitation of HEK-derived

MAPK7 did not confirm the protein microarray results. These findings may suggest the involvement of a paraneoplastic background of the encephalitis in patient Ip2.

Interestingly, $GABA_AR$ function is regulated by a zinc-binding site, which is located to an N-terminal cysteine-loop of the α-subunit [120]. Common zinc-coordinating residues Cys, His, Glu and Asp [216] are thought to form the binding site [120]. In contrast, in all LIM-domain proteins, zinc-ions are bound by the consensus LIM-motif [217]. The two distinct zinc-binding motifs are illustrated in Figure 4-1.

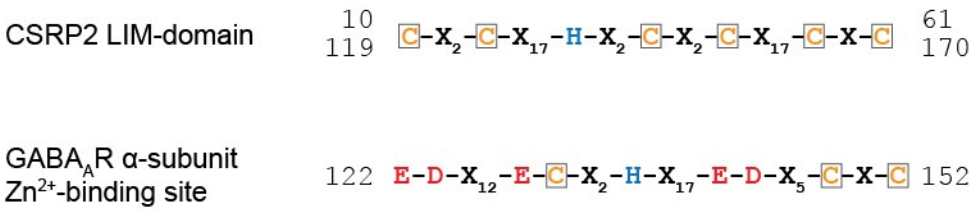

Figure 4-1: Comparison of Zn^{2+}-binding Motifs in CSRP2 and the $GABA_AR$ α-subunit.
The upper row depicts the LIM-domain consensus sequence found in CSRP2. CSRP2 carries an N-terminal (AA10-61) and a C-terminal (AA119-170) LIM-domain. Regulatory zinc-binding in the $GABA_AR$ α-subunit may be mediated by negatively charged AA in a cysteine-loop (lower row). Binding of zinc ions may also involve residues of neighboring subunits. Residues are color-coded: cysteine: orange, boxed, histdine: blue, negatively charged AA: red, black: any other AA.

The LIM-domain coordinates zinc mainly with cysteine-residues, whereas negatively charged residues play a crucial role in zinc binding by $GABA_AR$. As the primary sequence of the motifs is quite distinct, structural analysis is needed to clarify whether the cross-reactivity of rAb-Ip2 to $GABA_AR$ and CSRP2 relates to the zinc-binding site.

Figure 4-2 highlights the localization of (potential) zinc-binding residues in a $GABA_A$-receptor subunit and in CSRP2. The zinc binding site of the $GABA_AR$ appears to be located in the extracellular domain facing the extracellular space. This location may be accessible to antibodies in tissue. Thus, the zinc-binding sites in CSRP2 and $GABA_AR$ may present a potential common structural feature that could form the basis for cross-reactivity of rAb-Ip2 and a potential paraneoplastic background. Co-crystallization of rAb-Ip2 with $GABA_AR$ and CSRP2 may elucidate the target epitope.

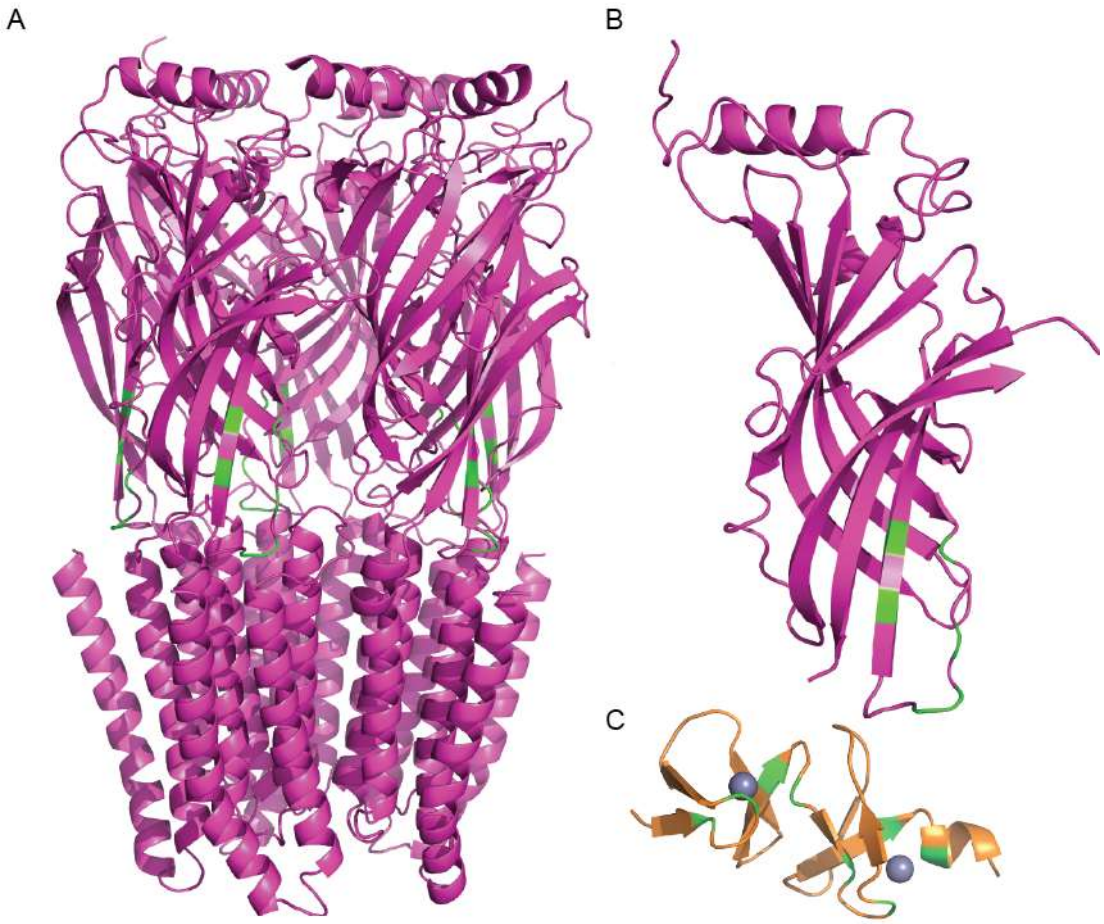

Figure 4-2: Ribbon-diagram of a $GABA_AR$-pentamer, single Subunit, and CSRP2 C-terminus.

Comparison of putative zinc-binding sites in a $GABA_AR$ β3-pentamere (A), a single subunit (B, both 4COF) and the C-terminal part of CSRP2 (C, 1QLI) are depicted. Putative zinc-binding residues are highlighted in green. CSRP2 is depicted with zinc ions (grey spheres). In both proteins, zinc-binding residues are located to beta-sheet secondary structures and in flexible loops. From this model, both putative zinc-binding sites appear to be localized on the protein's surface and may be accessible for antibodies. Note that the structural information depicted here is deduced from $GABA_AR$ β3-subunit and corresponding residues of the α1-subunit are highlighted as zinc-binding. The illustrations of 4COF and 1QLI are modified from [114] and [218] respectively.

Immunofluorescence staining of non-transfected HEK293E-cells, which endogenously express high levels of CSRP2, medium levels of CSRP1 and CRIP2, but not $GABA_AR$, yielded signals in perinuclear regions (Figure 3-29). This is in accordance with the expected intracellular localization of the LIM-domain proteins [219, 220]. These results further substantiate the reactivity of rAb-Ip2 with CSRP2. Whether rAb-Ip2 recognizes CSRP2 *in vivo* remains to be formally demonstrated.

In patient Ip2 no tumor could be detected [111]. As neurologic symptoms regularly occur prior to cancer diagnosis [108] and underlying malignancies may be small [34], a paraneoplastic etiology is conceivable. In such a scenario, rAb-Ip2 would have been raised in a primary immune response against CSRP2 (peripheral tumor antigen), which may be exposed due to effective tumor destruction, and was cross-reactive to $GABA_AR$ (CNS-specific antigen). The cross-reactivity may be mediated by the structurally similar zinc-binding sites of the two antigens. This finding may suggest the presence of a malignancy that initiated the production of rAb-Ip2.

4.6 Future Prospects

a) MS-OCBs

In this study, three ubiquitous intracellular proteins were identified as targets of OCB antibodies from MS patients. The target antigens presented here suggest that MS-OCBs represent a highly variable and seemingly patient-specific population of expanded antibodies. To confirm that a majority of OCBs recognizes ubiquitous, intracellular proteins, a larger number of distinct OCB-derived antibodies should be analyzed. Recognition of ubiquitous intracellular proteins by OCB-antibodies points to a rather non-pathogenic role of OCBs. In MS, most patients present with a relapsing-remitting disease course. However, in case of an expanded antibody targeting a CNS-specific, accessible antigen, the disease course is probably expected to be monophasic and fulminant as has been observed with paraneoplastic encephalitides for example. One potential functional role of OCB-antibodies, in agreement with the present data, may be opsonization of cellular debris to facilitate phagocytic clearance processes. To strengthen this hypothesis, it is important to clarify whether the antigens described here are also targeted *in vivo* and to characterize more OCB-antibodies.

Importantly, the antigens presented here are clearly not exclusive and each of the antibodies holds the potential to recognize multiple other related or un-related structures. Therefore, infectious agents may be reconsidered. Suspected causative pathogens may play a role as a trigger of disease [221] possibly through induction of autoreactivity. Full length OCB-derived antibodies were not yet analyzed with regard to infectious agents and potential cross-reactivity cannot be excluded.

Analyzing potential changes of OCB reactivity during the disease course could elucidate whether the reactivity spectrum is as stable as OCB-patterns are. To this end, OCB-antibody specificities from patients in distinct disease states, i.e. relapses vs. remission could be compared. Similarly, profiling the antigen-specificity in longitudinal follow-up CSF-samples of a patient could hold information. However, these samples are sparse because lumbar punctures are generally only done at the time of diagnosis.

Genetic factors play a role in MS etiology [222], thus the risk to develop the disease is increased if family members are affected. Monitoring of relatives of MS patients offers the opportunity to diagnose the disease in very early stages, even before clinical signs are detectable. Studies of MS-discordant monozygotic twins showed that non-MS diagnosed twins occasionally present signs of MS, such as clinically-silent lesions in MRI-scans or OCBs (E. Beltran, K. Held, unpublished data). Identifying the specificity of OCB-antibodies from such incipient MS patients may promote the understanding of early pathogenetic processes in the disease.

b) $GABA_AR$-encephalitis

rAb-Ip2 was found to recognize the $GABA_AR$ α1-subunit and to cross-react with a ubiquitously expressed antigen, CSRP2 and related LIM-domain proteins. The number of $GABA_AR$-encephalitis cases, which may be caused by a paraneoplastic syndrome is extremely small [111, 223]. Identification of the cross-reactive CSRP2 protein provides a hint for a systemic antigen to play a role, but direct evidence of a malignancy in patient Ip2 is not available. To this end, studies on CSF and serum samples of other patients are necessary. So far, few patients with $GABA_AR$-encephalitis and co-existing thymoma are described [121]. CSRP2-reactivity in CSF and/or serum of these patients could be assessed to test whether this cross-reactivity is specific for patient Ip2 or a common feature in $GABA_AR$-encephalitis. Implementation of an ELISA to screen patient samples would allow rapid identification of CSRP2-reactivity in other $GABA_AR$-encephalitis patients using minimal amounts of CSF. Identification of a malignancy that may cause a neurologic syndrome could help to improve diagnosis and treatment of the disorder. Removal of malignant tissue has proven effective in other paraneoplastic syndromes [211] and in most cases tumors are only diagnosed after the onset of neurologic symptoms [34]. Knowledge on associated tumors could help diagnosing patients early.

Functionally, Petit-Pedrol et al. showed that CSF from patient Ip2 downregulates synaptical $GABA_AR$, thereby impeding inhibitory signals [111]. This finding could account for seizures and psychic symptoms that may be caused by disturbed synaptic activity. Thus, electrophysiological experiments using rAb-Ip2 could clarify whether this antibody causes changes in synaptical expression of $GABA_AR$ and thereby may induce pathologic symptoms.

The occurrence of paraneoplastic syndromes had been ascribed to ectopic expression of neuronal antigens in tumor-tissue that are targeted by the immune response [108]. However, pathogenic antibodies may also derive from anti-tumor responses to non-CNS-antigens that are cross-reactive with CNS-tissue. In this case, the antibody's cross-reactivity may be based on the recognition of either structurally similar or distinct epitopes on different proteins. rAb-Ip2 recognized multiple proteins containing LIM-domains and other zinc-binding proteins on the protein microarray, suggesting that zinc-binding motifs may play a role for cross-reactivity. Understanding the molecular basis for the cross-reactivity of CSRP2 and the $GABA_AR$ α1-subunit would offer mechanistic insights and allow predictions on other proteins that potentially cross-react. As discussed earlier, crystallization experiments could elucidate whether the zinc-binding sites of $GABA_AR$ and CSRP2 are epitopes of rAb-Ip2. Crystals of antibody-antigen-complexes will be analyzed by x-ray diffraction and allow for identification of molecular structures involved in recognition by rAb-Ip2.

References

1. Ehrlich, P., *Experimentelle Untersuchungen über Immunität. II. Über Abrin.* Deutsche Medizinische Wochenschrift, 1891(17): p. 1218-1219.
2. Abbas, A.K., A.H. Lichtman, and S. Pillai, *Cellular and molecular immunology*. 8. ed. ed. 2015, Philadelphia, PA: Elsevier Saunders. VIII, 535 S.
3. MacLennan, I.C., *Germinal centers.* Annu Rev Immunol, 1994. **12**: p. 117-39.
4. Muramatsu, M., et al., *Class switch recombination and hypermutation require activation-induced cytidine deaminase (AID), a potential RNA editing enzyme.* Cell, 2000. **102**(5): p. 553-63.
5. Cambier, J.C., et al., *B-cell anergy: from transgenic models to naturally occurring anergic B cells?* Nat Rev Immunol, 2007. **7**(8): p. 633-43.
6. Stoop, J.W., et al., *Serum immunoglobulin levels in healthy children and adults.* Clin Exp Immunol, 1969. **4**(1): p. 101-12.
7. Irani, D.N., *CHAPTER 10 - Properties and Composition of Normal Cerebrospinal Fluid*, in *Cerebrospinal Fluid in Clinical Practice*, D.N. Irani, Editor. 2009, W.B. Saunders: Philadelphia. p. 69-89.
8. Harris, L.J., E. Skaletsky, and A. McPherson, *Crystallographic structure of an intact IgG1 monoclonal antibody.* J Mol Biol, 1998. **275**(5): p. 861-72.
9. Tapryal, S., et al., *Structural evaluation of a mimicry-recognizing paratope: plasticity in antigen-antibody interactions manifests in molecular mimicry.* J Immunol, 2013. **191**(1): p. 456-63.
10. Sundberg, E.J. and R.A. Mariuzza, *Molecular recognition in antibody-antigen complexes*, in *Advances in Protein Chemistry*. 2002, Academic Press. p. 119-160.
11. Lutterotti, A. and R. Martin, *Getting specific: monoclonal antibodies in multiple sclerosis.* Lancet Neurol, 2008. **7**(6): p. 538-47.
12. Wardemann, H., et al., *Predominant autoantibody production by early human B cell precursors.* Science, 2003. **301**(5638): p. 1374-7.
13. Zhou, Z.H., et al., *The broad antibacterial activity of the natural antibody repertoire is due to polyreactive antibodies.* Cell Host Microbe, 2007. **1**(1): p. 51-61.
14. Dimitrov, J.D., et al., *Antibody polyreactivity in health and disease: statu variabilis.* J Immunol, 2013. **191**(3): p. 993-9.
15. Alam, S.M., et al., *The role of antibody polyspecificity and lipid reactivity in binding of broadly neutralizing anti-HIV-1 envelope human monoclonal antibodies 2F5 and 4E10 to glycoprotein 41 membrane proximal envelope epitopes.* J Immunol, 2007. **178**(7): p. 4424-35.
16. Girard, D. and J.L. Senecal, *Anti-microfilament IgG antibodies in normal adults and in patients with autoimmune diseases: immunofluorescence and immunoblotting analysis of 201 subjects reveals polyreactivity with microfilament-associated proteins.* Clin Immunol Immunopathol, 1995. **74**(2): p. 193-201.
17. van Esch, W.J., et al., *Polyreactivity of human IgG Fc-binding phage antibodies constructed from synovial fluid CD38+ B cells of patients with rheumatoid arthritis.* J Autoimmun, 2002. **19**(4): p. 241-50.
18. Yaniv, G., et al., *A volcanic explosion of autoantibodies in systemic lupus erythematosus: a diversity of 180 different antibodies found in SLE patients.* Autoimmun Rev, 2015. **14**(1): p. 75-9.
19. Linnington, C., M. Webb, and P.L. Woodhams, *A novel myelin-associated glycoprotein defined by a mouse monoclonal antibody.* J Neuroimmunol, 1984. **6**(6): p. 387-96.
20. Mariuzza, R.A., *Multiple paths to multispecificity.* Immunity, 2006. **24**(4): p. 359-61.
21. McFarland, B.J. and R.K. Strong, *Thermodynamic analysis of degenerate recognition by the NKG2D immunoreceptor: not induced fit but rigid adaptation.* Immunity, 2003. **19**(6): p. 803-12.
22. Stanfield, R.L., et al., *Major antigen-induced domain rearrangements in an antibody.* Structure, 1993. **1**(2): p. 83-93.
23. Yin, J., et al., *Structural plasticity and the evolution of antibody affinity and specificity.* J Mol Biol, 2003. **330**(4): p. 651-6.
24. Wedemayer, G.J., et al., *Structural insights into the evolution of an antibody combining site.* Science, 1997. **276**(5319): p. 1665-9.
25. James, L.C., P. Roversi, and D.S. Tawfik, *Antibody multispecificity mediated by conformational diversity.* Science, 2003. **299**(5611): p. 1362-7.

26. Sethi, D.K., et al., *Differential epitope positioning within the germline antibody paratope enhances promiscuity in the primary immune response.* Immunity, 2006. **24**(4): p. 429-38.
27. Zhou, Z.-h., et al., *Polyreactive Antibodies Plus Complement Enhance the Phagocytosis of Cells Made Apoptotic by UV-Light or HIV.* Scientific Reports, 2013. **3**: p. 2271.
28. Gunti, S. and A.L. Notkins, *Polyreactive Antibodies: Function and Quantification.* J Infect Dis, 2015. **212 Suppl 1**: p. S42-6.
29. Gay, D., et al., *Receptor editing: an approach by autoreactive B cells to escape tolerance.* J Exp Med, 1993. **177**(4): p. 999-1008.
30. Nemazee, D.A. and K. Burki, *Clonal deletion of B lymphocytes in a transgenic mouse bearing anti-MHC class I antibody genes.* Nature, 1989. **337**(6207): p. 562-6.
31. Goodnow, C.C., et al., *Altered immunoglobulin expression and functional silencing of self-reactive B lymphocytes in transgenic mice.* Nature, 1988. **334**(6184): p. 676-82.
32. Coutinho, A., M.D. Kazatchkine, and S. Avrameas, *Natural autoantibodies.* Curr Opin Immunol, 1995. **7**(6): p. 812-8.
33. Mouquet, H., et al., *Polyreactivity increases the apparent affinity of anti-HIV antibodies by heteroligation.* Nature, 2010. **467**(7315): p. 591-5.
34. Albert, M.L. and R.B. Darnell, *Paraneoplastic neurological degenerations: keys to tumour immunity.* Nat Rev Cancer, 2004. **4**(1): p. 36-44.
35. Lennon, V.a., et al., *IgG marker of optic-spinal multiple sclerosis binds to the aquaporin-4 water channel.* The Journal of experimental medicine, 2005. **202**: p. 473-477.
36. Dalmau, J., et al., *Paraneoplastic anti-N-methyl-D-aspartate receptor encephalitis associated with ovarian teratoma.* Ann Neurol, 2007. **61**(1): p. 25-36.
37. Stepulak, A., et al., *Expression of glutamate receptor subunits in human cancers.* Histochem Cell Biol, 2009. **132**(4): p. 435-45.
38. Liblau, R., B. Benyahia, and J.Y. Delattre, *The pathophysiology of paraneoplastic neurological syndromes.* Ann Med Interne (Paris), 1998. **149**(8): p. 512-20.
39. Rosenblum, M.D., K.A. Remedios, and A.K. Abbas, *Mechanisms of human autoimmunity.* J Clin Invest, 2015. **125**(6): p. 2228-33.
40. Hayter, S.M. and M.C. Cook, *Updated assessment of the prevalence, spectrum and case definition of autoimmune disease.* Autoimmun Rev, 2012. **11**(10): p. 754-65.
41. Cooper, G.S., M.L. Bynum, and E.C. Somers, *Recent insights in the epidemiology of autoimmune diseases: improved prevalence estimates and understanding of clustering of diseases.* J Autoimmun, 2009. **33**(3-4): p. 197-207.
42. Steinman, L., *Multiple sclerosis: a two-stage disease.* Nat Immunol, 2001. **2**(9): p. 762-764.
43. Sawcer, S., et al., *Genetic risk and a primary role for cell-mediated immune mechanisms in multiple sclerosis.* Nature, 2011. **476**(7359): p. 214-9.
44. Hohlfeld, R., et al., *The search for the target antigens of multiple sclerosis, part 1: autoreactive CD4+ T lymphocytes as pathogenic effectors and therapeutic targets.* The Lancet Neurology, 2016. **15**(2): p. 198-209.
45. Ramagopalan, S.V., D.A. Dyment, and G.C. Ebers, *Genetic epidemiology: the use of old and new tools for multiple sclerosis.* Trends Neurosci, 2008. **31**(12): p. 645-52.
46. Wingerchuk, D.M., *Smoking: effects on multiple sclerosis susceptibility and disease progression.* Ther Adv Neurol Disord, 2012. **5**(1): p. 13-22.
47. Ascherio, A., K.L. Munger, and K.C. Simon, *Vitamin D and multiple sclerosis.* Lancet Neurol, 2010. **9**(6): p. 599-612.
48. Levin, L.I., et al., *Primary infection with the Epstein-Barr virus and risk of multiple sclerosis.* Ann Neurol, 2010. **67**(6): p. 824-30.
49. Hemmer, B., M. Kerschensteiner, and T. Korn, *Role of the innate and adaptive immune responses in the course of multiple sclerosis.* Lancet Neurol, 2015. **14**(4): p. 406-19.
50. Ang, C.W., B.C. Jacobs, and J.D. Laman, *The Guillain-Barre syndrome: a true case of molecular mimicry.* Trends Immunol, 2004. **25**(2): p. 61-6.
51. Hohlfeld, R., et al., *The search for the target antigens of multiple sclerosis, part 2: CD8+ T cells, B cells, and antibodies in the focus of reverse-translational research.* Lancet Neurol, 2016. **15**(3): p. 317-31.
52. Pollinger, B., et al., *Spontaneous relapsing-remitting EAE in the SJL/J mouse: MOG-reactive transgenic T cells recruit endogenous MOG-specific B cells.* J Exp Med, 2009. **206**(6): p. 1303-16.
53. Bar-Or, A., et al., *Abnormal B-cell cytokine responses a trigger of T-cell-mediated disease in MS?* Annals of Neurology, 2010. **67**: p. 452-461.
54. Lanzavecchia, A., *Antigen-specific interaction between T and B cells.* Nature, 1985. **314**(6011): p. 537-9.

55. Brodbelt, A. and M. Stoodley, *CSF pathways: a review.* Br J Neurosurg, 2007. **21**(5): p. 510-20.
56. Felgenhauer, K., *Protein size and cerebrospinal fluid composition.* Klin Wochenschr, 1974. **52**(24): p. 1158-64.
57. Reiber, H. and M. Uhr, *Liquordiagnostik*, in *Klinische Neurologie*, P. Berlit, Editor. 2012, Springer Berlin Heidelberg. p. 143-178.
58. Kabat, E.A., D.H. Moore, and H. Landow, *AN ELECTROPHORETIC STUDY OF THE PROTEIN COMPONENTS IN CEREBROSPINAL FLUID AND THEIR RELATIONSHIP TO THE SERUM PROTEINS.* J Clin Invest, 1942. **21**(5): p. 571-7.
59. Kabat, E.A., M. Glusman, and V. Knaub, *Quantitative estimation of the albumin and gamma globulin in normal and pathologic cerebrospinal fluid by immunochemical methods.* Am J Med, 1948. **4**(5): p. 653-62.
60. Lowenthal, A., D. Karcher, and M. Van Sande, *Electrophophoretic studies of central nervous system proteins.* Exp Neurol, 1959. **1**: p. 233-47.
61. Bourahoui, A., et al., *CSF isoelectrofocusing in a large cohort of MS and other neurological diseases.* Eur J Neurol, 2004. **11**(8): p. 525-9.
62. Vandvik, B., et al., *Oligoclonal measles virus-specific IgG antibodies isolated from cerebrospinal fluids, brain extracts, and sera from patients with subacute sclerosing panencephalitis and multiple sclerosis.* Scand J Immunol, 1976. **5**(8): p. 979-92.
63. Coyle, P.K. and J.S. Wolinsky, *Characterization of immune complexes in progressive rubella panencephalitis.* Ann Neurol, 1981. **9**(6): p. 557-62.
64. Vartdal, F., et al., *Neurosyphilis: intrathecal synthesis of oligoclonal antibodies to Treponema pallidum.* Ann Neurol, 1982. **11**(1): p. 35-40.
65. Burgoon, M.P., et al., *Oligoclonal immunoglobulins in cerebrospinal fluid during varicella zoster virus (VZV) vasculopathy are directed against VZV.* Ann Neurol, 2003. **54**(4): p. 459-63.
66. Link, H. and Y.M. Huang, *Oligoclonal bands in multiple sclerosis cerebrospinal fluid: an update on methodology and clinical usefulness.* J Neuroimmunol, 2006. **180**(1-2): p. 17-28.
67. McLean, B.N., R.W. Luxton, and E.J. Thompson, *A study of immunoglobulin G in the cerebrospinal fluid of 1007 patients with suspected neurological disease using isoelectric focusing and the Log IgG-Index. A comparison and diagnostic applications.* Brain, 1990. **113 (Pt 5)**: p. 1269-89.
68. Obermeier, B., et al., *Matching of oligoclonal immunoglobulin transcriptomes and proteomes of cerebrospinal fluid in multiple sclerosis.* Nat Med, 2008. **14**(6): p. 688-93.
69. Beltran, E., et al., *Intrathecal somatic hypermutation of IgM in multiple sclerosis and neuroinflammation.* Brain, 2014.
70. Lucchinetti, C., et al., *Heterogeneity of multiple sclerosis lesions: implications for the pathogenesis of demyelination.* Ann Neurol, 2000. **47**(6): p. 707-17.
71. Weinshenker, B.G., *Therapeutic plasma exchange for acute inflammatory demyelinating syndromes of the central nervous system.* J Clin Apher, 1999. **14**(3): p. 144-8.
72. Sospedra, M. and R. Martin, *Immunology of multiple sclerosis.* Annu Rev Immunol, 2005. **23**: p. 683-747.
73. Bronstein, J.M., et al., *A humoral response to oligodendrocyte-specific protein in MS: a potential molecular mimic.* Neurology, 1999. **53**(1): p. 154-61.
74. Lovato, L., et al., *Transketolase and 2',3'-cyclic-nucleotide 3'-phosphodiesterase type I isoforms are specifically recognized by IgG autoantibodies in multiple sclerosis patients.* Mol Cell Proteomics, 2008. **7**(12): p. 2337-49.
75. Banki, K., et al., *Oligodendrocyte-specific expression and autoantigenicity of transaldolase in multiple sclerosis.* J Exp Med, 1994. **180**(5): p. 1649-63.
76. Niehaus, A., et al., *Patients with active relapsing-remitting multiple sclerosis synthesize antibodies recognizing oligodendrocyte progenitor cell surface protein: implications for remyelination.* Ann Neurol, 2000. **48**(3): p. 362-71.
77. Mathey, E.K., et al., *Neurofascin as a novel target for autoantibody-mediated axonal injury.* The Journal of experimental medicine, 2007. **204**: p. 2363-2372.
78. Silber, E., et al., *Patients with progressive multiple sclerosis have elevated antibodies to neurofilament subunit.* Neurology, 2002. **58**(9): p. 1372-81.
79. Bornstein, N.M., et al., *Antibodies to brain antigens following stroke.* Neurology, 2001. **56**(4): p. 529-30.
80. Couratier, P., et al., *Serum autoantibodies to neurofilament proteins in sporadic amyotrophic lateral sclerosis.* J Neurol Sci, 1998. **154**(2): p. 137-45.
81. Wingerchuk, D.M., et al., *International consensus diagnostic criteria for neuromyelitis optica spectrum disorders.* Neurology, 2015. **85**(2): p. 177-89.

82. Quintana, F.J., et al., *Antigen microarrays identify CNS-produced autoantibodies in RRMS.* Neurology, 2012. **78**(8): p. 532-9.
83. Sueoka, E., et al., *Autoantibodies against heterogeneous nuclear ribonucleoprotein B1 in CSF of MS patients.* Ann Neurol, 2004. **56**(6): p. 778-86.
84. Mayo, I., et al., *The proteasome is a major autoantigen in multiple sclerosis.* Brain, 2002. **125**(Pt 12): p. 2658-67.
85. Williamson, R.A., et al., *Anti-DNA antibodies are a major component of the intrathecal B cell response in multiple sclerosis.* Proc Natl Acad Sci U S A, 2001. **98**(4): p. 1793-8.
86. Ilyas, A.A., Z.W. Chen, and S.D. Cook, *Antibodies to sulfatide in cerebrospinal fluid of patients with multiple sclerosis.* J Neuroimmunol, 2003. **139**(1-2): p. 76-80.
87. Brennan, K.M., et al., *Lipid arrays identify myelin-derived lipids and lipid complexes as prominent targets for oligoclonal band antibodies in multiple sclerosis.* J Neuroimmunol, 2011. **238**(1-2): p. 87-95.
88. Libbey, J.E., M.F. Cusick, and R.S. Fujinami, *Role of pathogens in multiple sclerosis.* Int Rev Immunol, 2014. **33**(4): p. 266-83.
89. Reiber, H., S. Ungefehr, and C. Jacobi, *The intrathecal, polyspecific and oligoclonal immune response in multiple sclerosis.* Mult Scler, 1998. **4**(3): p. 111-7.
90. Wandinger, K., et al., *Association between clinical disease activity and Epstein-Barr virus reactivation in MS.* Neurology, 2000. **55**(2): p. 178-84.
91. Fraussen, J., et al., *Targets of the humoral autoimmune response in multiple sclerosis.* Autoimmunity Reviews, 2014.
92. Hauser, S.L., et al., *B-cell depletion with rituximab in relapsing-remitting multiple sclerosis.* N Engl J Med, 2008. **358**(7): p. 676-88.
93. Kappos, L., et al., *Ocrelizumab in relapsing-remitting multiple sclerosis: a phase 2, randomised, placebo-controlled, multicentre trial.* The Lancet. **378**(9805): p. 1779-1787.
94. Kanter, J.L., et al., *Lipid microarrays identify key mediators of autoimmune brain inflammation.* Nature medicine, 2006. **12**: p. 138-143.
95. Querol, L., et al., *Protein array-based profiling of CSF identifies RBPJ as an autoantigen in multiple sclerosis.* Neurology, 2013. **81**: p. 956-963.
96. von Budingen, H.C., et al., *Clonally expanded plasma cells in the cerebrospinal fluid of MS patients produce myelin-specific antibodies.* Eur J Immunol, 2008. **38**(7): p. 2014-23.
97. Owens, G.P., et al., *Antibodies produced by clonally expanded plasma cells in multiple sclerosis cerebrospinal fluid.* Ann Neurol, 2009. **65**(6): p. 639-49.
98. Dornmair, K., E. Meinl, and R. Hohlfeld, *Novel approaches for identifying target antigens of autoreactive human B and T cells.* Seminars in Immunopathology, 2009. **31**(4): p. 467-477.
99. Brändle, S., *Analysis of oligoclonally expanded antibodies in the cerebrospinal fluid of patients with multiple sclerosis* 2013, WWU Münster.
100. Obermeier, B., *Multiple Sklerose: Charakterisierung oligoklonaler Antikörper im Liquor von Patienten*. 2011, LMU München.
101. Brändle, S., et al., *Distinct oligoclonal band antibodies in multiple sclerosis recognize ubiquitous self-proteins.* Proc Natl Acad Sci U S A, in press.
102. Bruder, J., *Antigenerkennung bei autoaggressiven Lymphozyten*. 2012, Bayrische Julius-Maximilians-Universität: Würzburg.
103. Venkatesan, A., *Epidemiology and outcomes of acute encephalitis.* Curr Opin Neurol, 2015. **28**(3): p. 277-82.
104. Armangue, T., F. Leypoldt, and J. Dalmau, *Autoimmune encephalitis as differential diagnosis of infectious encephalitis.* Curr Opin Neurol, 2014. **27**(3): p. 361-8.
105. Lai, M., et al., *AMPA receptor antibodies in limbic encephalitis alter synaptic receptor location.* Ann Neurol, 2009. **65**(4): p. 424-34.
106. Lancaster, E., et al., *Antibodies to the GABA(B) receptor in limbic encephalitis with seizures: case series and characterisation of the antigen.* Lancet Neurol, 2010. **9**(1): p. 67-76.
107. Lai, M., et al., *Investigation of LGI1 as the antigen in limbic encephalitis previously attributed to potassium channels: a case series.* Lancet Neurol, 2010. **9**(8): p. 776-85.
108. Graus, F. and J. Dalmau, *Paraneoplastic neurological syndromes.* Curr Opin Neurol, 2012. **25**(6): p. 795-801.
109. Darnell, R., R.B. Darnell, and J.B. Posner, *Paraneoplastic Syndromes*. 2011: Oxford University Press, USA.
110. Lancaster, E. and J. Dalmau, *Neuronal autoantigens--pathogenesis, associated disorders and antibody testing.* Nat Rev Neurol, 2012. **8**(7): p. 380-90.
111. Petit-Pedrol, M., et al., *Encephalitis with refractory seizures, status epilepticus, and antibodies to the GABAA receptor: a case series, characterisation of the antigen, and analysis of the effects of antibodies.* Lancet Neurol, 2014. **13**(3): p. 276-86.

112. Goodkin, H.P., J.L. Yeh, and J. Kapur, *Status epilepticus increases the intracellular accumulation of GABAA receptors.* J Neurosci, 2005. **25**(23): p. 5511-20.
113. Miller, P.S. and T.G. Smart, *Binding, activation and modulation of Cys-loop receptors.* Trends in Pharmacological Sciences, 2010. **31**(4): p. 161-174.
114. Miller, P.S. and a.R. Aricescu, *Crystal structure of a human GABAA receptor.* Nature, 2014. **512**: p. 270-275.
115. Simon, J., et al., *Analysis of the set of GABA(A) receptor genes in the human genome.* J Biol Chem, 2004. **279**(40): p. 41422-35.
116. Sigel, E. and M.E. Steinmann, *Structure, function, and modulation of GABA(A) receptors.* J Biol Chem, 2012. **287**(48): p. 40224-31.
117. Benarroch, E.E., *GABAA receptor heterogeneity, function, and implications for epilepsy.* Neurology, 2007. **68**(8): p. 612-4.
118. Karlin, A. and M.H. Akabas, *Toward a structural basis for the function of nicotinic acetylcholine receptors and their cousins.* Neuron, 1995. **15**(6): p. 1231-44.
119. Rudolph, U. and F. Knoflach, *Beyond classical benzodiazepines: novel therapeutic potential of GABAA receptor subtypes.* Nat Rev Drug Discov, 2011. **10**(9): p. 685-97.
120. Hosie, A.M., et al., *Zinc-mediated inhibition of GABA(A) receptors: discrete binding sites underlie subtype specificity.* Nature neuroscience, 2003. **6**: p. 362-369.
121. Ohkawa, T., et al., *Identification and Characterization of GABAA Receptor Autoantibodies in Autoimmune Encephalitis.* The Journal of Neuroscience, 2014. **34**(24): p. 8151-8163.
122. Simabukuro, M.M., et al., *GABA(A) receptor and LGI1 antibody encephalitis in a patient with thymoma.* Neurology® Neuroimmunology & Neuroinflammation, 2015. **2**(2): p. e73.
123. Graus, F., et al., *Anti-Hu-associated paraneoplastic encephalomyelitis: analysis of 200 patients.* Brain, 2001. **124**(Pt 6): p. 1138-48.
124. Dalmau, J., et al., *Anti-NMDA-receptor encephalitis: case series and analysis of the effects of antibodies.* Lancet Neurol, 2008. **7**(12): p. 1091-8.
125. Durocher, Y., S. Perret, and A. Kamen, *High-level and high-throughput recombinant protein production by transient transfection of suspension-growing human 293-EBNA1 cells.* Nucleic acids research, 2002. **30**: p. E9.
126. Gorman, C.M., et al., *The human cytomegalovirus major immediate early promoter can be trans-activated by adenovirus early proteins.* Virology, 1989. **171**: p. 377-385.
127. Linington, C., et al., *Augmentation of demyelination in rat acute allergic encephalomyelitis by circulating mouse monoclonal antibodies directed against a myelin/oligodendrocyte glycoprotein.* The American journal of pathology, 1988. **130**: p. 443-454.
128. Bird, R., et al., *Single-chain antigen-binding proteins.* Science, 1988. **242**(4877): p. 423-426.
129. Palmer, I. and P.T. Wingfield, *Preparation and extraction of insoluble (inclusion-body) proteins from Escherichia coli.* Curr Protoc Protein Sci, 2004. **Chapter 6**: p. Unit 6 3.
130. Peterson, G.L., *Review of the Folin phenol protein quantitation method of Lowry, Rosebrough, Farr and Randall.* Anal Biochem, 1979. **100**(2): p. 201-20.
131. Laemmli, U.K., *Cleavage of structural proteins during the assembly of the head of bacteriophage T4.* Nature, 1970. **227**(5259): p. 680-5.
132. Shevchenko, A., et al., *Mass spectrometric sequencing of proteins from silver-stained polyacrylamide gels.* Analytical Chemistry, 1996. **68**: p. 850-858.
133. Provencher, S.W. and J. Glockner, *Estimation of globular protein secondary structure from circular dichroism.* Biochemistry, 1981. **20**(1): p. 33-7.
134. Jones, D.T., *Protein secondary structure prediction based on position-specific scoring matrices.* J Mol Biol, 1999. **292**(2): p. 195-202.
135. Sievers, F., et al., *Fast, scalable generation of high-quality protein multiple sequence alignments using Clustal Omega.* Mol Syst Biol, 2011. **7**: p. 539.
136. Robert, X. and P. Gouet, *Deciphering key features in protein structures with the new ENDscript server.* Nucleic Acids Research, 2014. **42**(W1): p. W320-W324.
137. Li, W., et al., *The EMBL-EBI bioinformatics web and programmatic tools framework.* Nucleic Acids Res, 2015. **43**(W1): p. W580-4.
138. Pröbstel, a.K., et al., *Antibodies to MOG are transient in childhood acute disseminated encephalomyelitis.* Neurology, 2011. **77**: p. 580-588.
139. Tetin, S., et al., *Comparative circular dichroism studies of an anti-fluorescein monoclonal antibody (Mab 4-4-20) and its derivatives.* Biochemistry, 1992. **31**(48): p. 12029-34.
140. Mallender, W.D., J. Carrero, and E.W. Voss, Jr., *Comparative properties of the single chain antibody and Fv derivatives of mAb 4-4-20. Relationship between interdomain interactions and the high affinity for fluorescein ligand.* J Biol Chem, 1996. **271**(10): p. 5338-46.
141. Breithaupt, C., et al., *Structural insights into the antigenicity of myelin oligodendrocyte glycoprotein.* Proc Natl Acad Sci U S A, 2003. **100**(16): p. 9446-51.

142. Apweiler, R., et al., *UniProt: the Universal Protein knowledgebase.* Nucleic Acids Research, 2004. **32**(Database issue): p. D115-D119.
143. Uhlen, M., et al., *Proteomics. Tissue-based map of the human proteome.* Science, 2015. **347**(6220): p. 1260419.
144. Vermeulen, N., et al., *Identification of a novel autoantigen in inflammatory bowel disease by protein microarray.* Inflammatory Bowel Diseases, 2011. **17**: p. 1291-1300.
145. Tetin, S.Y., F.G. Prendergast, and S.Y. Venyaminov, *Accuracy of protein secondary structure determination from circular dichroism spectra based on immunoglobulin examples.* Anal Biochem, 2003. **321**(2): p. 183-7.
146. Xiao, B.G., C. Linington, and H. Link, *Antibodies to myelin-oligodendrocyte glycoprotein in cerebrospinal fluid from patients with multiple sclerosis and controls.* J Neuroimmunol, 1991. **31**(2): p. 91-6.
147. Wajgt, A. and M. Gorny, *CSF antibodies to myelin basic protein and to myelin-associated glycoprotein in multiple sclerosis. Evidence of the intrathecal production of antibodies.* Acta Neurol Scand, 1983. **68**(5): p. 337-43.
148. Warren, K.G. and I. Catz, *Relative frequency of autoantibodies to myelin basic protein and proteolipid protein in optic neuritis and multiple sclerosis cerebrospinal fluid.* J Neurol Sci, 1994. **121**(1): p. 66-73.
149. Mayer, M.C. and E. Meinl, *Glycoproteins as targets of autoantibodies in CNS inflammation: MOG and more.* Therapeutic Advances in Neurological Disorders, 2012. **5**(3): p. 147-159.
150. Ben-Nun, A., et al., *From classic to spontaneous and humanized models of multiple sclerosis: impact on understanding pathogenesis and drug development.* J Autoimmun, 2014. **54**: p. 33-50.
151. Rupprecht, T.A., et al., *The pathogenesis of lyme neuroborreliosis: from infection to inflammation.* Mol Med, 2008. **14**(3-4): p. 205-12.
152. Djukic, M., et al., *Cerebrospinal fluid findings in adults with acute Lyme neuroborreliosis.* J Neurol, 2012. **259**(4): p. 630-6.
153. Hansen, K., M. Cruz, and H. Link, *Oligoclonal Borrelia burgdorferi-specific IgG antibodies in cerebrospinal fluid in Lyme neuroborreliosis.* J Infect Dis, 1990. **161**(6): p. 1194-202.
154. Barbour, A.G., et al., *A genome-wide proteome array reveals a limited set of immunogens in natural infections of humans and white-footed mice with Borrelia burgdorferi.* Infect Immun, 2008. **76**(8): p. 3374-89.
155. Martin, R., et al., *Persistent intrathecal secretion of oligoclonal, Borrelia burgdorferi-specific IgG in chronic meningoradiculomyelitis.* J Neurol, 1988. **235**(4): p. 229-33.
156. Martin, J.R., *Herpes simplex virus types 1 and 2 and multiple sclerosis.* Lancet, 1981. **2**(8250): p. 777-81.
157. Soldan, S.S., et al., *Association of human herpes virus 6 (HHV-6) with multiple sclerosis: increased IgM response to HHV-6 early antigen and detection of serum HHV-6 DNA.* Nat Med, 1997. **3**(12): p. 1394-7.
158. Cepok, S., et al., *Identification of Epstein-Barr virus proteins as putative targets of the immune response in multiple sclerosis.* J Clin Invest, 2005. **115**(5): p. 1352-60.
159. Derfuss, T., et al., *Intrathecal antibody production against Chlamydia pneumoniae in multiple sclerosis is part of a polyspecific immune response.* Brain, 2001. **124**(Pt 7): p. 1325-35.
160. Kolln, J., et al., *Triosephosphate isomerase- and glyceraldehyde-3-phosphate dehydrogenase-reactive autoantibodies in the cerebrospinal fluid of patients with multiple sclerosis.* J Immunol, 2006. **177**(8): p. 5652-8.
161. Michaud, G.A., et al., *Analyzing antibody specificity with whole proteome microarrays.* Nat Biotechnol, 2003. **21**(12): p. 1509-12.
162. Robinson, W.H., L. Steinman, and P.J. Utz, *Protein arrays for autoantibody profiling and fine-specificity mapping.* Proteomics, 2003. **3**(11): p. 2077-84.
163. Quintana, F.J., et al., *Antigen microarrays identify unique serum autoantibody signatures in clinical and pathologic subtypes of multiple sclerosis.* Proc Natl Acad Sci U S A, 2008. **105**(48): p. 18889-94.
164. Beyer, N.H., et al., *Investigation of autoantibody profiles for cerebrospinal fluid biomarker discovery in patients with relapsing-remitting multiple sclerosis.* Journal of Neuroimmunology, 2012. **242**: p. 26-32.
165. Korn, T. and H. Tumani, *Patterns of intrathecal autoreactive antibodies in MS using antigen microarrays.* Neurology, 2012. **78**(8): p. 522-3.
166. Jarvis, D.L., *Developing baculovirus-insect cell expression systems for humanized recombinant glycoprotein production.* Virology, 2003. **310**(1): p. 1-7.
167. Schena, M., ed. *Protein microarrays*. 2005, Jones and Bartlett: Sudbury, MA. 469.

168. Guggenmos, J., et al., *Antibody cross-reactivity between myelin oligodendrocyte glycoprotein and the milk protein butyrophilin in multiple sclerosis.* J Immunol, 2004. **172**(1): p. 661-8.
169. Buxade, M., J.L. Parra-Palau, and C.G. Proud, *The Mnks: MAP kinase-interacting kinases (MAP kinase signal-integrating kinases).* Front Biosci, 2008. **13**: p. 5359-73.
170. Knauf, U., C. Tschopp, and H. Gram, *Negative Regulation of Protein Translation by Mitogen-Activated Protein Kinase-Interacting Kinases 1 and 2.* Molecular and Cellular Biology, 2001. **21**(16): p. 5500-5511.
171. Diab, S., et al., *MAP Kinase-Interacting Kinases—Emerging Targets against Cancer.* Chemistry & Biology, 2014. **21**(4): p. 441-452.
172. Kobayashi, T., et al., *A gene encoding a family with sequence similarity 84, member a (FAM84A) enhanced migration of human colon cancer cells.* International Journal of Oncology, 2006. **29**: p. 341-347.
173. Bouloukos, A., et al., *Immunoglobulins in cerebrospinal fluid in various neurologic disorders.* Clinical Chemistry, 1980. **26**(1): p. 115-6.
174. Obermeier, B., et al., *Related B cell clones that populate the CSF and CNS of patients with multiple sclerosis produce CSF immunoglobulin.* J Neuroimmunol, 2011. **233**(1-2): p. 245-8.
175. Xavier, R.J. and D.K. Podolsky, *Unravelling the pathogenesis of inflammatory bowel disease.* Nature, 2007. **448**(7152): p. 427-434.
176. Marrie, R.A., et al., *A systematic review of the incidence and prevalence of comorbidity in multiple sclerosis: overview.* Mult Scler, 2015. **21**(3): p. 263-81.
177. Langer-Gould, A., et al., *Autoimmune diseases prior to the diagnosis of multiple sclerosis: a population-based case-control study.* Mult Scler, 2010. **16**(7): p. 855-61.
178. Jarnæss, E., et al., *Splicing factor arginine/serine-rich 17A (SFRS17A) is an A-kinase anchoring protein that targets protein kinase A to splicing factor compartments.* Journal of Biological Chemistry, 2009. **284**: p. 35154-35164.
179. Mangs, A.H., et al., *XE7: a novel splicing factor that interacts with ASF/SF2 and ZNF265.* Nucleic Acids Res, 2006. **34**(17): p. 4976-86.
180. Mouquet, H. and M.C. Nussenzweig, *Polyreactive antibodies in adaptive immune responses to viruses.* Cell Mol Life Sci, 2012. **69**(9): p. 1435-45.
181. Lafer, E.M., et al., *Polyspecific monoclonal lupus autoantibodies reactive with both polynucleotides and phospholipids.* J Exp Med, 1981. **153**(4): p. 897-909.
182. Yurasov, S., et al., *Persistent expression of autoantibodies in SLE patients in remission.* The Journal of Experimental Medicine, 2006. **203**(10): p. 2255-2261.
183. Svarcova, J., et al., *Cerebrospinal fluid antibodies to tubulin are elevated in the patients with multiple sclerosis.* Eur J Neurol, 2008. **15**(11): p. 1173-9.
184. Willis, S.N., et al., *Investigating the antigen specificity of multiple sclerosis central nervous system-derived immunoglobulins.* Frontiers in Immunology, 2015. **6**.
185. Rahman, A. and D.A. Isenberg, *Systemic Lupus Erythematosus.* New England Journal of Medicine, 2008. **358**(9): p. 929-939.
186. Nihtyanova, S.I. and C.P. Denton, *Autoantibodies as predictive tools in systemic sclerosis.* Nat Rev Rheumatol, 2010. **6**(2): p. 112-116.
187. Racanelli, V., et al., *Autoantibodies to intracellular antigens: generation and pathogenetic role.* Autoimmun Rev, 2011. **10**(8): p. 503-8.
188. Hansen, M.H., H.V. Nielsen, and H.J. Ditzel, *Translocation of an intracellular antigen to the surface of medullary breast cancer cells early in apoptosis allows for an antigen-driven antibody response elicited by tumor-infiltrating B cells.* J Immunol, 2002. **169**(5): p. 2701-11.
189. Munoz, L.E., et al., *The role of defective clearance of apoptotic cells in systemic autoimmunity.* Nat Rev Rheumatol, 2010. **6**(5): p. 280-9.
190. Casciola-Rosen, L., et al., *Cleavage by granzyme B is strongly predictive of autoantigen status: implications for initiation of autoimmunity.* J Exp Med, 1999. **190**(6): p. 815-26.
191. Prineas, J.W. and J.S. Graham, *Multiple sclerosis: capping of surface immunoglobulin G on macrophages engaged in myelin breakdown.* Ann Neurol, 1981. **10**(2): p. 149-58.
192. Storch, M.K., et al., *Multiple sclerosis: in situ evidence for antibody- and complement-mediated demyelination.* Ann Neurol, 1998. **43**(4): p. 465-71.
193. Reindl, M., M. Khalil, and T. Berger, *Antibodies as biological markers for pathophysiological processes in MS.* J Neuroimmunol, 2006. **180**(1-2): p. 50-62.
194. Genain, C.P., et al., *Identification of autoantibodies associated with myelin damage in multiple sclerosis.* Nat Med, 1999. **5**(2): p. 170-5.
195. Reindl, M., et al., *The spectrum of MOG autoantibody-associated demyelinating diseases.* Nat Rev Neurol, 2013. **9**(8): p. 455-61.
196. Dalmau, J. and M.R. Rosenfeld, *Autoimmune encephalitis update.* Neuro Oncol, 2014. **16**(6): p. 771-8.

197. Wekerle, H. and R. Hohlfeld, *Molecular mimicry in multiple sclerosis.* N Engl J Med, 2003. **349**(2): p. 185-6.
198. Samarkos, M. and G. Vaiopoulos, *The role of infections in the pathogenesis of autoimmune diseases.* Curr Drug Targets Inflamm Allergy, 2005. **4**(1): p. 99-103.
199. Owens, G.P., et al., *Viruses and multiple sclerosis.* Neuroscientist, 2011. **17**(6): p. 659-76.
200. Poon, I.K.H., et al., *Apoptotic cell clearance: basic biology and therapeutic potential.* Nature reviews. Immunology, 2014. **14**: p. 166-180.
201. Baumann, I., et al., *Impaired uptake of apoptotic cells into tingible body macrophages in germinal centers of patients with systemic lupus erythematosus.* Arthritis Rheum, 2002. **46**(1): p. 191-201.
202. Archelos, J.J., M.K. Storch, and H.P. Hartung, *The role of B cells and autoantibodies in multiple sclerosis.* Ann Neurol, 2000. **47**(6): p. 694-706.
203. Grabar, P., *"Self"and "not-self" in immunology.* Lancet, 1974. **1**(7870): p. 1320-2.
204. Trotter, J., L.J. DeJong, and M.E. Smith, *Opsonization with antimyelin antibody increases the uptake and intracellular metabolism of myelin in inflammatory macrophages.* J Neurochem, 1986. **47**(3): p. 779-89.
205. Bieber, A.J., et al., *Humoral autoimmunity as a mediator of CNS repair.* Trends in Neurosciences, 2001. **24, Supplement 1**: p. 39-44.
206. Grimaldi, L.M., et al., *IgG1,3 and 4 oligoclonal bands in multiple sclerosis and other neurological diseases.* Ital J Neurol Sci, 1986. **7**(5): p. 507-13.
207. Losy, J., P.D. Mehta, and H.M. Wisniewski, *Identification of IgG subclasses' oligoclonal bands in multiple sclerosis CSF.* Acta Neurol Scand, 1990. **82**(1): p. 4-8.
208. Warrington, A.E., et al., *Human monoclonal antibodies reactive to oligodendrocytes promote remyelination in a model of multiple sclerosis.* Proc Natl Acad Sci U S A, 2000. **97**(12): p. 6820-5.
209. Vargas, M.E., et al., *Endogenous antibodies promote rapid myelin clearance and effective axon regeneration after nerve injury.* Proc Natl Acad Sci U S A, 2010. **107**(26): p. 11993-8.
210. Compston, A. and A. Coles, *Multiple sclerosis.* Lancet, 2008. **372**(9648): p. 1502-17.
211. Lancaster, E., E. Martinez-Hernandez, and J. Dalmau, *Encephalitis and antibodies to synaptic and neuronal cell surface proteins.* Neurology, 2011. **77**(2): p. 179-89.
212. Weiskirchen, R. and K. Günther, *The CRP/MLP/TLP family of LIM domain proteins: Acting by connecting.* BioEssays, 2003. **25**: p. 152-162.
213. Schmeichel, K.L. and M.C. Beckerle, *The LIM domain is a modular protein-binding interface.* Cell, 1994. **79**(2): p. 211-9.
214. Louis, H.A., et al., *Comparison of three members of the cysteine-rich protein family reveals functional conservation and divergent patterns of gene expression.* J Biol Chem, 1997. **272**(43): p. 27484-91.
215. Matthews, J.M., et al., *LIM-domain-only proteins in cancer.* Nat Rev Cancer, 2013. **13**(2): p. 111-122.
216. Auld, D.S., *Zinc coordination sphere in biochemical zinc sites.* Biometals, 2001. **14**(3-4): p. 271-313.
217. Sanchez-Garcia, I. and T.H. Rabbitts, *The LIM domain: a new structural motif found in zinc-finger-like proteins.* Trends Genet, 1994. **10**(9): p. 315-20.
218. Konrat, R., et al., *Solution structure of the carboxyl-terminal LIM domain from quail cysteine-rich protein CRP2.* Journal of Biological Chemistry, 1997. **272**: p. 12001-12007.
219. Weiskirchen, R., et al., *LIM-domain protein cysteine- and glycine-rich protein 2 (CRP2) is a novel marker of hepatic stellate cells and binding partner of the protein inhibitor of activated STAT1.* Biochem J, 2001. **359**(Pt 3): p. 485-96.
220. Arber, S. and P. Caroni, *Specificity of single LIM motifs in targeting and LIM/LIM interactions in situ.* Genes and Development, 1996. **10**: p. 289-300.
221. Goodin, D.S., *The epidemiology of multiple sclerosis: insights to disease pathogenesis.* Handb Clin Neurol, 2014. **122**: p. 231-66.
222. Dendrou, C.A., L. Fugger, and M.A. Friese, *Immunopathology of multiple sclerosis.* Nat Rev Immunol, 2015. **15**(9): p. 545-58.
223. Pettingill, P., et al., *Antibodies to GABAA receptor alpha1 and gamma2 subunits: clinical and serologic characterization.* Neurology, 2015. **84**(12): p. 1233-41.
224. Zhang, J., R. MacKenzie, and Y. Durocher, *Production of chimeric heavy-chain antibodies.* Methods Mol Biol, 2009. **525**: p. 323-36, xv.

Appendix

Vector Maps

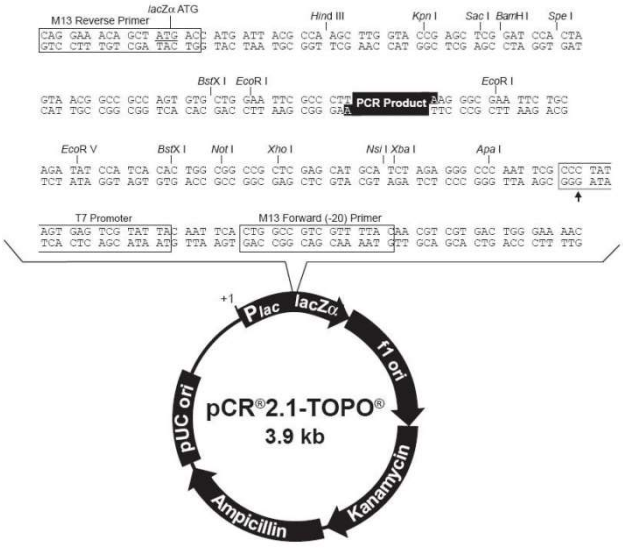

Vector map of pCR2.1-TOPO.

This vector was used intermediate steps during molecular cloning. Abbreviations: P*lac*: promoter of the *lac*Z-gene, *lac*Zα: α-galactosidase (α-fragment)-gene, f1 ori: f1 phage origin of replication, pUC ori: origin of replication for bacterial plasmid propagation. The illustration is taken from the “TOPO®TA Cloning” handbook (Invitrogen).

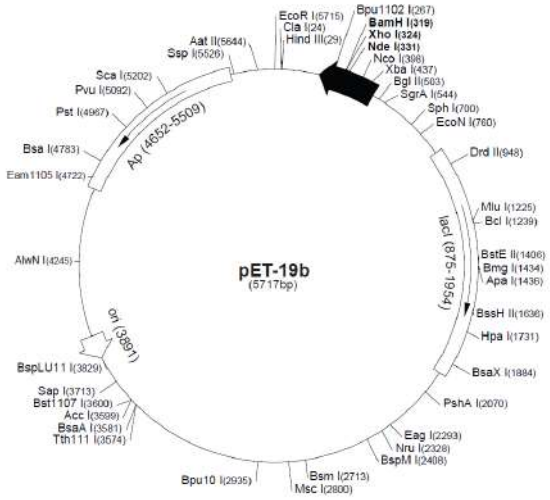

Vector map of pET-19b.

This vector was used for recombinant expression of the scF$_v$-MS2-s5 in *E. coli*. Abbreviations: *lac*I: lac inhibitor, ori: origin of replication, Ap: ampicillin resistance gene, rbs: ribosomal binding site. The illustration is taken from the Novagen datasheet.

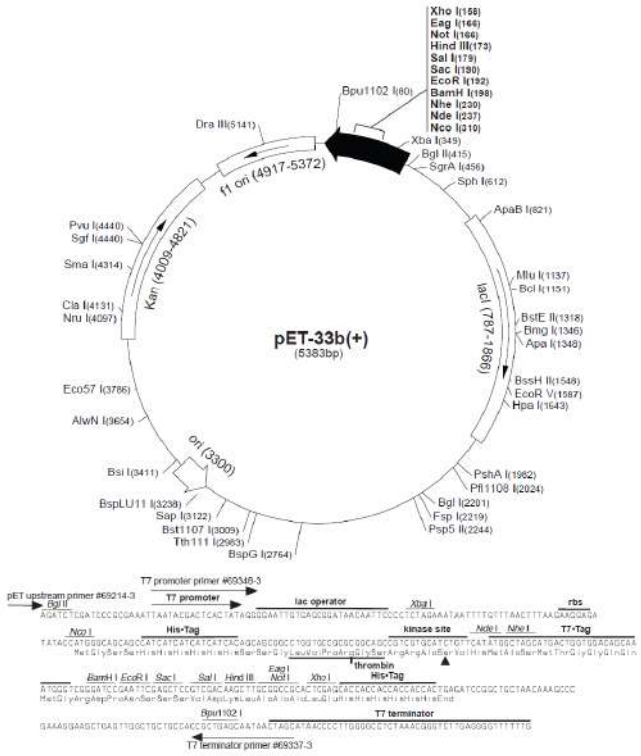

Vector map of pET-33b(+).

This vector was used for recombinant expression of FAM84A, FAM84A-mutants, and $GABA_AR\alpha1ex$ in *E. coli*. Abbreviations: *lac*I: lac inhibitor, ori: origin of replication, Kan: kanamycin resistance gene, f1 ori: f1 phage origin of replication, rbs: ribosomal binding site. The illustration is taken from the Novagen datasheet.

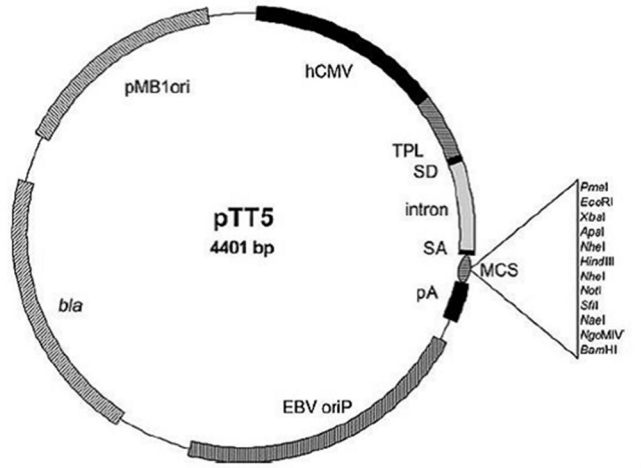

Vector map of pTT5.

This vector was used to recombinantly express full length antibodies and the AKAP17A-protein in HEK293E-cells. Abbreviations: hCMV: Promotor of the human Cytomegalovirus, TPL: Tripartite leader sequence of the Adenovirus, SD: Splice donor, SA: splice acceptor, MCS: multiple cloning site, pA: polyadenylation site, EBV oriP: origin of replication from the Epstein-Barr-Virus, pMB1 ori: origin of replication for bacterial propagation, *bla*: β-lactamase gene conferes ampicillin resistence. The illustration is taken from [224].

Amino Acid Sequences

Full length Antibodies

Each antibody heavy chain was cloned with and without V5-tag, it is therefore depicted as grey letters.

rAb-	Sequence
MS3-s1	H-chain QVQLQESGPRLVKPSEALSLTCIVSGGSINSNTYYWDWLRQPPGKGLEWIGSISYSGGTYYNPSLKNRVTMSVDTSNNQFSLK LSSVTAADTAVYYCARHTPRQAYYNILTSSQDYYYYGMDVWGQGTTVTVSSASTKGPSVFPLAPSSKSTSGGTAALGCLVKDY FPEPVTVSWNSGALTSGVHTFPAVLQSSGLYSLSSVVTVPSSSLGTQTYICNVNHKPSNTKVDKKVEPKSCDKTHTCPPCPAP ELLGGPSVFLFPPKPKDTLMISRTPEVTCVVVDVSHEDPEVKFNWYVDGVEVHNAKTKPREEQYNSTYRVVSVLTVLHQDWLN GKEYKCKVSNKALPAPIEKTISKAKGQPREPQVYTLPPSRDELTKNQVSLTCLVKGFYPSDIAVEWESNGQPENNYKTTPPVL DSDGSFFLYSKLTVDKSRWQQGNVFSCSVMHEALHNHYTQKSLSLSPGKGKPIPNPLLGLDSTHHHHHH

	L-chain DIVMTQSPLSLPVTPGEAASISCRSSQSLLHSSGNNYLDWYLQKPGQPPQLLIYLGSNRASGVPDRFSGSGSGTDFTLKISRV EAEDVGVYYCMQALETPPITFGQGTRLEIKRTVAAPSVFIFPPSDEQLKSGTASVVCLLNNFYPREAKVQWKVDNALQSGNSQ ESVTEQDSKDSTYSLSSTLTLSKADYEKHKVYACEVTHQGLSSPVTKSFNRGEC
MS1-s8	H-chain QVQLVQSGGGLVQPGESVRLSCAVSGFSSTTYWMSWVRQAPGKGLEWVANINQDGRQEYYVDSVKGRFTISRDNAENSLYLQM NSLRAEDTAVYYCARRTYDFWSGSSLAFDVWGQGTMVIVSSASTKGPSVFPLAPSSKSTSGGTAALGCLVKDYFPEPVTVSWN SGALTSGVHTFPAVLQSSGLYSLSSVVTVPSSSLGTQTYICNVNHKPSNTKVDKKVEPKSCDKTHTCPPCPAPELLGGPSVFL FPPKPKDTLMISRTPEVTCVVVDVSHEDPEVKFNWYVDGVEVHNAKTKPREEQYNSTYRVVSVLTVLHQDWLNGKEYKCKVSN KALPAPIEKTISKAKGQPREPQVYTLPPSRDELTKNQVSLTCLVKGFYPSDIAVEWESNGQPENNYKTTPPVLDSDGSFFLYS KLTVDKSRWQQGNVFSCSVMHEALHNHYTQKSLSLSPGKGKPIPNPLLGLDSTHHHHHH L-chain DIQMTQSPVTLSASVGDRVTITCRASQSVSSYLNWYQQKPGEAPKLLIYAASRLHSGVPSRFSGSGSGTHFTLTVTSLLPEDF ATYYCQQSYSNPTFGQGTKLEIKRTVAAPSVFIFPPSDEQLKSGTASVVCLLNNFYPREAKVQWKVDNALQSGNSQESVTEQD SKDSTYSLSSTLTLSKADYEKHKVYACEVTHQGLSSPVTKSFNRGEC
MS1-s9	H-chain QVQLVQSGGGLVQPGGPLRLSCAASGFTFTNYEMNWVRQAPGKGLEWVSYISISGRTIYYADSVKGRFTISRDNARNSLYLQM NSLRAEDTAVYYCARELSHWDGMIVVDSDAFDIWGQGTMVTVSSASTKGPSVFPLAPSSKSTSGGTAALGCLVKDYFPEPVTV SWNSGALTSGVHTFPAVLQSSGLYSLSSVVTVPSSSLGTQTYICNVNHKPSNTKVDKKVEPKSCDKTHTCPPCPAPELLGGPS VFLFPPKPKDTLMISRTPEVTCVVVDVSHEDPEVKFNWYVDGVEVHNAKTKPREEQYNSTYRVVSVLTVLHQDWLNGKEYKCK VSNKALPAPIEKTISKAKGQPREPQVYTLPPSRDELTKNQVSLTCLVKGFYPSDIAVEWESNGQPENNYKTTPPVLDSDGSFF LYSKLTVDKSRWQQGNVFSCSVMHEALHNHYTQKSLSLSPGKGKPIPNPLLGLDSTHHHHHH L-chain EIVMTQSPATLSVSPGERATLSCRASQNVSSNLAWYQQKPGQVPRLLIYGASTRATGIPARFSGSGSGTEFTLTISSLQSEDF AVYYCQQYNDWPRTFGRGTKVEIKRTVAAPSVFIFPPSDEQLKSGTASVVCLLNNFYPREAKVQWKVDNALQSGNSQESVTEQ DSKDSTYSLSSTLTLSKADYEKHKVYACEVTHQGLSSPVTKSFNRGEC
MS4	H-chain QVQLQESGPGLVKPSQTLSLTCTVSGGSITSGSYYWSWVRQSAGKGLEWIGRISATGSTNYNPSLWSRVTISVDTSKNQFSLK LTSVTAADTAVYYCARHSSYSDSSYLPYWGQGTLVTVSSASTKGPSVFPLAPSSKSTSGGTAALGCLVKDYFPEPVTVSWNSG ALTSGVHTFPAVLQSSGLYSLSSVVTVPSSSLGTQTYICNVNHKPSNTKVDKKVEPKSCDKTHTCPPCPAPELLGGPSVFLFP PKPKDTLMISRTPEVTCVVVDVSHEDPEVKFNWYVDGVEVHNAKTKPREEQYNSTYRVVSVLTVLHQDWLNGKEYKCKVSNKA LPAPIEKTISKAKGQPREPQVYTLPPSRDELTKNQVSLTCLVKGFYPSDIAVEWESNGQPENNYKTTPPVLDSDGSFFLYSKL TVDKSRWQQGNVFSCSVMHEALHNHYTQKSLSLSPGKGKPIPNPLLGLDSTHHHHHH L-chain DIQMTQSPVTLSASVGDRVSITCRASQGISNYLAWYQQKPGKVPKLLIYAASTLKSGVPSRFSGSGSGTDFTLTITSLQPEDV ATYYCQKYYSTPRTFGQGTKVEIKRTVAAPSVFIFPPSDEQLKSGTASVVCLLNNFYPREAKVQWKVDNALQSGNSQESVTEQ DSKDSTYSLSSTLTLSKADYEKHKVYACEVTHQGLSSPVTKSFNRGEC
MS1-s2	H-chain QVQLVQSGGGLVHPGGSLRLSCATSGFTFNSYNMNWVRQAPGKGLEWLAYINSDSSTTYYADSVKGRFTISRDDARRSLDLQM NSLRAEDTAVYYCARLSGYDWYSDESVLYHDYWGQGTLVTVSSTSTKGPSVFPLAPSSKSTSGGTAALGCLVKDYFPEPVTVS WNSGALTSGVHTFPAVLQSSGLYSLSSVVTVPSSSLGTQTYICNVNHKPSNTKVDKKVEPKSCDKTHTCPPCPAPELLGGPSV FLFPPKPKDTLMISRTPEVTCVVVDVSHEDPEVKFNWYVDGVEVHNAKTKPREEQYNSTYRVVSVLTVLHQDWLNGKEYKCKV SNKALPAPIEKTISKAKGQPREPQVYTLPPSRDELTKNQVSLTCLVKGFYPSDIAVEWESNGQPENNYKTTPPVLDSDGSFFL YSKLTVDKSRWQQGNVFSCSVMHEALHNHYTQKSLSLSPGKGKPIPNPLLGLDSTHHHHHH L-chain SYELTQPPSVSVSPGQTARITCSGDGLPKKYAYWYQQKSGQAPVLVIYQNTARPSGIPERFSGSTSGNTAALIISGTQAVDEA DYYCQAWDGSTVVFGRGTKLTVLRTVAAPSVFIFPPSDEQLKSGTASVVCLLNNFYPREAKVQWKVDNALQSGNSQESVTEQD SKDSTYSLSSTLTLSKADYEKHKVYACEVTHQGLSSPVTKSFNRGEC
r8-18C5	H-chain QVQLQQSGAELMKPGASVEISCKATGYTFSSFWIEWVKQRPGHGLEWIGEILPGRGRTNYNEKFKGKATFTAETSSNTAYMQL SSLTSEDSAVYYCATGNTMVNMPYWGQGTTLTVSSASTKGPSVFPLAPSSKSTSGGTAALGCLVKDYFPEPVTVSWNSGALTS GVHTFPAVLQSSGLYSLSSVVTVPSSSLGTQTYICNVNHKPSNTKVDKKVEPKSCDKTHTCPPCPAPELLGGPSVFLFPPKPK DTLMISRTPEVTCVVVDVSHEDPEVKFNWYVDGVEVHNAKTKPREEQYNSTYRVVSVLTVLHQDWLNGKEYKCKVSNKALPAP IEKTISKAKGQPREPQVYTLPPSRDELTKNQVSLTCLVKGFYPSDIAVEWESNGQPENNYKTTPPVLDSDGSFFLYSKLTVDK SRWQQGNVFSCSVMHEALHNHYTQKSLSLSPGKGKPIPNPLLGLDSTHHHHHH L-chain DIVMTQSPSSLSVSAGEKVTMSCKSSQSLLNSGNQKNYLAWYQQKPGQPPKLLIYGASTRESGVPDRFTGSGSGTDFTLTISS VQAEDLAVYYCQNDHSYPLTFGAGTKLELKRTVAAPSVFIFPPSDEQLKSGTASVVCLLNNFYPREAKVQWKVDNALQSGNSQ ESVTEQDSKDSTYSLSSTLTLSKADYEKHKVYACEVTHQGLSSPVTKSFNRGEC
MS2-s5	H-chain QVQLVQSGGGVVQPGRSLRLSCEGAGFTFSSYVVHWVRQTPDKGLEWVALISYDGNNRDYADAVKGRFIISRDNSKNTVYLEM HSLRSEDTSIYYCARGLSWVDLLYTVDWFDPWGQGTLVTVSSASTKGPSVFPLAPSSKSTSGGTAALGCLVKDYFPEPVTVSW NSGALTSGVHTFPAVLQSSGLYSLSSVVTVPSSSLGTQTYICNVNHKPSNTKVDKKVEPKSCDKTHTCPPCPAPELLGGPSVF LFPPKPKDTLMISRTPEVTCVVVDVSHEDPEVKFNWYVDGVEVHNAKTKPREEQYNSTYRVVSVLTVLHQDWLNGKEYKCKVS NKALPAPIEKTISKAKGQPREPQVYTLPPSRDELTKNQVSLTCLVKGFYPSDIAVEWESNGQPENNYKTTPPVLDSDGSFFLY SKLTVDKSRWQQGNVFSCSVMHEALHNHYTQKSLSLSPGKGKPIPNPLLGLDSTHHHHHH L-chain DIQMTQSPSSLSASVGDRVTIPCRASQDISNYLNWYQQKPGKAPKLLIYDTSNLETGVPSRFTGSGSGTEFTLTISSLQPEDI AIYYCQQYDSLPLTFGGGTKVEIKRTVAAPSVFIFPPSDEQLKSGTASVVCLLNNFYPREAKVQWKVDNALQSGNSQESVTEQ DSKDSTYSLSSTLTLSKADYEKHKVYACEVTHQGLSSPVTKSFNRGEC
Ip2	H-chain EVQLVESGGGLVKPGGSLRLSCAASGFTSSFYSMNWVRQAPGKGLEWVSSISSSSSYIYYADSVKGRFTISRDNAKNSLYLQM SSLRADDTAVYYCARVGIMEWSDPRFVDEKYGMDVWGQGTTVTVSSASTKGPSVFPLAPSSKSTSGGTAALGCLVKDYFPEPV TVSWNSGALTSGVHTFPAVLQSSGLYSLSSVVTVPSSSLGTQTYICNVNHKPSNTKVDKKVEPKSCDKTHTCPPCPAPELLGG

PSVFLFPPKPKDTLMISRTPEVTCVVVDVSHEDPEVKFNWYVDGVEVHNAKTKPREEQYNSTYRVVSVLTVLHQDWLNGKEYK
CKVSNKALPAPIEKTISKAKGQPREPQVYTLPPSRDELTKNQVSLTCLVKGFYPSDIAVEWESNGQPENNYKTTPPVLDSDGS
FFLYSKLTVDKSRWQQGNVFSCSVMHEALHNHYTQKSLSLSPGKGKPIPNPLLGLDSTHHHHHH

L-chain
EIVLTQSPGTLSLSPGERATLSCRASQSVSSRYLAWYQQKPGQAPRLLIYGASSRATGIPDRFSGSGSGTDFILTISRLEPED
FAVYYCQQYGSSLYTFGQGTKLEIKRTVAAPSVFIFPPSDEQLKSGTASVVCLLNNFYPREAKVQWKVDNALQSGNSQESVTE
QDSKDSTYSLSSTLTLSKADYEKHKVYACEVTHQGLSSPVTKSFNRGEC

Single chain variable Fragment of rOCB-MS2-s5

Ab-	Sequence
scF_v-MS2-s5	MGQLVQSGGGVVQPGRSLRLSCEGAGFTFSSYVVHWVRQTPDKGLEWVALISYDGNNRDYADAVKGRFIISRDNSKNTV YLEMHSLRSEDTAIYYCARGLSWVDLLYTVDWFDPWGQGTLVTVSSGGGGSGGGGSGGGGSDIQMTQSPSSLSASVGDR VTIPCRASQDISNYLNWYQQKPGKAPKLLIYDTSNLETGVPSRFTGSGSGTEFTLTISSLQPEDIAIYYCQQYDSLPLT FGGGTKVEIKGKPIPNPLLGLDSTHHHHHH

Candidate Antigens

Antibody	Sequence
MKNK1	MVSSQKLEKPIEMGSSEPLPIADGDRRRKKKRRGRATDSLPGKFEDMYKLTSELLGEGAYAKVQGAVSLQNGKEYAVKII EKQAGHSRSRVFREVETLYQCQGNKNILELIEFFEDDTRFYLVFEKLQGGSILAHIQKQKHFNEREASRVVRDVAAALDF LHTKDKVSLCHLGWSAMAPSGLTAAPTSLGSSDPPTSASQVAGTTGIAHRDLKPENILCESPEKVSPVKICDFDLGSGMK LNNSCTPITTPELTTPCGSAEYMAPEVVEVFTDQATFYDKRCDLWSLGVVLYIMLSGYPPFVGHCGADCGWDRGEVCRVC QNKLFESIQEGKYEFPDKDWAHISSEAKDLISKLLVRDAKQRLSAAQVLQHPWVQGQAPEKGLPTPQVLQRNSSTMDLTL FAAEAIALNRQLSQHEENELAEEPEALADGLCSMKLSPPCKSRLARRRALAQAGRGEDRSPPTALTRTRPLEQKLISEED LAANDILDYKDDDDKV
FAM84A wt	MGNQLDRITHLNYSELPTGDPSGIEKDELRVGVAYFFSDDEEDLDERGQPDKFGVKAPPGCTPCPESPSRHHHHLLHQLV LNETQFSAFRGQECIFSKVSGGPQGADLSVYAVTALPALCEPGDLLELLWLQHAPEPPAPAPHWAVYVGGGQIIHLHQGE IRQDSLYEAGAANVGRVVNSWYRYRPLVAELVVQNACGHLGLKSEEICWTNSESFAAWCRFGKREFKAGGEVPAGTQPPQ QQYYLKVHLGENKVHTARFHSLEDLIREKRRIDASGRLRVLQELADLVDDKEGKPIPNPLLGLDSQHHHHHH
AKAP17A	NSTMKHLWFFLLLVAAPRWVLSMAAATIVHDTSEAVELCPAYGLYLKPITKMTISVALPQLKQPGKSISNWEVMERLKGM VQNHQFSTLRISKSTMDFIRFEGEVENKSLVKSFLACLDGKTIKLSGFSDILKVRAAEFKIDFPTRHDWDSFFRDAKDMN ETLPGERPDTIHLEGLPCKWFALKESGSEKPSEDVLVKVFEKFGEIRNVDIPMLDSYREEMTGRNFHTFSFGGHLNFEAY VQYREYMGFIQAMSALRGMKLMYKGEDGKAVACNIKVSFDSTKHLSDASIKKRQLERQKLQELEQQREEQKRREKEAEER QRAEERKQKELEELERERKREEKLRKREQKQRDRELRRNQKKLEKLQAEEQKQLQEKIKLEERKLLLAQRNLQSIRLIAE LLSRAKVPGGSLCSRQPRPGCPQCPPLKCGRRHGAVSPPAAAVATKPALMPRMTAPSREGVALVCRSRGKPIPNPLLGLD STHHHHHH
FAM20B	YPYDVPDYANLDTSAANREDQRAFHRMMTGLRVELAPKLDHTLQSPWEIAAQWVVPREVYPEETPELGAVMHAMATKKII KADVGYKGTQLKALLILEGGQKVVFKPKRYSRDHVVEGEPYAGYDRHNAEVAAFHLDRILGFHRAPLVVGRFVNLRTEIK PVATEQLLSTFLTVGNNTCFYGKCYYCRETEPACADGDIMEGSVTLWLPDVWPLQKHRHPWGRTYREGKLARWEYDESYC DAVKKTSPYDSGPRLLDIIDTAVFDYLIGNADRHHYESFQDDEGASMLILLDNAKSFGNPSLDERSILAPLYQCCIIRVS TWNRLNYLKNGVLKSALKSAMAHDPISPVLSDPHLDAVDQRLLSVLATVKQCTDQFGMDTVLVEDRMPLSHL
CHD2	MMRNKDKSQEEDSSLHSNASSHSASEEASGSDSGSQSESEQGSDPGSGHGSESNSSSESSESQSESESESESAGSKSQPVLP EAKEKPASKKERIADVKKMWEEYPDVYGVRRSNRSRQEPSRFNIKEEASSGSESGSPKRRGQRQLKKQEKWKQEPSEDEQ EQGTSAESEPEQKKVKARRPVPRRTVPKPRVKKQPKTQRGKRKKQDSSDEDDDDDEAPKRQTRRRAAKNVSYKEDDDFET DSDDLIEMTGEGVDEQQDNSETIEKVLDSRLGKKGATGASTTVYAIEANGDPSGDFDTEKDEGEIQYLIKWKGWSYIHST WESEESLQQQKVKGLKKLENFKKKEDEIKQWLGKVSPEDVEYFNCQQELASELNKQYQIVERVIAVKTSKSTLGQTDFPA HSRKPAPSNEPEYLCKWMGLPYSECSWEDEALIGKKFQNCIDSFHSRNNSKTIPTRECKALKQRPRFVALKKQPAYLGGE NLELRDYQLEGLNWLAHSWCK
MAPK7	MAEPLKEEDGEDGSAEPPGPVKAEPAHTAASVAAKNLALLKARSFDVTFDVGDEYEIIETIGNGAYGVVSSARRRLTGQQ VAIKKIPNAFDVVTNAKRTLRELKILKHFKHDNIIAIKDILRPTVPYGEFKSVYVVLDLMESDLHQIIHSSQPLTLEHVR YFLYQLLRGLKYMHSAQVIHRDLKPSNLLVNENCELKIGDFGMARGLCTSPAEHQYFMTEYVATRWYRAPELMLSLHEYT QAIDLWSVGCIFGEMLARRQLFPGKNYVHQLQLIMMVLGTPSPAVIQAVGAERVRAYIQSLPPRQPVPWETVYPGADRQA LSLLGRMLRFEPSARISAAAALRHPFLAKYHDPDDEPDCAPPFDFAFDREALTRERIKEAIVAEIEDFHARREGIRQQIR FQPSLQPVASEPGCPDVEMPSPWAPSGDCAMESPPPAPPPCPGPAPDTIDLTLQPPPPVSEPAPPKKDGAISDNTKAALK AALLKSLRSRLRDGPSAPLEAPEPRKPVTAQERQREREEKRRRRQERAKEREKRRQERERKERGAGASGGPSTDPLAGLV LSDNDRSLLERWTRMARPAAPALTSVPAPAPAPTPTPTPVQPTSPPPGPVAQPTGPQPQSAGSTSGPVPQPACPPPGPAP HPTGPPGPIPVPAPPQIATSTSLLAAQSLVPPPGLPGSSTPGVLPYFPPGLPPPDAGGAPQSSMSESPDVNLVTQQLSKS QVEDPLPPVFSGTPKGSGAGYGVGFDLEEFLNQSFDMGVADGPQDGQADSASLSASLLADWLEGHGMNPADIESLQREIQ MDSPMLLADLPDLQDPTRTRPLEQKLISEEDLAANDILDYKDDDDKV
CRIP2	MASKCPKCDKTVYFAEKVSSLGKDWHKFCLKCERCSKTLTPGGHAEHDGKPFCHKPCYATLFGPKGVNIGGAGSYIYEKP LAEGPQVTGPIEVPAARAEERKASGPPKGPSRASSVTTFTGEPNTCPRCSKKVYFAEKVTSLGKDWHRPCLRCERCGKTL TPGGHAEHDGQPYCHKPCYGILFGPKGVNTGAVGSYIYDRDPEGKVQPTRTRPLEQKLISEEDLAANDILDYKDDDDKV
CSRP2	MPVWGGGNKCGACGRTVYHAEEVQCDGRSFHRCCFLCMVCRKNLDSTTVAIHDEEIYCKSCYGKKYGPKGYGYGQGAGTL NMDRGERLGIKPESVQPHRPTTNPNTSKFAQKYGGAEKCSRCGDSVYAAEKIIGAGKPWHKNCFRCAKCGKSLESTTLTE KEGEIYCKGCYAKNFGPKGFGYGQGAGALVHAQTRTRPLEQKLISEEDLAANDILDYKDDDDKV
$GABA_AR$ α1ex	MGQPSLQDELKDNTTVFTRILDRLLDGYDNRLRPGLGERVTEVKTDIFVTSFGPVSDHDMEYTIDVFFRQSWKDERLKFK GPMTVLRLNNLMASKIRTPDTFFHNGKKSVAHNMTMPNKLLRITEDGTLLYTMRLTVRAECPMHLEDFPMDAHACPLKFG SYAYTRAEVVYEWTREPARSVVVAEDGSRLNQYDLLGQTVDSGIVQSSTGEYVVMTTHFHLKRKIGGSGGGKPIPNPLLG LDSTHHHHHH
hMOG	METDTLLLWVLLLWVPGSTGDAAGGSGQFRVIGPRHPIRALVGDEVELPCRISPGKNATGMEVGWYRPPFSRVVHLYRNG KDQDGDQAPEYRGRTELLKDAIGEGKVTLRIRNVRFSDEGGFTCFFRDHSYQEEAAMELKVEDPFYWVSPGSGMGMGMGM MGLNDIFEAQKIEWHESGGSGHHHHHHS

FAM84A-Mutants

Mutant	Sequence
188VA	MGNQLDRITHLNYSELPTGDPSGIEKDELRVGVAYFFSDDEEDLDERGQPDKFGVKAPPGCTPCPESPSRHHHHLLHQL VLNETQFSAFRGQECIFSKVSGGPQGADLSVYAVTALPALCEPGDLLELLWLQHAPEPPAPAPHWAVYVGGGQIIHLHQ GEIRQDSLYEAGAANVGRVVNSWYRYRPL**A**AELVVQNACGHLGLKSEEICWTNSESFAAWCRFGKREFKAGGEVPAGTQ PPQQQYYLKVHLGENKVHTARFHSLEDLIREKRRIDASGRLRVLQELADLVDDKEGKPIPNPLLGLDSQHHHHHH
190EA	MGNQLDRITHLNYSELPTGDPSGIEKDELRVGVAYFFSDDEEDLDERGQPDKFGVKAPPGCTPCPESPSRHHHHLLHQL VLNETQFSAFRGQECIFSKVSGGPQGADLSVYAVTALPALCEPGDLLELLWLQHAPEPPAPAPHWAVYVGGGQIIHLHQ GEIRQDSLYEAGAANVGRVVNSWYRYRPLVA**A**LVVQNACGHLGLKSEEICWTNSESFAAWCRFGKREFKAGGEVPAGTQ PPQQQYYLKVHLGENKVHTARFHSLEDLIREKRRIDASGRLRVLQELADLVDDKEGKPIPNPLLGLDSQHHHHHH
191LA	MGNQLDRITHLNYSELPTGDPSGIEKDELRVGVAYFFSDDEEDLDERGQPDKFGVKAPPGCTPCPESPSRHHHHLLHQL VLNETQFSAFRGQECIFSKVSGGPQGADLSVYAVTALPALCEPGDLLELLWLQHAPEPPAPAPHWAVYVGGGQIIHLHQ GEIRQDSLYEAGAANVGRVVNSWYRYRPLVAE**A**VVQNACGHLGLKSEEICWTNSESFAAWCRFGKREFKAGGEVPAGTQ PPQQQYYLKVHLGENKVHTARFHSLEDLIREKRRIDASGRLRVLQELADLVDDKEGKPIPNPLLGLDSQHHHHHH
263EA	MGNQLDRITHLNYSELPTGDPSGIEKDELRVGVAYFFSDDEEDLDERGQPDKFGVKAPPGCTPCPESPSRHHHHLLHQL VLNETQFSAFRGQECIFSKVSGGPQGADLSVYAVTALPALCEPGDLLELLWLQHAPEPPAPAPHWAVYVGGGQIIHLHQ GEIRQDSLYEAGAANVGRVVNSWYRYRPLVAELVVQNACGHLGLKSEEICWTNSESFAAWCRFGKREFKAGGEVPAGTQ PPQQQYYLKVHLGENKVHTARFHSL**A**DLIREKRRIDASGRLRVLQELADLVDDKEGKPIPNPLLGLDSQHHHHHH
264DA	MGNQLDRITHLNYSELPTGDPSGIEKDELRVGVAYFFSDDEEDLDERGQPDKFGVKAPPGCTPCPESPSRHHHHLLHQL VLNETQFSAFRGQECIFSKVSGGPQGADLSVYAVTALPALCEPGDLLELLWLQHAPEPPAPAPHWAVYVGGGQIIHLHQ GEIRQDSLYEAGAANVGRVVNSWYRYRPLVAELVVQNACGHLGLKSEEICWTNSESFAAWCRFGKREFKAGGEVPAGTQ PPQQQYYLKVHLGENKVHTARFHSLE**A**LIREKRRIDASGRLRVLQELADLVDDKEGKPIPNPLLGLDSQHHHHHH
267RA	MGNQLDRITHLNYSELPTGDPSGIEKDELRVGVAYFFSDDEEDLDERGQPDKFGVKAPPGCTPCPESPSRHHHHLLHQL VLNETQFSAFRGQECIFSKVSGGPQGADLSVYAVTALPALCEPGDLLELLWLQHAPEPPAPAPHWAVYVGGGQIIHLHQ GEIRQDSLYEAGAANVGRVVNSWYRYRPLVAELVVQNACGHLGLKSEEICWTNSESFAAWCRFGKREFKAGGEVPAGTQ PPQQQYYLKVHLGENKVHTARFHSLEDLI**A**EKRRIDASGRLRVLQELADLVDDKEGKPIPNPLLGLDSQHHHHHH
268EA	MGNQLDRITHLNYSELPTGDPSGIEKDELRVGVAYFFSDDEEDLDERGQPDKFGVKAPPGCTPCPESPSRHHHHLLHQL VLNETQFSAFRGQECIFSKVSGGPQGADLSVYAVTALPALCEPGDLLELLWLQHAPEPPAPAPHWAVYVGGGQIIHLHQ GEIRQDSLYEAGAANVGRVVNSWYRYRPLVAELVVQNACGHLGLKSEEICWTNSESFAAWCRFGKREFKAGGEVPAGTQ PPQQQYYLKVHLGENKVHTARFHSLEDLIR**A**KRRIDASGRLRVLQELADLVDDKEGKPIPNPLLGLDSQHHHHHH
271RA	MGNQLDRITHLNYSELPTGDPSGIEKDELRVGVAYFFSDDEEDLDERGQPDKFGVKAPPGCTPCPESPSRHHHHLLHQL VLNETQFSAFRGQECIFSKVSGGPQGADLSVYAVTALPALCEPGDLLELLWLQHAPEPPAPAPHWAVYVGGGQIIHLHQ GEIRQDSLYEAGAANVGRVVNSWYRYRPLVAELVVQNACGHLGLKSEEICWTNSESFAAWCRFGKREFKAGGEVPAGTQ PPQQQYYLKVHLGENKVHTARFHSLEDLIREKR**A**IDASGRLRVLQELADLVDDKEGKPIPNPLLGLDSQHHHHHH

List of Abbreviations

A	alanine
AA	amino acid
ADCC	antibody-dependent cell-mediated cytotoxicity
ADH5	alcohol dehydrogenase 5, chi polypeptide
AID	activation-induced cytidine deaminase
AKAP17A	A-kinase anchoring protein 17A
AMPAR	α-amino-3-hydroxy-5-methyl-4-isoxazolepropionic acid receptor
APC	antigen-presenting cell
AU	arbitrary unit
BCR	B-cell receptor
BS^3	bis(sulfosuccinimidyl)suberate
BSA	bovine serum albumine
CASPR2	contactin-associated protein-like 2
CD	circular dichroism
cDNA	complementary desoxyribonucleic acid
CDR	complementary-determining region
CHD2	Chromodomain helicase DNA binding protein 2
CHO	chinese hamster ovary
CNP	cranial nerve palsies
CNS	central nervous system
CRIP2	cystein-rich protein 2
CSF	cerebrospinal fluid
CSRP2	Cystein and serine rich protein 2
C-terminal	carboxy-terminal
CV	coulmn volume
CYB5R3	Cytochrome b5 reductase 3
D	aspartic acid
Da	Dalton
DNA	desoxyribonucleic acid
dNTP	desoxynucleosid triphosphate
DTT	dithiothreitol
E	glutamic acid
E. coli	*Escherichia coli*
EAE	experimental autoimmune encephalitis
ECL	enhanced chemiluminescence
ELISA	enzyme-linked immunosorbent assay
F_{ab}	antigen-binding fragment
FAM20B	Family with sequence similarity 20 B
FAM84A	Family with sequence similarity 84 A
for	forward
g	gravitational force
$GABA_AR$	γ-aminobutyric acid-A receptor
$GABA_AR\alpha1$ ex	extracellular domain of γ-aminobutyric acid-A receptor α1-subunit
$GABA_BR$	γ-aminobutyric acid-B receptor
GAPDH	glyceraldehyd-3-phosphate dehydrogenase
GC	germinal centre
h	hours
H-chain	heavy chain
HEK	human embryonic kidney cell
HIV	human immunodeficiency virus
HRP	horseradish peroxidase
IB	inclusion body
IBD	inflammatory bowel disease
IEF	isoelectric focusing
Ig	immunoglobulin
IgA	immunoglobulin subclass A, D, G ,E, M
IMAC	immobilized metal affinity chromatography
IPTG	isopropyl-thio-β-galactoside
L	leucine
LB	Luria-Broth
L-chain	light-chain
LGI1	leucine-rich glioma inactivated protein 1
LPS	lipopolysccharide
M	molar
MAG	myelin-associated glycoprotein
MALDI	matrix-assisted laser/desorption/ionization
MAPK7	mitogen-activated protein kinase 7
MBP	myelin basic protein
MKNK1	MAP-kinase interacting kinase 1
ml	milliliter
MOG	myelin oligodendrocyte glycoprotein

mRNA	messenger ribonucleic acid
MRZ	measles-varizella-zoster
MS	multiple sclerosis
MW	molecular weight
NB	neuroborreliosis
NIND	non-inflammatory neurologic disorder
NMDAR	N-methyl-D-aspartate receptor
NMO	neorumyelitis optica
N-terminal	amino-terminal
OCB	oligoclonal band
OD	optical density
OID	other inflammatory disorder
p	probability
PBMC	peripheral blood mononuclear cell
PBS	phosphate-buffered saline
PBS-T	phosphate-buffered saline with tween
PCR	polymerase chain reaction
PEI	polyethylen imine
PLP	proteolipid protein
PMSF	phenylmethanesulfonyl fluoride
PMT	photomultiplier-tube
PTM	posttranslational modification
PVDF	polyvinylidene fluoride
R	arginine
rAb	recombinant antibody
rev	reverse
RT	room temperature
scF_v	single chain variable Fragment
SD	standard deviation
SDS	sodium dodecyl sulfate
SDS-PAGE	sodium dodecyl sulfate polyacrylamid gel electrophoresis
SLE	systemic lupus erythematosus
STUB1	STIP homology and U-box containing protein 1
Taq	*thermus aquaticus*
TBE	tris-boric acid-EDTA buffer
TMB	3,3′,5,5′-Tetramethylbenzidin
TOF	time-of-flight
Tris	tris(hydroxymethyl)-aminomethan
UV	ultraviolet light
V	valine
V(D)J	variable (diversity) junctional gene segments
v/v	volume per volume
w/v	weight per volume
WB	Western blot

List of Figures and Tables

Eidesstattliche Erklärung

Ich erkläre hiermit an Eides statt, dass ich die vorliegende Dissertation mit dem Thema

„Analysis of oligoclonal band antibodies from patients with neurological diseases“

selbständig verfasst, mich außer der angegebenen keiner weiteren Hilfsmittel bedient und alle Erkenntnisse, die aus dem Schrifttum ganz oder annähernd übernommen sind, als solche kenntlich gemacht und nach ihrer Herkunft unter Bezeichnung der Fundstelle einzeln nachgewiesen habe.

Ich erkläre des Weiteren, dass die hier vorgelegte Dissertation nicht in gleicher oder in ähnlicher Form bei einer anderen Stelle zur Erlangung eines akademischen Grades eingereicht wurde.

München, 06.06.16 Simone Brändle